Targeting the EPHA2 receptor tyrosine kinase in *KRAS* and *EGFR* mutant lung cancer

By

Katherine Renee Amato

Dissertation

Submitted to the Faculty of the

Graduate School of Vanderbilt University

in partial fulfillment of the requirements

for the degree of

DOCTOR OF PHILOSOPHY

in

Cancer Biology

May 2015

Nashville, Tennessee

Approved:

Pierre Massion, M.D.

Jin Chen, M.D., Ph.D.

Rebecca Cook, Ph.D.

Deborah Lannigan, Ph.D.

ORIGINAL PUBLICATIONS

1. **Amato KR**, Wang S, Tan L, Hastings AK, Lovly CM, Ye F, Lu P, Balko JM, Colvin DC, Cates JM, Pao W, Gray NS, Chen J. EPHA2 inhibition overcomes acquired resistance to EGFR TKIs in lung cancer. (Submitted)

2. Wang S, **Amato KR**, Song W, Youngblood V, Lee K, Boothby M, Brantley-Sieders DM, and Chen J. Regulation of endothelial cell proliferation and vascular assembly through distinct mTORC2 signaling pathways. ***Mol Cell Biol***. 2015.

3. Chen J, Song W, **Amato K**. Eph receptor tyrosine kinases in cancer stem cells. ***Cytokine Growth Factor Rev***. 2014.

4. **Amato KR**, Wang S, Hastings AK, Youngblood VM, Santapuram PR, Chen H, Cates JM, Colvin DC, Ye F, Brantley-Sieders DM, Cook RS, Tan L, Gray NS, and Chen J. Genetic and pharmacologic inhibition of EPHA2 promotes apoptosis in NSCLC. ***J Clin Invest***. 2014; 124:2037–49.

5. Zhuang G, Song W, **Amato K**, Hwang Y, Lee K, Boothby M, Ye F, Guo Y, Shyr Y, Lin L, Carbone DP, Brantley-Sieders DM, Chen J. Effects of cancer-associated EPHA3 mutations on lung cancer. ***J Natl Cancer Inst***. 2012; 104:1182-97.

6. Chmielecki J, Foo J, Oxnard GR, Hutchinson K, Ohashi K, Somwar R, Wang L, **Amato KR**, Arcila M, Sos ML, Socci ND, Viale A, de Stanchina E, Ginsberg MS, Thomas RK, Kris MG, Inoue A, Ladanyi M, Miller VA, Michor F, Pao W. Optimization of dosing for EGFR-mutant non-small cell lung cancer with evolutionary cancer modeling. ***Sci Transl Med***. 2011; 3:90ra59.

This is dedicated to the lung cancer patients whose tumors reveal no detectable driver mutations, whose tumors express mutations for which no therapies are currently available, or whose tumors are resistant to therapy.

This is also dedicated to my family (Gary and Janice Amato, Mitchell Amato, Mitchell and Delphine Wietchy, and Anthony and Louella Amato)
and to Andrew Hastings
for their unwavering support, encouragement, and love.

ACKNOWLEDGMENTS

There were countless individuals that contributed to the work documented here to whom I owe my utmost and most sincere gratitude. A partial list is provided below.

First, I must thank my mentor, Dr. Jin Chen. Being a student in her lab has truly been an unmatched opportunity to develop both as a scientist and as an individual. From my first day in her lab, Dr. Chen immediately offered me her highest confidence in my abilities, a gift that has not waned throughout the course of my studies and has infused my work with confidence and motivation. Not only did Dr. Chen provide me the space to do the experiments herein, she has also provided for me in many intangible ways, generously giving me guidance and advice as I attempted to navigate through many of my “firsts” as a scientist. Dr. Chen’s harmony of enthusiasm for my project, belief in me, and insistence that I continually strive to do better has pushed me to accomplish more than I could have imagined during my tenure in her lab. I am incredibly thankful to her for her wealth of support and assistance during my Ph.D. training.

I must also thank my past and present thesis committee members (Pierre Massion, Rebecca Cook, Deborah Lannigan, William Pao, David Carbone, and Stacey Huppert) who over the years have provided advice and critiques that have improved my project and have made me a stronger scientist. To Dr. Massion, my thesis committee chair, thank you for being a source of encouragement, for providing me with many valuable lung SPORE related opportunities and resources, and for so clearly modeling practical ways to give back to the cancer community. To Dr. Cook, thank you for always being interested and supportive, for making yourself available to listen and help, and for helping me see the big picture. To Dr. Pao, thank you for your service as my past thesis committee chair as well as my T32 training grant clinical mentor during my Ph.D. training. Thank you not only for your generous contribution of reagents and mice to this

thesis project, but also for the gift of scientific rigor that you brought to my committee meetings. To Drs. Lannigan, Carbone, and Huppert, thank you all for the good questions and helpful discussions.

I would also like to thank those who supported me financially during my graduate training making this work possible, specifically to Drs. Lynn Matrisian and Jin Chen for their Microenvironmental Influences in Cancer training grant (T32 CA009592) and to the National Cancer Institute for their pre-doctoral fellowship (F31 CA167878). I would also like to thank the Department of Cancer Biology, particularly Drs. Moses, Richmond, and Toni Shepard, for their dedication to the Cancer Biology graduate training program.

I would also like to thank the past and present members of the Chen lab who have been an instrumental part of my graduate training and experience by providing scientific advice, critiques, encouragement, and friendship. To Drs. David Vaught and Meghana Rao, former graduate students who were critical to my initial training in the lab, thank you for your generous patience, encouragement, and friendship. To Dr. Shan Wang, who I initially got to know through frequent mouse room runs and who I now consider family, thank you a million times over. Thank you for your positivity, your encouragement, and your constant willingness to help me no matter what. To Dr. Tammy Sobolik, thank you for making my last year of graduate school so much richer and more colorful. Your listening ear and sincere friendship have meant more to me than you know. To Dr. Dana Brantley-Sieders, who imparted a variety of her mouse-related expertise to me and was always willing to help, thank you. Additional thanks to lab members Victoria Youngblood, Dr. Deanna Edwards, Dr. Wenqiang Song, and Yoonha Hwang for their variety of helpful contributions.

Throughout my graduate training I have had the pleasure to work with many collaborators both at Vanderbilt University and elsewhere. I would like to thank Dr. Nathanael Gray and Dr. Li Tan (Harvard Medical School) for their collaboration and

enthusiasm in the development of the EPHA2 small molecule inhibitor, ALW-II-41-27. I would like to thank Dr. Fei Ye and Pengcheng Lu (Vanderbilt University) for their assistance in dataset analysis and biostatistics. I would also like to thank Dr. Christine Lovly (Vanderbilt University) for always having an encouraging word and for her help accessing patient tumor samples for our study. Furthermore, I would like to thank all of the courageous patients who were treated with EGFR TKI therapies and who selflessly agreed to donate their tumor tissue for the research performed herein, thank you. Additionally, I would also like to acknowledge Dr. Justin Balko, Dr. Daniel Colvin, and Dr. Justin Cates for their various contributions to this project.

Lastly, I must thank my family whose support, encouragement, and unconditional love have made this work possible. To my parents whom have sacrificed so much to get me to where I am today, thank you is not nearly enough. To my dad, Gary Amato, who worked tirelessly to provide for my education, who "helped" me craft my first science fair project, who taught me to enjoy an attention to detail, and who taught me the importance of carefully planning a project well before its commencement, thank you. To my mom, Janice Amato, who has been a constant cheerleader, who sacrificed her career to invest wholly in my upbringing, who has never once been too busy to listen (even about tumors and mice), and who instilled in me the importance of maintaining balance and perspective, thank you. To my brother, Mitchell Amato, who has been a lifelong friend, always challenging me and keeping me laughing, thank you. To my grandma, Delphine Wietchy, who has always inspired me with her generosity and love, thank you. To my grandparents, Anthony and Louella Amato, who have always shared their love and support even from afar, thank you.

To Andrew Hastings, there are not words enough to thank you or acknowledge you properly for your contribution to this work both emotionally and scientifically. Your presence from the beginning of this challenging journey has infused it with positivity,

peace, and joy. Thank you for your unwavering support and love which have made this project much more than I ever could have alone. Thank you∞.

For the honor and privilege to work each day immersing myself in the complex and enigmatic world of human cancer with the hope that my efforts and discoveries may help someone someday, thank You.

TABLE OF CONTENTS

LIST OF TABLES

LIST OF FIGURES

LIST OF ABBREVIATIONS

ABTS	2,2'-Azinobis [3-Ethylbenzothiazoline-6-Sulfonic Acid]-Diammonium Salt
ABL	Abelson Murine Leukemia Viral Oncogene Homolog 1
ADCC	Antibody Dependent Cell Mediated Cytotoxicity
ALDH	Aldehyde Dehydrogenase
ALK	Anaplastic Lymphoma Kinase
ANOVA	Analysis of Variance
APAF1	Apoptotic Protease Activating Factor 1
APC	Antigen Presenting Cell
ATP	Adenosine Triphosphate
AUC	Area Under the Curve
BAD	Bcl-2 Associated Death Promoter
BAX	Bcl-2 Associated X Protein
BCL-xL	B Cell Lymphoma- Extra Large
BIM	Bcl-2 Interacting Mediator of Cell Death
BrdU	Bromodeoxyuridine
CAD	Caspase Activated DNase
CCSP	Clara (Club) Cell Secretory Protein
$CD8^+$	Cytotoxic T Lymphocyte
CTLA4	Cytotoxic T Lymphocyte Associated Protein 4
CXCR4	C-X-C Chemokine Receptor Type 4
DAB	Diaminobenzidine Tetrahydrochloride
DAPI	4',6-Diamidino-2-Phenylindole
DMEM	Dulbecco’s Modified Eagle’s Media
DMSO	Dimethyl Sulfoxide

DOX	Doxycycline
ECK	Epithelial Cell Kinase
ECL	Enhanced Chemiluminscence
EDTA	Ethylenediaminetetraacetic Acid
EGF	Epidermal Growth Factor
EGFR	Epidermal Growth Factor Receptor
EMT	Epithelial to Mesenchymal Transition
ERBB2	Erythroblastic Leukemia Viral Oncogene Homolog 2
ELISA	Enzyme Linked Immunosorbent Assay
EPH	Erythropoietin Producing Hepatocellular Carcinoma Receptor
Ephrin	EPH Family Receptor Interacting Proteins
ERK	Extracellular Signal Regulated Kinase (MAPK)
FAK	Focal Adhesion Kinase
FBS	Fetal Bovine Serum
FDR	False Discovery Rate
FGFR	Fibroblast Growth Factor Receptor
$FOXN1^{nu}$	Forkhead Box N1 - Nude
GAP	GTPase Activating Protein
GDP	Guanosine Diphosphate
GEF	Guanine Nucleotide Exchange Factor
GPI	Glycosylphosphatidlinositol
GTP	Guanosine Triphosphate
HER2	Human Epidermal Growth Factor Receptor 2
HCl	Hydrochloric Acid
HRAS	Harvey Rat Sarcoma Viral Oncogene Homolog
IGF1R	Insulin-like Growth Factor 1 Receptor

IFNγ	Interferon Gamma
IHC	Immunohistochemistry
IC_{50}	Half Maximal Inhibitory Concentration
IP	Immunoprecipitation
JNK	C-Jun N-Terminal Kinase
KRAS	Kirsten Rat Sarcoma Viral Oncogene Homolog
LAG3	Lymphocyte Activation Gene 3
LKB1	Liver Kinase B1
LMW-PTP	Low Molecular Weight Protein Tyrosine Phosphatase
mAb	Monoclonal Antibody
MAPK	Mitogen Activated Protein Kinase
MCL-1	Myeloid Cell Leukemia 1
MEK	Mitogen Activated Protein Kinase Kinase (MAPKK)
MeOH	Methanol
MHCI	Major Histocompatibility Complex I
MHCII	Major Histocompatibility Complex II
MNK	MAPK Interacting Kinase
MSK	Mitogen and Stress Activated Protein Kinase
mTOR	Mammalian Target of Rapamycin
MTT	(3-(4,5-Dimethylthiazol-2-yl)-2,5-Diphenyltetrazolium Bromide)
MYC	Avian Myelocytomatosis Viral Oncogene Homolog
NRAS	Neuroblastoma Rat Sarcoma Viral Oncogene Homolog
NSCLC	Non Small Cell Lung Cancer
p90-RSK	90 kDa Ribosomal Protein S6 Kinase 1
PAGE	Polyacrylamide Gel Electrophoresis
PARP	Poly (ADP-ribose) Polymerase

PBS	Phosphate Buffered Saline
PD-1	Programmed Death-1
PD-L1	Programmed Death Ligand-1
PD-L2	Programmed Death Ligand-2
PCNA	Proliferating Cell Nuclear Antigen
PCR	Polymerase Chain Reaction
PEG	Polyethylene Glycol
PKCα	Protein Kinase C Alpha
PZD	PSD95/DIg/ZO1 Motif
PIP3	Phosphatidylinositol 3,4,5-Triphosphate
PI3K	Phosphatidylinositol 3 Kinase
RAC1	RAS Related C3 Botulinum Toxin Substrate 1
RAF	Rapidly Accelerated Fibrosarcoma (MAPKKK)
RBD	RAS Binding Domain
RHOA	RAS Homology Gene Family, Member A
RIPA	Radioimmunoprecipitation Assay
RNAi	RNA Interference
RPMI	Roswell Park Memorial Institute Media
RTK	Receptor Tyrosine Kinase
rtTA	Reverse Tetracycline Controlled Transactivator
S6	Ribosomal Protein S6
S6K1	Ribosomal Protein S6 Kinase Beta-1
SAM	Sterile-α-Motif
SCLC	Small Cell Lung Cancer
SD	Standard Deviation
SDS	Sodium Dodecyl Sulfate

SEM	Standard Error of the Mean
SGK1	Serum Glucocorticoid Regulated Kinase
SH2	Src Homology 2
siRNA	Small Interfering RNA
shRNA	Small Hairpin RNA
TetO	Tetracycline Operator
TGFα	Transforming Growth Factor Alpha
TIM3	T Cell Immunoglobulin Domain and Mucin Domain 3
TKI	Tyrosine Kinase Inhibitor
TTF-1	Thyroid Transcription Factor 1
TUNEL	Terminal Deoxynucleotidyl Transferase dUTP Nick-End Labeling
VEGF	Vascular Endothelial Growth Factor
vWF	von Willebrand Factor

CHAPTER I

INTRODUCTION

Overview

Lung cancer remains the leading cause of cancer related deaths in the United States despite a significant number of advancements in the molecular diagnosis and treatment of this disease. Although some aberrant gene products have been readily actionable using targeted therapeutics, intrinsic and acquired resistance to these inhibitors inform the necessity of identifying novel targets to mitigate the limitations of these drugs. Recent genome wide expression analyses of human lung cancer has identified a number of receptor tyrosine kinases (RTKs) as overexpressed and potentially representing molecular drivers of lung cancer. Among these RTKs identified was EPHA2, which belongs to the largest family of RTKs, the EPH family. Although previous studies have provided correlative data linking high EPHA2 expression to poor clinical outcomes in lung cancer, the role of EPHA2 in lung cancer, specifically in distinct molecular subtypes of lung cancer, had not been investigated. Herein we dissected the role of EPHA2 in a variety of molecular subtypes of lung cancer and discovered that *KRAS* and $EGFR^{T790M}$ mutant lung cancers were most vulnerable to EPHA2 inhibition by either genetic or pharmacological methods. We demonstrated the first functional evidence in vivo that the EPHA2 receptor is required for tumor growth and survival in both $Kras^{G12D}$ and $EGFR^{L858R+T790M}$ mutant transgenic mouse models of lung cancer. We also showed that EPHA2 controls viability in lung cancer through regulation of apoptosis, specifically by controlling activation of components of the PI3K/mTOR signaling pathway. Additionally, we identified a novel ATP competitive, EPHA2 RTK inhibitor, ALW-II-41-27, which was capable of inhibiting *KRAS* and *EGFR* mutant lung cancer cell

viability both in vitro and in vivo. Overall, we have provided genetic, functional, mechanistic, and pharmacologic evidence that EPHA2 signaling promotes the progression and survival of lung cancer. These studies suggest that EPHA2 may be a promising therapeutic target for both *KRAS* and *EGFR*^{T790M} mutant lung cancer.

Lung Cancer

Lung cancer is the leading cause of cancer related deaths in the United States with a 5 year survival rate of 18% (1). Cancers of the lung are responsible for approximately 160,000 deaths per year, more deaths than the next three most deadly cancers (colon, breast, and pancreatic) combined (1). Although approximately 80-90% of malignant transformation observed in the lung epithelium can be traced back to a history of smoking (2), other environmental exposures (e.g. asbestos, radon, mustard gas, polycyclic hydrocarbons, chloromethyl ethers, chromium, nickel, and arsenic) as well as a host of aberrant genetic factors are known to contribute to lung cancer as well (3-10). It is also well established that lung cancer is a disease of the middle-aged and elderly with the odds of developing lung cancer starting at approximately 1 in 560 between ages of 1-49 and growing to 1 in 17.5 by age 70 (1). Although simply defined, lung cancer can be viewed as a malignant neoplasm of the pulmonary epithelium, it is clear that lung cancer is not a single disease but is rather represented by a variety of histological appearances as well as molecular characteristics.

Histological Classification

There are two main histological subtypes of lung cancer: small cell lung cancer (SCLC) and non-small cell lung cancer (NSCLC). SCLCs comprise about 15% of all lung cancers and boast the highest association to smoking history of any type of lung cancer (11). Histologically, SCLC is defined by the presence of a large nuclei, a small

rim of cytoplasm, and neuroendocrine features (Figure 1.1A) (11, 12). NSCLC is the most common histological subtype of lung cancer accounting for approximately 85% of lung cancer cases. NSCLC can be further divided into three large subsets: adenocarcinoma, squamous cell carcinoma, and large cell carcinoma. Adenocarcinomas account for 41% of NSCLCs and are defined as neoplasias arising from bronchial mucosal glands or cells occupying the surface epithelium of the lung, specifically the alveoli (Figure 1.1B) (11, 12). Histologically, adenocarcinomas are frequently heterogeneous, displaying a variety of growth patterns including acinar, papillary, bronchioloalveolar as well as solid, mucin producing structures (11). Assessment of adenocarcinoma in the lung can be accomplished by positive staining for

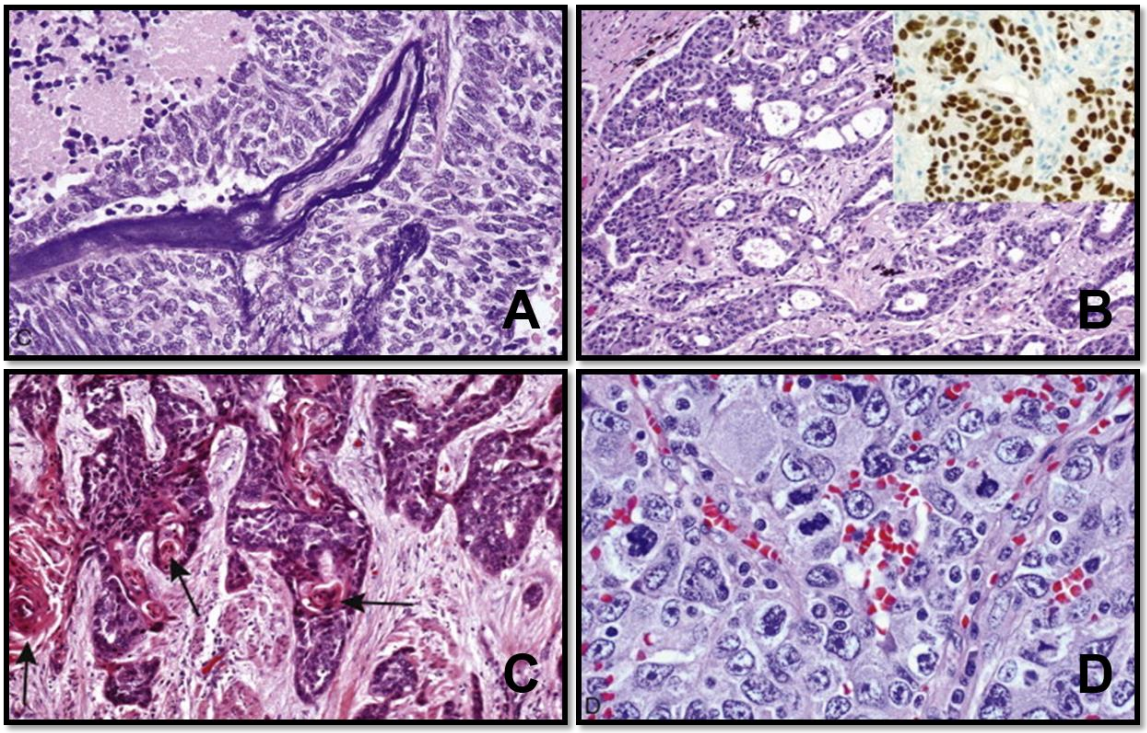

Figure 1.1 Histological subtypes of lung cancer. (A) Small cell carcinoma **(B)** Adenocarcinoma; top inset shows thyroid transcription factor 1 (TTF-1) **(C)** Squamous cell carcinoma; arrows show keratinization **(D)** Large cell carcinoma (Adapted from Robbins and Cotran Pathologic Basis of Disease, 9th Edition, (13)).

cytokeratin 7, thyroid transcription factor 1 (TTF-1), and surfactant apoprotein A; however, metastatic adenocarcinomas at secondary sites are typically negative for TTF-1 (12). Squamous cell carcinomas, also known as epidermoid carcinomas, arise in the proximal bronchi and are identified histologically by the presence of keratinization and intercellular bridges (Figure 1.1C) (11). This tumor type, which accounts for 34% of NSCLCs, has the highest association with a history of smoking compared to other forms of NSCLC (12). Large cell carcinomas, which account for 8% of NSCLCs, arise in the bronchi and are defined by their large nuclei as well as the absence of glandular or squamous differentiation, features of adenocarcinoma and squamous cell carcinoma, respectively (Figure 1.1D) (11, 12). Historically, lung cancers have largely been treated based upon their histological presentation at the time of diagnosis due to a determination that different histological subtypes had varying responses to chemotherapeutic agents (14).

Molecular Classification

Over the past decade through efforts to assess the sequence of the human genome and subsequently the cancer genome, it has become evident that tumors often harbor recurrent, oncogenic mutations, amplifications, or rearrangements in genes that "drive" growth and survival. These driver alterations are rarely found concurrently in the same tumor. Tumor cells can become addicted to the signaling from oncogenic, mutant proteins, thereby becoming vulnerable to specific, targeted therapeutic interventions (15). These principles have led to a paradigm shift in lung cancer classification and treatment which is now focused on molecular criteria rather than histology. A myriad of genetic alterations have already been discovered to drive tumorigenesis in NSCLCs, including those in *AKT1, ALK, BRAF, DDR2, EGFR, FGFR1, HER2, KRAS, MEK1, MET, NRAS, NTRK1, PIK3CA, PTEN, RET, and ROS1* (Table 1.1) (16).

Gene	Alteration	Frequency in NSCLC
AKT1	Mutation	1%
ALK	Rearrangement	3-7%
BRAF	Mutation	1-3%
DDR2	Mutation	4%
EGFR	Mutation	10-35%
FGFR1	Amplification	20%
HER2	Mutation	2-4%
KRAS	Mutation	15-25%
MEK1	Mutation	1%
MET	Amplification	2-4%
NRAS	Mutation	1%
NTRK1	Rearrangement	3%
PI3KCA	Mutation	1-3%
PTEN	Mutation	4-8%
RET	Rearrangement	1%
ROS1	Rearrangement	1%

Table 1.1 Frequency of mutations in non-small cell lung cancer (NSCLC) (Adapted from (16)).

Two of these aberrant protein products driven by mutations in the epidermal growth factor receptor (EGFR) and the anaplastic lymphoma kinase (ALK), already have FDA-approved small molecule inhibitors developed for use in NSCLC. A number of other alterations such as those in *BRAF, DDR2, HER2, MEK1, and RET* have existing FDA-approved drugs in other cancer types that may be transferable to lung cancer in the near future.

It is important to note that in lung cancer a number of recurrent mutations have also been observed in tumor suppressors, such as p53 and LKB1, contributing to tumorigenesis. Additionally, genetic analysis of tumors from both smoker and nonsmoker patients has revealed distinct molecular differences. For example, *KRAS* mutations have positively correlated with lung tumors of patients with a history of

smoking, while *EGFR* mutations are more closely associated with lung tumors from individuals without a history of smoking (17-21).

Mutant *KRAS*

RAS, a member of the RAS superfamily of proteins, is a GTPase that regulates intracellular signaling by acting as a molecular switch to turn on and off downstream signaling. In its inactive form, RAS is bound to guanosine diphosphate (GDP). In response to upstream signaling, RAS can be activated by binding of guanine nucleotide exchange factors (GEFs), which release GDP and allow guanosine triphosphate (GTP) loading (Figure 1.2) (22, 23).

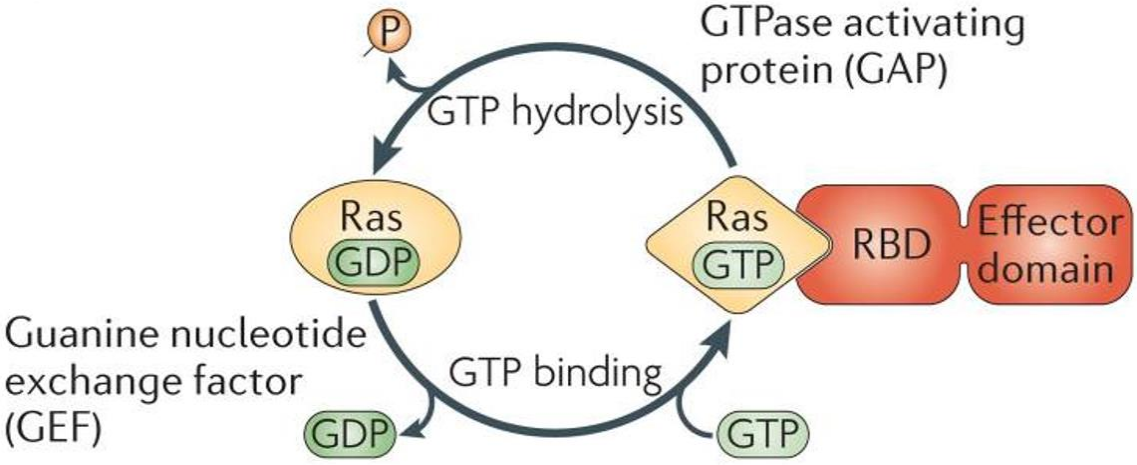

Figure 1.2 RAS GDP/GTP cycle. Inactive, GDP-bound RAS is activated by a GEF that induces the release of GDP and thereby permits GTP to bind. GTP binding induces a marked conformational change in RAS that allows it to bind effectors via their RAS binding domains (RBD). (Adapted from (24))

Binding of GTP to RAS prompts a structural change in RAS permitting it to bind to downstream effector proteins by their RAS-binding domain (RBD) (24). Classically, RAS binds to RAF (MAPKKK), which activates MEK (MAPKK), which activates ERK (MAPK) (25). Activated ERK can phosphorylate a variety of downstream proteins including p90-

RSK (subsequently controlling the phosphorylation of Fos, SRF, and CREB) (26-28), MNK (subsequently controlling the phosphorylation of eIF4E) (29), MSK (subsequently controlling the phosphorylation of CREB, ATF1, Histone H3, and HMG-14) (30-33), ELK1 (34), MYC (35), BRF1 (36), and UBF (37). It is also known that RAS proteins can activate the PI3K, RalGDS, TIAM1, PLCε, and RIN1 pathways as well (Figure 1.3) (22, 38, 39). Ultimately, RAS activation is associated with phenotypes of cell growth, survival, differentiation, and migration (40). In addition to GTP binding to promote its activity, RAS also requires modification via isoprenylation to efficiently transmit signals to effector proteins (41). In this post-translational modification a farnesyl group is added to the C-terminal tail of the protein allowing it to anchor in the cell membrane thereby facilitating its interactions with the appropriate effector molecules (24, 42, 43).

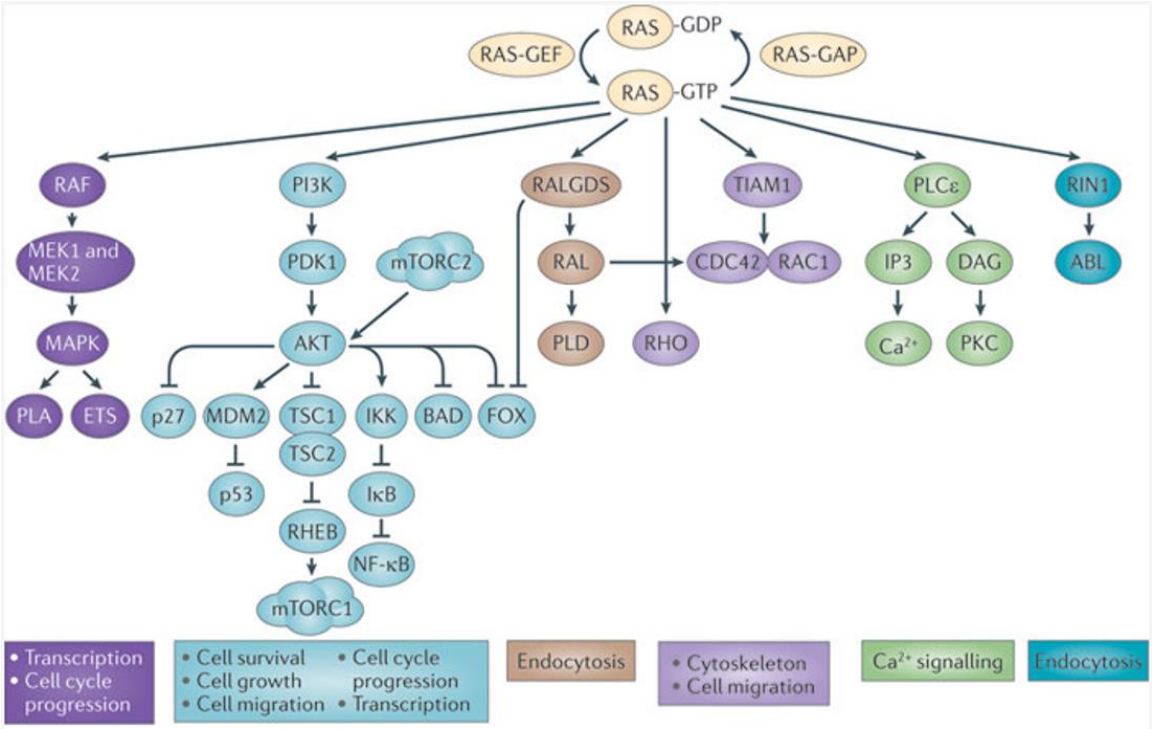

Figure 1.3 RAS signaling pathways. The GTPase, RAS, functions as a molecular switch based on binding of GTP and GDP. RAS is located at the apex of many signaling pathways and regulates many essential cellular functions including proliferation and survival (44).

Mutations in *RAS*, which inhibit guanine nucleotide exchange factor (GAP)-mediated GTP hydrolysis lock RAS in its activated form resulting in constitutive growth and survival signals. Mutations in *RAS* have been shown to have transformative potential in both cell culture and animal models (45-47). Although there are three major RAS isoforms expressed in humans (H, K, and N), mutations in *KRAS* are by far the most common, occurring in 33% of all cancers and 20% of NSCLCs (45, 47, 48). In lung cancer *KRAS* mutations are classically missense and occur most frequently at codon 12 although mutations are also known to occur at codons 13 and 61. $KRAS^{G12C}$ mutations are the most common in lung cancer and strongly correlate to tobacco smoke exposure as well as activation of the RalGDS pathway (49). $KRAS^{G12D}$ mutations on the other hand have been more closely associated with activation of the mitogen activated protein kinase (MAPK) and phosphatidylinositol 3 kinase (PI3K) pathways (50).

Mutant KRAS proteins present a unique challenge for small molecule inhibition by conventional nucleotide competition due to the high affinity of GTP to KRAS, demonstrated by its sub-nanomolar dissociation constant (51). In recent years various targeted inhibition methods have attempted to block oncogenic RAS signals including the use of RNA interference (52, 53), farnesyltransferase inhibitors (54-56), combinations of farnesyltransferase/ geranylgeranyltransferase inhibitors (57), immunotherapies (58, 59), and blockade of various downstream effectors such as RAF, MEK, and mTOR (60, 61). Unfortunately these attempts have resulted in minimal success often associated with significant toxicities.

Mutant *EGFR*

The epidermal growth factor receptor (EGFR) or ERBB1 is a receptor tyrosine kinase belonging to the ERBB family of RTKs which also includes HER2 (ERBB2), HER3 (ERBB3), and HER4 (ERBB4) (22). Structurally, EGFR is composed of three

main domains: an extracellular ligand-binding domain, a transmembrane domain, and an intracellular domain. Upon ligand binding (e.g. EGF or TGFα), EGFR monomers undergo a conformational change that facilitates dimerization either with another EGFR monomer (homodimerization) or with another ERBB family member (heterodimerization) (22). The receptor complex is then autophosphorylated on tyrosine residues through the acquisition of adenosine triphosphate (ATP) in the intracellular kinase domain of the receptor. Activated EGFR then recruits a variety of adaptor and signaling molecules with SRC homology 2 (SH2) domains as well as tyrosine binding domains to bind the phosphotyrosines on its C-terminal end and activate downstream effector molecules (22). EGFR most notably activates the MAPK and the PI3K/AKT pathways which together support multiple cellular processes including proliferation and survival (22, 62).

Overexpression of EGFR has been observed in many cancer types including breast, colon, lung, and prostate, which led to the development of targeted agents

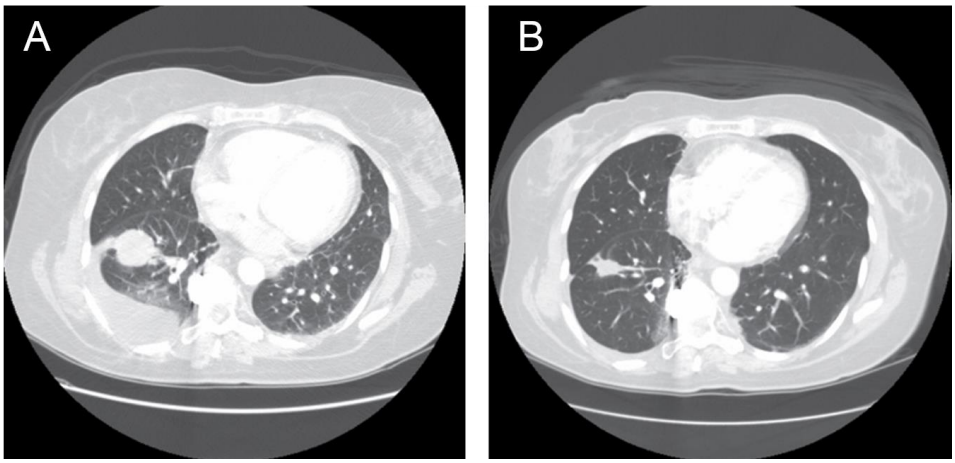

Figure 1.4 Treatment response to the EGFR TKI, erlotinib. A female patient with no smoking history presented with a primary lung adenocarcinoma which was determined to have a deletion in exon 19 of EGFR. The pre-treatment CT shows the primary lung tumor prior to erlotinib **(A)**; CT imaging after 4 months of erlotinib therapy revealed a significant response **(B)** (Adapted from (12)).

against wild-type EGFR in the 1990s (63). These included two ATP-competitive, small molecule tyrosine kinase inhibitors (TKIs), erlotinib (Tarceva; Genetech/OSI Pharmaceuticals) and gefitinib (Iressa; AstraZeneca), and one human-murine chimeric IgG1 monoclonal antibody therapeutic, cetuximab (Erbitux; ImClone/Merck/Bristol-Myers Squibb) (Figure 1.6A and 1.6B) (64). Upon introduction of the EGFR targeted therapy (gefitinib) in lung cancer, few patients responded. Interestingly, the patients that did respond had some similar, informative features including East Asian ethnicity, a non-smoking history, and tumors of adenocarcinoma histology (21, 65). In 2004, the laboratories of Haber, Meyerson, and Varmus independently published that the presence of oncogenic *EGFR* mutations in lung cancer correlated to increased tumor sensitivity to the EGFR tyrosine kinase inhibitors gefitinib and erlotinib (Figure 1.4) (66-68). *EGFR* mutations are found in 10-35% of lung cancer patients, and 85-90% of these mutations occur in exons encoding the kinase domain (exons 18-21) particularly manifesting as a deletion in exon 19 of the amino acids LREA or a point mutation in exon 21 (L858R) (Figure 1.5) (69). These mutations are activating and enhance EGFR kinase activity leading to constitutive activation of its downstream effector molecules.

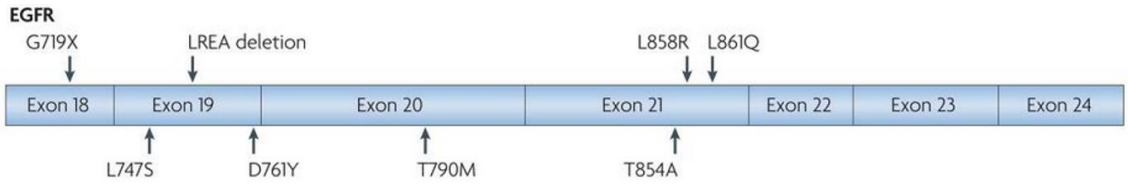

Figure 1.5 EGFR TKI sensitive and TKI resistance mutations. Activating drug-sensitive mutations are shown on the top of the epidermal growth factor (EGFR) kinase domain (exons 18-24). Mutations associated with TKI resistance are depicted on the bottom of the kinase domain schematic (Adapted from (63)).

In 2009 the Iressa Pan-Asia Study (IPASS) and WJTOG3405 trials unequivocally demonstrated that patients with *EGFR*-mutant tumors on gefitinib had a significantly longer progression free survival than patients receiving chemotherapy (carboplatin+paclitaxel or cisplatin+docetaxel for the respective studies) (70, 71). It was determined that successful cell death by these EGFR TKIs was dependent on the upregulation of pro-apoptotic, BCL-2 family member, BIM, and downregulation of the anti-apoptotic protein, MCL-1 (72-76). Unfortunately, all patients treated with EGFR TKIs acquire resistance to these therapies approximately a year after commencing treatment (77, 78). Sequencing efforts have revealed that tumors with acquired resistance to EGFR TKIs commonly gain an additional mutation in exon 20, T790M, in the gatekeeper position of the kinase domain of EGFR (79, 80). Biochemical analysis has revealed that this mutation confers resistance by sterically hindering drug-kinase interactions as well as by increasing the affinity of the mutant receptor for ATP (81, 82).

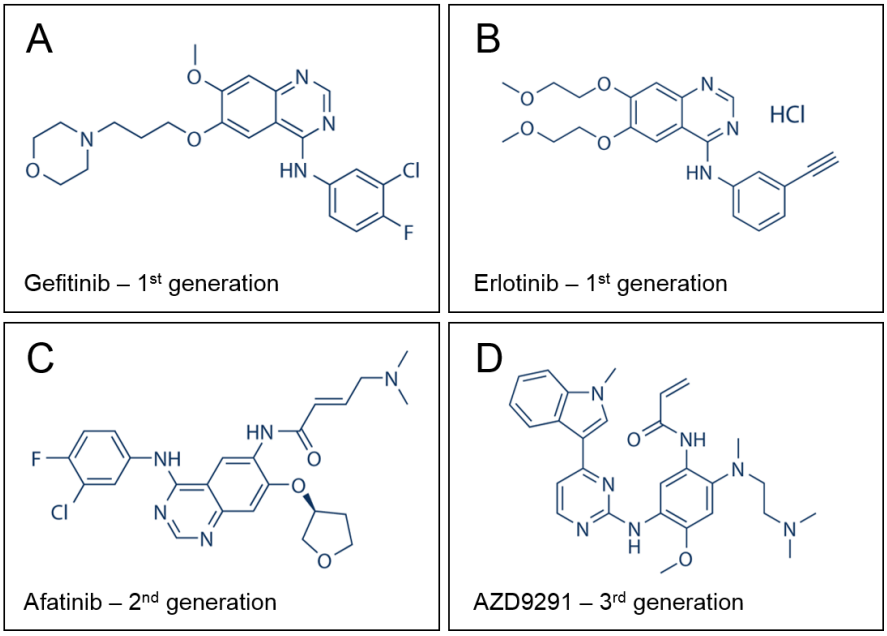

Figure 1.6 Structure of EGFR tyrosine kinase inhibitors. (A) Gefitinib (Iressa) and **(B)** Erlotinib (Tarceva) are reversible, 1st generation EGFR TKIs. **(C)** Afatinib (Gilotrif) is an irreversible, 2nd generation EGFR and HER2 inhibitor. **(D)** AZD9291 is a 3rd generation *EGFR*^{T790M} mutant specific inhibitor that is EGFR wild-type sparing.

Currently, there are limited options for the treatment of acquired resistance to first-generation, EGFR TKIs (e.g. gefitinib, erlotinib), although some success has been observed with administration of second (e.g. afatinib) (Figure 1.6C) (83, 84) and third (Figure 1.6D) (e.g. AZD9291) (85, 86) generation EGFR TKIs or by combining afatinib and cetuximab (87). Molecular analysis of EGFR TKI resistant tumors has suggested a role for the mammalian target of rapamycin (mTOR) activation in the maintenance of the acquired resistance phenotype (88, 89). mTOR is a serine/threonine kinase that regulates a myriad of cellular processes including cellular growth, survival, and metabolism by signaling in two distinct complexes (mTORC1 and mTORC2) (90, 91). Canonically, mTORC1 is activated downstream of PI3K and AKT (T308 phosphorylation) (92), and it is capable of phosphorylating p70 S6K1 (and subsequently S6) (93), BAD (94, 95), and 4E-BP1 (and subsequently eIF4E). mTORC2 most notably signals through AKT (S473), SGK1, and PKCα (91, 96-98). While mTOR has been implicated in EGFR TKI resistance (88), to date mTOR inhibitors have had limited success clinically due to a disruption of feedback mechanisms between the two complexes as well as dose limiting toxicities.

Risks of persistent and/or mutation-specific targeting of EGFR include the likely development of alternative mechanisms of TKI resistance distinct from further mutations in EGFR (85), including oncogene addiction to other kinases. Such “bypass” RTK signaling has been a well-documented mechanism of EGFR TKI resistance as evidenced by compensatory activation of MET, HER2, AXL, IGF1R, and FGFR in the context of EGFR TKI acquired resistance (99-105). Identifying bypass pathways responsible for mediating EGFR TKI resistance may provide novel targets needed for therapeutic intervention.

Apoptosis

Genetic or pharmacological inhibition of a genetically activated kinase to which a cell displays signaling addiction often results in proliferative arrest and in many cases induces a program of cell death called apoptosis. At a cellular level this process includes steps of chromatin condensation and fragmentation, cell shrinkage, and formation of intact apoptotic bodies that contain nuclear and cytoplasmic material. Molecularly, there are two distinct pathways that lead to apoptosis. The first which is initiated through the mitochondria is called the intrinsic apoptosis pathway, and the second which is initiated by pro-apoptotic receptors on the cell surface is called the extrinsic apoptosis pathway. The intrinsic apoptosis pathway, a known regulator of apoptosis induced by DNA damage (106-108) has emerged as a key regulator of apoptosis induced by molecularly targeted therapy (109-111). Intrinsic apoptosis occurs by inducing a rearrangement of pro-apoptotic (e.g. BAX, BAK, BID, BAD, BIM, and BIK) and anti-apoptotic (BLC-2, BLC-xL, and MCL1) protein interactions to regulate the balance between survival and death (112). As apoptosis commences, inhibition of upstream PI3K/AKT/mTOR signaling decreases phosphorylation of BAD (113) and increases expression of BIM (75, 111, 114), allowing these proteins to bind and sequester the anti-apoptotic family members, BCL-2, BCL-xL, and MCL-1 (111). In addition to these new interactions, anti-apoptotic proteins often exhibit decreased expression upon kinase inhibition further decreasing the anti-apoptotic protein's functional abilities in response to targeted therapy (112). In the absence of suppression from anti-apoptotic family members, the pro-apoptotic, BCL-2 family members, BAX and BAK, are liberated and capable of association with the mitochondrial membrane where they oligomerize and form pores to initiate the release of cytochrome C into the cytoplasm (115, 116). Cytochrome C then binds to the apoptotic protease activating factor (APAF1) to facilitate the formation of the apoptosome and the activation of the

initiator caspase, caspase 9 (117, 118). Caspase 9 is then able to bind and activate caspase 3 through a cleavage event at aspartate residue 175 (119), which is responsible for activation of the caspase activated DNase (CAD) (120), cleavage of the nuclear enzyme poly (ADP-ribose) polymerase (PARP) (121, 122), and induction of apoptotic body formation (115).

EPH receptors and ephrin ligands

The EPH family of receptors are the largest family of receptor tyrosine kinases comprised of 15 receptors (EPHA1-EPHA10, EPHB1-EPHB4, and EPHB6) although only 14 receptors (excluding EPHA9) are encoded in the human genome (Table 1.2) (123-125). EPH receptors and their ligands, called ephrins (EPH family interacting

EPH Receptor	Ephrin Ligand
A CLASS	
EPHA1	EphrinA1
EPHA2	EphrinA2
EPHA3	EphrinA3
EPHA4	EphrinA4
EPHA5	EphrinA5
EPHA6	EphrinA6
EPHA7	
EPHA8	
EPHA10	
B CLASS	
EPHB1	EphrinB1
EPHB2	EphrinB2
EPHB3	EphrinB3
EPHB4	
EPHB5	

Table 1.2 EPH receptor tyrosine kinases and ephrin ligands encoded in the human genome (Adapted from (126)).

proteins), are divided into two classes, A and B, which differ based on the EPH receptor sequence homology and ligand binding affinities. Unlike many classical RTK ligands, ephrins are unique in that they are membrane bound. A class ephrins (ephrinA1-ephrinA6) are tethered to the membrane by a glycosylphosphatidlinositol (GPI) anchor, while B class ephrins (ephrin B1- ephrin B3) are transmembrane in nature and include a small cytosolic region (125, 127). EPH receptors typically interact with ephrins of the same class (e.g. A class EPH RTKs bind A class ephrin ligands) although promiscuous binding has been described with some receptors including EPHA4 and EPHB2. EPH receptors consist of an extracellular portion, containing a highly conserved N-terminal ligand binding domain, a cysteine-rich region (including an epidermal growth factor-like motif), and two fibronectin type-III repeats. A transmembrane region connects to the intracellular portion which is composed of a tyrosine kinase domain, a sterile-α-motif (SAM) domain, and a PSD95/Dlg/ZO1 (PDZ)-binding motif (128) (Figure 1.7). Structural analysis of EPH-ephrin interactions has contributed significantly to the understanding of the signaling properties of this family of receptors and ligands. Classically, a monomeric interaction is mediated between a receptor and ligand *in trans* by insertion of the hydrophobic loop of an ephrin ligand into a cleft of the N-terminal domain of an EPH RTK (129-131). Ligand binding is known to initiate a conformation change in these interacting partners enabling the EPH-ephrin complexes to oligomerize and commence autophosphorylation of the intracellular portion of the EPH receptor (132-134). Two highly conserved tyrosine residues in the juxtamembrane domain of the EPH receptor are phosphorylated in response to ligand binding (135, 136), which prompts an additional structural rearrangement further exposing the kinase domain (135). This allows for a cascade of phosphorylation events involving the EPH receptors fourteen conserved, cytosolic tyrosine residues (130, 131, 134) preparing the kinase for docking of signaling effector molecules with SRC homology 2 (SH2) domains (137, 138).

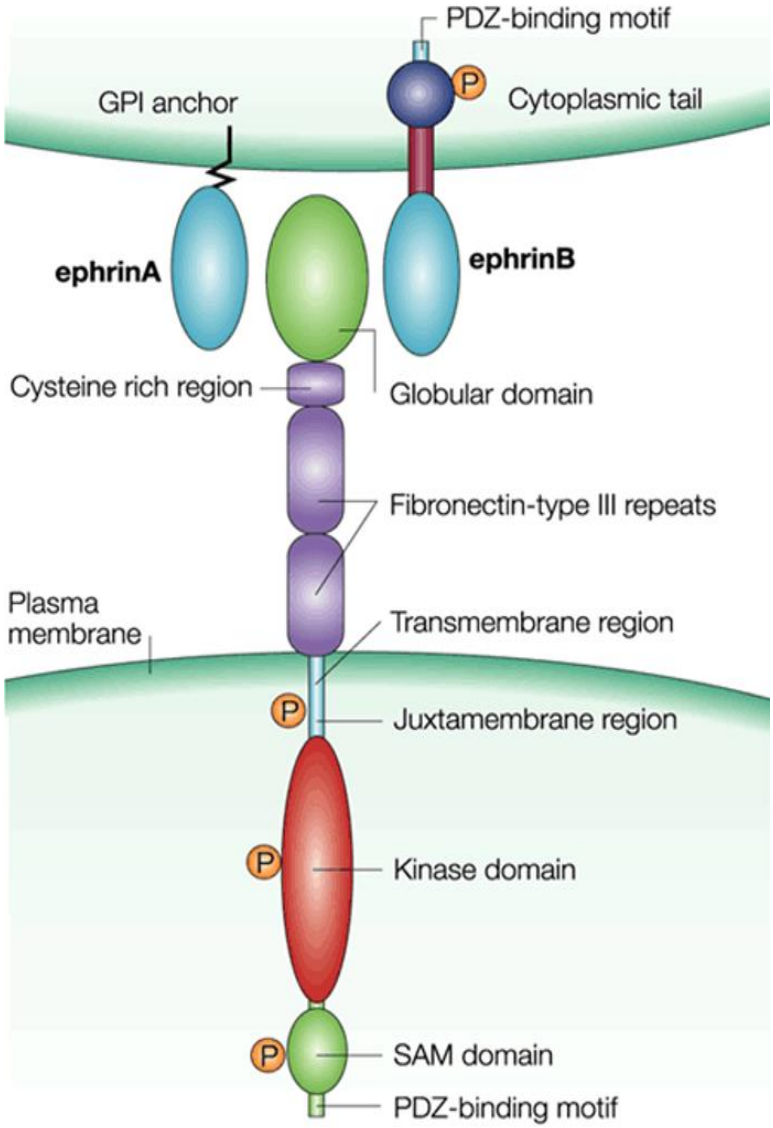

Figure 1.7 EPH receptor and ephrin ligand structure. Schematic diagram of EPH receptors and ephrin ligands. The top of the figure shows an ephrin expressing cell and the bottom half of the figure shows and EPH RTK expressing cell (Adapted from (126)).

EPH-ephrin signaling is often complicated by the co-expression of a variety of EPH and ephrin family members that can co-cluster and co-signal both *in cis* and *in trans* (139). In addition, signaling can be variable dependent on EPH receptor and ephrin ligand densities, which differ based on tissue type and pathology (140).

Signaling mechanisms

EPH receptor and ligand complexes are capable of binding to a variety of proteins thereby activating signaling pathways with diverse functions including adhesion, bone remodeling, cell morphology, invasion, immunity, migration, proliferation, and synaptic plasticity (123, 124). To date a number of proteins have been found to interact with EPH receptors directly including: Ephexin, FAK, GRB2, LMW-PTP, the p85 regulatory subunit of PI3K, SHP2, SRC family members, VAV GEFs, EGFR, and HER2 (137, 141-149). The wide spectrum of binding partners is informative of the phenotypic variety that can results from this family of RTKs.

Forward signaling versus reverse signaling

One unique feature of EPH-ephrin complexes is their ability to signal bidirectionally through both the receptor (forward signaling) and ligand (reverse signaling) (124). Because both EPH receptors and ephrin ligands are tethered to the cell membrane these interactions often require cell-cell contact. “Forward” or receptor-mediated signaling is stimulated by the phosphorylation of tyrosine residues in the kinase domain of the EPH receptor and successive downstream activation of signaling molecules. EPH receptors have been most notably associated with forward signaling through the RAS/MAPK (149-151), PI3K/AKT/mTOR (152, 153), ABL/CRK (154, 155), and the RHO/RAC/CDC42 (149, 156-158) pathways. Signaling pathways utilized by EPH receptors and ligands are often specific to tissue and pathological condition, as

evidenced by divergent pathways used by EPHA2 in breast and lung cancers, RAS/MAPK and PI3K/AKT/mTOR, respectively (149, 153).

"Reverse" or ligand-mediated signaling differs depending on the ephrin class, A or B. "B" class ephrins are able to signal by tyrosine phosphorylation of their C-terminal tails through interactions with SRC family proteins as well as a variety of other RTKs and effector proteins (159). "A" class ephrins are also able to engage in reverse signaling, although in a more enigmatic way, as they lack the cytoplasmic tail region of B class ligands. It is thought that A class ephrin ligands mediate signal transduction through acquisition of signaling partners, such as has been described with integrins and the p75 neurotrophin receptor (160-162). The functional significance of reverse signaling is still being uncovered although existing data suggests it provides an important function in axonal guidance for the organization of the nervous system particularly during embryogenesis (163-165).

Ligand independent versus ligand dependent signaling

Another unique aspect of EPH receptor signaling is its ability to occur both in the presence (ligand dependent) and absence (ligand independent) of an ephrin ligand. Ligand dependent activation of EPH receptors is accompanied by rapid internalization and degradation of the receptors (163, 166), which has been associated with inhibition of EPH related signaling pathways including ABL/CRK (155), integrins (142), RAS/MAPK (167), RHO/RAC (141), and PI3K/AKT/mTOR (168) pathways. As these pathways are regulators of cell proliferation, survival, and migration, ephrin stimulation is often associated with the inhibition of these cellular processes.

In addition to ligand stimulated forward signaling, EPH receptors can also activate downstream signals in the absence of a ligand by interacting with a host of other cellular proteins as demonstrated by the binding of A class EPH receptors with ERBB

family members EGFR and HER2 (147, 149, 169). Other reports have identified a direct interaction with EPHA4 and FGFR (170, 171) as well as interactions with EPHB receptors and CXCR4 (172, 173), which have resulted in an activation of downstream signals responsible for cell proliferation in glioma and T cell stimulation, respectively. A more complete list of known EPH RTK interacting receptors can be found in Table 1.3.

Ephrin dependent activation and suppression of EPH receptors illuminates seemingly conflicting data from the field which report the same EPH receptors having diametric signaling properties. For example, EPHA2 has been shown to regulate integrin signaling both positively and negatively (142, 163, 174, 175). This was shown to be due to the ability of EPHA2 to interact with FAK, a component of integrin signaling, in

EPH receptor	Crosstalk receptor	Signaling outcome	Reference
EPHA	CXCR4	CDC42 inhibition	(176)
EPHA	Integrins	RAC1 inhibition	(177)
EPHA2	EGFR and HER2	Modulate cell motility	(147, 149)
EPHA2	Claudin4	Claudin4 phosphorylation	(178)
EPHA2	Integrins	FAK inhibition	(142)
EPHA2	E-Cadherin	EPHA2 activation	(179)
EPHA4	Integrins	Integrin activation	(180)
EPHA4	FGFR	MAPK activation	(170)
EPHA4	EGFR	EGFR phosphorylation	(169)
EPHA8	Integrins	PI3K activation	(181)
EPHB	NMDA receptor	NMDAR phosphorylation	(182)
EPHB	E-Cadherin	E-Cadherin redistribution	(183)
EPHB2	Syndecan2	Syndecan2 phosphorylation	(184)
EPHB2	L1	L1 phosphorylation	(185)
EPHB2 an B4	CXCR4 receptor	AKT activation	(173)
EPHB2 and B3	RYK receptor	Tyrosine phosphorylation	(186)
EPHB6	T cell receptor	T cell activation	(172)

Table 1.3 Crosstalk between EPH receptors and other receptors.

a ligand independent manner to promote integrin signaling (142). In the presence of the preferential ligand for EPHA2, ephrinA1, the phosphatase SHP2 is recruited to the EPHA2-FAK-integrin complex, where FAK is subsequently dephosphorylated and inactivated (142). An additional example involves the interaction between EPHA2 and AKT. Ligand stimulated EPHA2 downregulates AKT phosphorylation as a downstream signaling effector, while in settings of EPHA2 overexpression (which equates to a lower intrinsic dependency on the ephrin ligand) AKT can directly phosphorylate EPHA2 at site S897 in turn regulating the receptor's activity (168). The basis for the regulation of this ligand dependent "switch" in signaling remains to be elucidated, but evidence suggests that the composition and concentration of receptors and ligands on opposing cell surfaces as well as the receptor and ligand avidity strongly contribute to the signaling consequences observed.

Role in normal physiology

EPH receptors are expressed in many tissues throughout the body and tend to be expressed at a higher level in the nervous system during development and in certain pathological conditions such as cancer. EPH receptors were first described for their role in axon guidance and subsequently tissue patterning, topographic mapping, and morphogenesis during embryonic development, where concentration gradients of receptors and ligands support motile behaviors through a series attractive and repulsive interactions (133, 163). In regard to tissue patterning, EPHA3 expression has been observed to inhibit the growth of the temporal retinal axon past the anterior tectum due to low ephrin expression there (187). Additionally, EPHB2 has been observed to be expressed at the ventral border of the pars posterior (acP), an axonal tract connecting the two temporal lobes of the brain, guiding axons along this track against an ephrinB1 gradient (164). EPHB2 also appears to be important in patterning of the peripheral

nervous system due to its overexpression in neural crest cells (188). Segmental patterning of the hindbrain has been attributed in part to EPHA2, EPHA4, EPHB2 and EPHB3 expression (189-192), while EPHA4 has been attributed to patterning of the forebrain (193).

In addition to the nervous system, EPH RTKs and ephrin ligands have also demonstrated a role in vascular biology. Expression of ephrinA1 and ephrinB1 have been detected in embryonic endothelial cells, suggestive of a role in endothelial cell segregation and vascular development (194-197). EphrinA1 has also been observed to participate in aortic and mitral valve formation as well as angiogenesis in normal and tumor tissue (133). Additionally, EPHB2, EPHB3, EPHB4, ephrinB1, and ephrinB2 have also been implicated in vascular development in mice with ephrinB2 demonstrating a particularly important role in embryonic vascular remodeling (194, 195, 198).

EPH RTKs and ephrins also have implications in epithelial tissue development particularly in branched organs such as the intestines (e.g. EPHB2, EPHB3, and eprhinB1) (199), kidney (e.g. EPHA2 and ephrinA1) (200, 201), mammary gland (e.g. EPHA2, EPHB4, and ephrinB2) (202), and thymus (e.g. EPHA4) (203). Additionally, our lab has shown that EPHA2 can regulate branching and penetration of the mammary gland into the fat pad during development and puberty (202).

Lastly, EPH receptors have been associated with both embryonic and adult stem cells, particularly in the brain and intestine (154, 204, 205). EphrinA2 has been observed to be expressed on neural progenitor cells regulating the proliferation and migration of neuroblasts to the olfactory bulb by the expression of EPHA7 on ependymal cells (206). Additionally, B class ephrins have been observed to be expressed in the subventricular zone guiding progenitor cell proliferation in that region by the presence or absence of B class EPH RTK forward signaling (207). In the intestines, high EPHB2 and EPHB3 expression is observed in stem cells at the base of the intestinal crypts, and this

expression progressively decreases as the cells differentiate and move to the top of the intestinal crypts (199). Interestingly, a gradient of B class ephrin expression is observed in a reverse and complimentary fashion to the B class EPH RTKs demonstrating the highest expression in the most differentiated cells at the top of the intestinal crypts (Figure 1.8) (199).

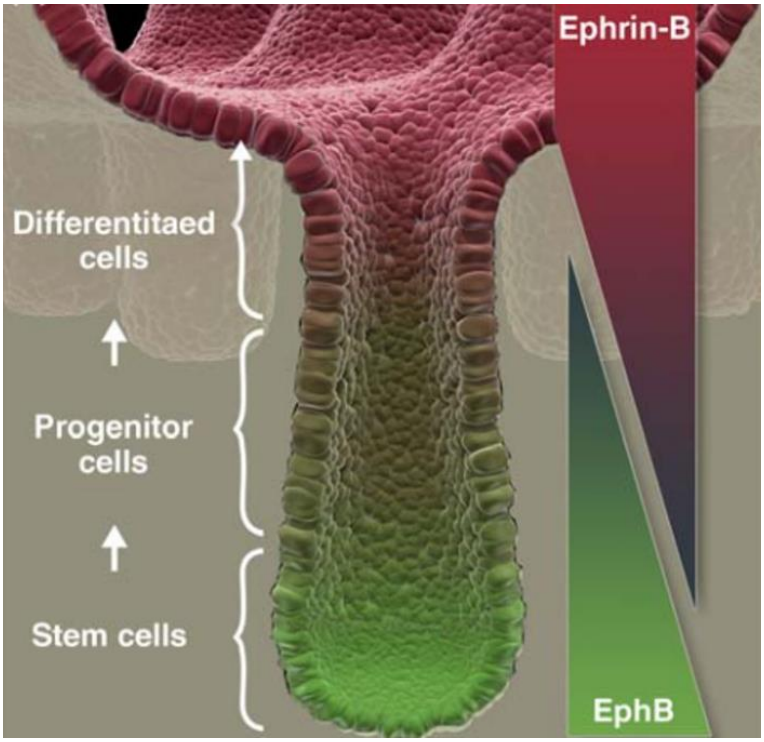

Table 1.8 EPHB signaling in adult intestinal stem cells. Stem cells residing at the bottom of the intestinal crypt express high levels of EPHB receptors (green) while more differentiated cells express high levels of ephrinB ligands (red) (Adapted from (208)).

Role in cancer

Overexpression and mutations in EPH RTKs have implicated this family of receptors in tumorigenesis for over 25 years (209, 210). EPH RTKs, particularly EPHA2, EPHB2, and EPHB4, have been observed to be overexpressed in a variety of malignant tissues including those of the brain, breast, lung, and skin. Additionally, the expression of many EPH receptors has positively correlated to a more aggressive tumor phenotype (211-214). Conversely, not all EPH RTKs are considered oncogenic, and there is

evidence of some EPH RTKs inhibiting tumorigenicity. Furthermore, the elevated expression of some EPH RTKs on tumor blood vessels has also suggested a role for EPH RTKs in the tumor microenvironment, particularly in the regulation of tumor angiogenesis (215, 216). Lastly, mutations have been detected in EPH RTKs, most notably EPHA3 and EPHA5 in lung cancers and EPHB2 in prostate, gastric, colorectal, and skin cancers although the functional consequences of these mutations is still being uncovered (217-223).

Tumor promotion

Genome-wide expression analysis has revealed EPH RTKs as overexpressed in many tissue types as compared to adjacent normal tissue with the degree of overexpression positively correlating to the level of malignancy (216). This has been observed for EPHA2 in lung cancer (224-226), breast cancer (227), pancreatic cancer (228), and esophageal cancer (229) as well as EPHB4 in breast cancer (227) and EPHB2 in brain cancer (230). Interestingly, EPH RTKs can be even further overexpressed in tumors as a mechanism of resistance to targeted therapies. This has been evidenced by EPHA2 overexpression in trastuzumab resistant breast cancer cells (231), tamoxifen insensitive breast cancer cells (232), vemurafenib resistant melanoma cells (233), and erlotinib resistant lung cancer cells (Chapter 3). Additionally, EPHB4 overexpression has been related to Imatinib resistance in Philadelphia chromosome positive acute lymphoblastic leukemia (ALL) (234).

The causal role of EPH RTKs in tumor promotion has been evidenced by the transforming potential of these receptors when overexpressed in vitro. This has been evidenced by the malignant transformation of normal-like, MCF-10A breast cancer cells (e.g. anchorage-independent growth) by EPHA2 overexpression (235) and the increased malignancy observed from overexpression of EPHA2 in pancreatic carcinoma cells

(228). Conversely, RNAi-mediated silencing of EPH RTKs has impaired cell viability and malignant progression in numerous cancer types. This has been evidenced by the decreased cell viability and migratory potential upon knockdown of EPHA2 in lung (153, 236), breast (149), skin (237), ovarian (238), and pancreatic (228) tumor cell lines and EPHB4 in breast cancer cell lines (239).

A tumor promoting role for EPH RTKs has also been observed in vivo using transgenic animal models. EPHA2 knockout mice crossed with any of the following oncogenic promotors, MMTV-Neu, *KRAS*^{G12D}, or *EGFR*$^{L858R+T790M}$ ((149, 153) and Chapter 3), led to decreased tumor progression and decreased tumor burden overall. Additionally, a model of EPHB4 overexpression crossed with MMTV-Neu accelerated tumor development and progression among these animals (239). These studies further support a role for EPH RTKs in tumor promotion.

A universal molecular mechanism by which EPH RTKs promote tumorigenesis remains elusive and may be a product of the highly dynamic and diverse nature of this family of RTKs. In tumor tissues it is hypothesized that EPH RTK overexpression drives tumor promotion by both amplifying survival signaling (e.g. RAS/MAPK, and PI3K/AKT/mTOR), migratory signaling (e.g. RHO/RAC), and increasing interactions with additional co-oncogenic receptors (e.g. EGFR, HER2, FGFR) (147, 149, 171). It is also possible that the loss of cellular organization in tumors exhibiting an epithelial to mesenchymal transition (EMT) phenotype can decrease the likelihood of EPH-ephrin interactions due to the requirement of cell-cell contact for bidirectional signaling (179, 205). Collectively, EPH RTK signaling is thought to promote tumorigenesis through a combination of receptor overexpression and ligand independent signaling.

Tumor angiogenesis and metastasis

Tumor cells require oxygen and nutrients for sustained proliferation and growth. In an effort to obtain these vital factors, tumors secrete proteins (e.g. VEGF and FGF) to stimulate vessel growth in the tumor microenvironment, a process called angiogenesis (22). This process is critical for tumor cell dissemination and malignant progression to distant sites as the vessels provide entry points into the circulatory system (240). Interestingly, EPH RTKs are often highly expressed in tumor vascular endothelial cells and inhibition of particular EPH family members, EPHA2 and ephrinB2, has successfully decreased tumor mediated vessel growth in vivo (241, 242). Elevated expression of EPH RTKs and ephrin ligands on tumor cells as well as the tumor vasculature may provide a dual therapeutic advantage when targeting this family of proteins as they hold the potential of inhibiting both cell viability and angiogenesis.

EPHA2 is not highly expressed in the developing or adult quiescent vasculature, however its expression has been found distinctly in tumor vessels. EphrinA1, however, has been found to be expressed in both developing and tumor vasculature with the ability to promote angiogenic responses in vitro and neovascularization in vivo (196, 243, 244). Notably, although ephrinA1 appears to be sufficient to support the development of the vasculature in embryogenesis, it does not appear to be essential. This is evidenced by the viability of ephrinA1 knockout mice which display few detectable vascular pathologies in addition to mild heart valve defects (197). Ligand dependent signaling via ephrinA1 is credited for the activation of EPHA2 (at Y587 and Y593) on endothelial cells resulting in downstream activation of RAC1 via interaction with the guanine nucleotide exchange factors, VAV2 and VAV3, which results in the regulation of endothelial cell migration and assembly (137, 245, 246). In vivo studies utilizing an EPHA2 knockout mouse or treatment with EPHA2-Fc fusion proteins on xenografted tumor cells have demonstrated significantly decreased breast cancer angiogenesis and metastatic

progression to the lung (245, 247-249). Additionally, EPHA2 has demonstrated a unique role in regulating angiogenesis induced by VEGF (250). This effect has been further suggested by the overexpression of ephrinA1 in the context of resistance to VEGF inhibitors in late stage pancreatic tumors in mice (251).

In contrast to EPHA2, ephrinB2 expression is detectable in the developing vasculature (195, 252). The role of ephrinB2 in angiogenesis is linked to the effects of its reverse signaling capabilities triggered by EPHB4 expression in both vascular and tumor cells. EphrinB2 mediated reverse signaling has been identified as contributing to vessel assembly, maturation, and maintenance of tumor-related vessels both in vitro and in vivo (253-255).

Tumor suppression

Although in cancer, EPH RTKs are largely considered to have an oncogenic role, there are many reports of this protein family also inhibiting tumor progression (139, 216). These conflicting data may be attributed to a host of factors including tissue type, disease stage, concentration gradients of EPH receptors and ephrin ligands, availability for receptor-ligand engagement, and the presence or absence of mutations in these receptors. By far the most documented context of EPH RTKs in tumor suppression has been in the presence of ligand-receptor engagement (155, 168, 256). This has been evidenced by decreased MAPK signaling in prostate epithelial cells, mouse embryonic fibroblasts, bovine endothelial cells, lung cancer cells, and breast cancer cells as a result of ephrinA1-Fc treatment (151, 167). In addition, decreased PI3K/AKT signaling following ephrinA1-Fc treatment has been observed in glioma cells (168) and decreased ABL/CRK signaling has been observed following ephrinB2 treatment in breast cancer (155). Evidence from our lab has also indicated that EPH RTK's tumor suppressive functions can be modulated by deletions or mutations in EPH receptors, as

demonstrated by loss-of-function mutations and the deleted focal locus 3p11.2 of EPHA3 in lung cancer (257). Others have also reported mutations that alter EPH RTK's tumor suppressive functions, such as an ephrin binding mutant (E53K) found in EPHA3 (258) and a kinase domain mutant (G787R) found in EPHB2 (259). Increased expression or activity of phosphotyrosine phosphatases such as LMW-PTP and PTPRO can also decrease EPH RTK signaling and transformation potential (144, 260).

EPH-based therapeutics in cancer

Despite the complexity of signaling properties of EPH RTKs, their role in tumor promotion has made them attractive targets for therapeutic intervention. A variety of strategies are being tested to target this family of receptors including agonistic monoclonal antibodies, soluble EPH and ephrin fusion proteins, inhibitors of EPH RTK expression, small molecule inhibitors, cytotoxic drug conjugates, and vaccine based immunotherapy. These novel therapeutics currently span a wide range of therapeutic development from early preclinical trials to phase III clinical trials.

Monoclonal antibodies

Due to the unique ligand mediated repression of EPH RTK signaling, agonistic monoclonal antibodies (mAb) were among the first therapeutics considered for use in targeting EPH RTKs (261). Mechanistically, these antibodies bind to their respective EPH RTK and induce receptor activation followed by receptor degradation (261). For EPHA2, two humanized mAb antibodies, 3F2-3M and 1C1-maleimidocaproyl-auristatin phenylalanine (mcMMAF) (MedImmune) (231, 262) were developed, the latter is conjugated to a potent tubulin polymerization inhibitor. Due to the overwhelming success of 1C1-mcMMAF in preclinical studies boasting limited toxicity and significant inhibition of tumor growth, it was promoted to phase I clinical trials (NCT00796055).

Unfortunately, due to drug related bleeding and coagulation complications the trial was discontinued (263). Additionally, mAbs against EPHB2 (2H9, Genetech) and EPHA3 (KB004, KaloBios Pharmaceuticals) have been developed for use in colon cancer and hematological malignancies, respectively (264). Phase I clinical trials are underway to test the safety and dosing of KB004.

Soluble EPH and ephrin fusion proteins, peptides, and siRNAs

Similar to mAb therapies, soluble EPH receptors and ephrin ligands have been suggested as possible therapeutics working as competitive agonists for the receptor-ligand complex. Preclinical studies have shown successful delivery of these soluble receptors and ligands as fusion constructs composed of segments of the EPH RTK or ephrin proteins fused to the Fc portion of a human immunoglobulin. EphrinB1-Fc and ephrinA1-Fc fusion proteins have been shown to inhibit proliferation of breast cancer (155, 253) and glioblastoma xenografts (265), respectively. It is possible that antibody-dependent cell-mediated cytotoxicity (ADCC) may be contributing to the success observed in vivo due to Fc fragment recognition from the immune system (266). In addition to peptide-Fc fusion fragments, antagonistic peptides have also been identified to inhibit EPH-ephrin engagement in both A and B classes (267-269).

Many reports using RNAi-mediated efforts to silence EPH RTK expression have shown dramatic inhibition of cell growth and survival in vitro although issues of RNA stability have directly limited the delivery of siRNAs against EPH RTKs in vivo. Promising studies using the neutral lipid 1,2-dioleoyl-sn-glycero-3-phosphatidylcholine (DOPC) to package siRNAs have demonstrated an ability to reduce tumor growth in vivo utilizing this strategy (238, 270).

Molecule	EPH-related Target	Inhibitor Class	Reference
Anilipyrimidine derivatives	EPHB4	Kinase inhibitor	(271, 272)
Benzenesulfonamide derivatives	EPHB4	Kinase inhibitor	(273)
XL-647	EPHB4	Kinase inhibitor	(274)
Xanthine derivative	EPHB4	Kinase inhibitor	(275, 276)
LDN-211904	EPHB3	Kinase inhibitor	(277)
Pyrido[2,3-d]pyrimidine PD173955	EPH RTKs	Kinase inhibitor	(278)
Nilotinib	EPHB1, EPHB2, and EPHB4	Kinase inhibitor	(279, 280)
Dasatinib	EPHA2, EPHB1, EPHB2, and EPHB4	Kinase inhibitor	(280-282)
JI-101	EPHB4	Kinase inhibitor	(283)
ALW-II-41-27	EPHA2	Kinase inhibitor	(153, 233)
Bosutinib	EPHB4 and EPHB1	Kinase inhibitor	(282)
Bafetinib	EPHA2, EPHA5, and EPHA8	Kinase inhibitor	(284)
NVP-BHG712	EPHB4	Kinase inhibitor	(285)
Liposomal siRNA delivery	EPHA2 and EPHB4	siRNA	(238, 256, 286-290)
Oligonucleotides	EPHA2 and EPHB4	Oligonucleotides	(287-291)
EPHA2-Fc and EPHA3-Fc	EphrinA	Soluble receptors	(248, 292-294)
sEPHB4	EphrinB	Soluble receptor	(295-297)
KYL, SNEW, or TNYL-RAW peptides	EPHA4, EPHB2, or EPHB4	Ephrin blocking peptide	(255, 268, 269, 298-301)
Dimethyl-pyrrole derivative	EPHA2 and EPHA4	Ephrin blocking compounds	(298, 302)
2H9 antagonistic mAb	EPHB2	Agonistic antibody	(264)
EA1.2, EA2, B233, 3F2-WT, EA5, Ab20, 1G9-H7, mAB208	EPHA2	Agonistic antibody	(261, 266, 303-306)
Dimerized IIIA4 mAb (KB004)	EPHA3	Agonistic antibody	(307)
EphrinA1-Fc	EPHA	Soluble ligand	(308)
EphrinB2-Fc	EPHB4	Soluble ligand	(254)
1C1 mAb-mc-MMAF conjugate	EPHA2	Cytotoxic conjugate	(262, 309)
bscEPHA2xCD3 mAb	EPHA2	Bispecific antibody	(310)
YSA modified adenovirus	EPHA2	Cytotoxic conjugate	(311)
EphrinA1-PE38QQR Pseudomonas exotoxin A	EPHA	Cytotoxic conjugate	(312)

conjugate			
EphrinA1 gold coated nanoshells	EPHA	Cytotoxic conjugate	(313)
2H9 mAB-vc-MMAE conjugate	EPHB2	Cytotoxic conjugate	(264)
EPHA2$_{833-891}$	EPHA2	Dendritic cell vaccine	(306)

Table 1.4 EPH receptor and ephrin ligand based therapeutics. Molecules in bold have been or are currently being evaluated in clinical trials (Adapted from (216)).

Small molecule inhibitors

A variety of small molecule inhibitors exist to inhibit EPH-ephrin binding and tyrosine kinase function (Table 1.4). The compounds 2,5-dimethylpyrrolyl benzoate (298), salicylate (314), lithocholic acid derivatives (315), and azurin (316) have been investigated for their abilities to inhibit EPH-ephrin interactions and reduce cell survival. Additionally, ATP-competitive small molecule multi-kinase inhibitors have been developed with potent EPH RTK inhibition of a spectrum of EPH RTKs (Table 1.4). XL-647, a second generation EGFR TKI inhibitor in phase III clinical trials (NCT0147174) and has been shown to inhibit ERBB2, VEGFR2, and EPHB4 (1.4nM) (274). Dasatinib, a SRC, BCR, ABL, PDGFR, KIT, EPHA2, EPHB1, EPHB2, and EPHB4 inhibitor, is in phase II clinical trials for advanced stage melanoma (280, 282, 317). Other TKIs with EPH-related inhibition include nilotinib (inhibits EPHB1, EPHB2, EPHB4) (280), bosutinib (inhibits EPHB4 and EPHB1) (282), bafetinib (inhibits EPHA2, EPHA5, EPHA8) (284), NVP-BHG712 (inhibits EPHB4) (285), and ALW-II-41-27 (inhibits EPHA2) (153).

Immunotherapy

Because of the prominent overexpression of various EPH RTKs on the surface of tumor cells, this family of receptors has been suggested as a candidate for vaccine based therapy. To date successful preclinical and phase I/II clinical trials

(NCT01876212) have demonstrated the utility of using dendritic cell vaccines loaded with EPHA2 and EPHB6 peptides to induce T cell activation and inhibit growth of glioma and renal cell carcinoma (318, 319). In addition to EPH targeted cancer vaccines, a bi-specific single-chain antibody construct has also been developed to simultaneously bind EPHA2 on tumor cells and CD3 on T cells (310).

EPHA2 receptor

EPHA2 was discovered in 1990 in a HeLa cell screen to identify novel proteins with tyrosine kinase activity, and it was originally called the epithelial cell kinase (ECK) due to its ubiquitous expression in epithelial cells (320). This transmembrane receptor tyrosine kinase is located on chromosome 1p36.1 and displays approximately 90% sequence conservation between mouse and human (321). In terms of size, it is 976 amino acids in length and has a molecular weight of approximately 130 kDa (322). High expression levels of EPHA2 can be observed in development, particularly in the distal region of the primitive streak, the hindbrain, the brachial arches, the ventricular zones, and also the developing bones (323). After development, EPHA2 expression is largely lost, although its expression is still maintained in tissues with proliferating epithelial cells such as the lung, ovaries, skin, and small intestines (320). Little is known about the functions of EPHA2 in non-malignant, adult tissues, but evidence from its role in malignancy indicate it as a key regulator of proliferation, survival, and migration.

EPHA2 expression in cancer

EPHA2 is overexpressed in a large number of cancer tissue types including breast (151, 235, 324), ovary (325, 326), prostate (327), pancreas (228, 328), brain (329-332), kidney (333), lung (225), melanoma (334), bladder (335), gastric (336), esophageal (229), colorectal (337), and cervix (338). In addition to being overexpressed

in many tumor tissues, the degree of EPHA2 overexpression has been observed to correlate with a tumor's aggressiveness and to the survival outcomes of patients. This was observed in a cohort of lung cancer patients (n=105). Patients that had high EPHA2 expression had a lower probability of cumulative survival, while patients with low EPHA2 expression had better survival outcomes (224) (Figure 1.9A). Similar results were seen when stratifying breast cancer patients based on EPHA2 expression using the Van de Vijver dataset (Figure 1.9B). It is therefore suggested that EPHA2 may serve as a prognostic marker for these two tumor types (211-214). In addition to prognosis, EPHA2 expression has been observed to positively correlate to increased angiogenesis and metastasis in a variety of cancer cell types. Specifically, this has been observed in HER2 driven breast cancer (149) as well as ovarian cancer (339), melanoma (334), and squamous cell carcinoma of the tongue (340).

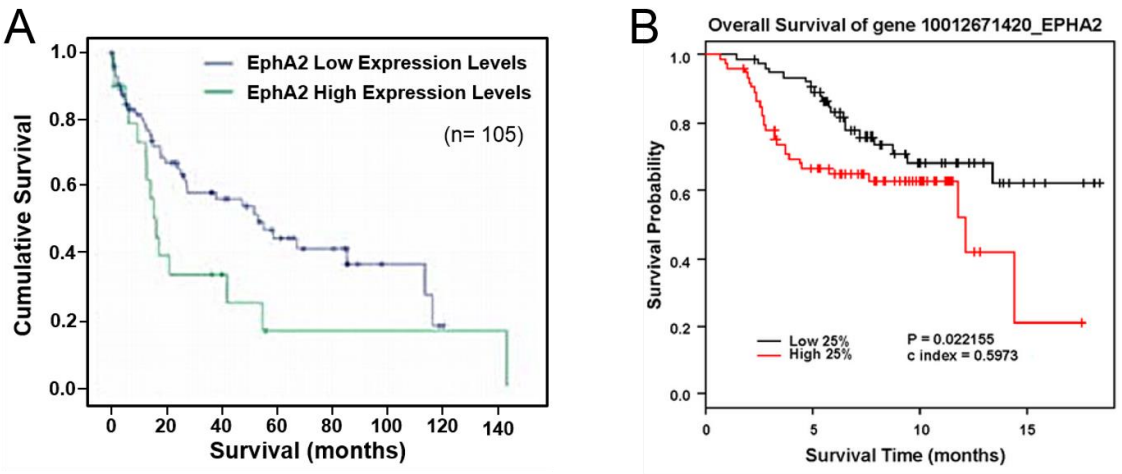

Figure 1.9 Survival analysis for EPHA2 expression in lung cancer and breast cancer. (A) Kaplan-Meier analysis of EPHA2 expression vs. survival with lung cancer patients stratified by EPHA2 expression levels, where low and high indicate expression relative to the mean (n=105) (Adapted from (224)). **(B)** Kaplan-Meier analysis of EPHA2 expression vs. survival in breast cancer (Van de Vijver dataset), where high EPHA2 expression was defined as tumors with the highest quartile of EPHA2 expression and low EPHA2 expression was defined as the lowest EPHA2 expressing quartile of tumors. Overall survival was defined as death due to any cause (n=295) (Adapted from (227)).

Overexpression of EPHA2 has been shown to be sufficient to transform cells, and it is the principle mechanism by which EPHA2 drives tumorigenesis (235). Although mutations in EPHA2 have been reported in cancer, they are rare in patient samples. EPHA2 has been found to be further overexpressed in tumor cells with resistance to molecularly targeted therapies (e.g. trastuzumab, vemurafenib, and erlotinib ((231, 233) and Figure 3.1D). EPHA2 has also been observed to be highly expressed in cancer stem-like cells both in malignant glioma and lung cancer (236, 265). In glioblastoma stem cell populations, EPHA2 was found to regulate both the cancer stem cell's ability to self-renew as well as their ability to be motile and invasive (265, 341). In lung cancer, EPHA2 expression was observed to positively correlate with the expression of the stem cell marker, aldehyde dehydrogenase (ALDH). In addition, EPHA2 expression was found to contribute to the formation of tumor spheroids in suspension and promote tumorigenicity in a limiting dilution xenograft model (236).

Regulation of EPHA2 expression

The molecular mechanisms which regulate EPHA2 expression in tumor cells are still not well understood. It is known, however, that EPHA2 is a transcriptional target of p53, EGFR, and RAS/MAPK pathway activation (147, 151, 342). EPHA2 expression levels are increased by the presence of p53, p63, or p73, which can bind to the p53 response element in the promoter region of EPHA2 to regulate its expression in addition to cell survival (342). Another transcription factor that has been found to regulate EPHA2 expression is C-MYC. Together with estrogen, MYC was observed to negatively regulate EPHA2 expression in breast cancer cells (343).

EPHA2 expression has also been observed to positively correlate to EGFR activation. Activation of EGFR by EGF was shown to increase both mRNA and protein expression of EPHA2 (147, 344). Conversely, treatment with an EGFR tyrosine kinase

inhibitor, was able to decrease EPHA2 expression after 2 hours in 1μM gefitinib or erlotinib (345). This regulation of expression was specific to EPHA2, as EGFR TKI treatment had no effect on the expression of other A class EPH family members, such as EPHA1, EPHA5, and EPHA6 (345). Additionally, recent work from our lab has demonstrated that cells with acquired resistance to erlotinib, demonstrate a time dependent increase in EPHA2 expression post removal of erlotinib from the culture medium (Figure 3.1E). Similarly, RAS transformed cells have been observed to have high levels of EPHA2 expression in vitro as well as in mouse models of HRAS mutant breast cancer and KRAS mutant lung cancer (153, 346). RAF activation has been found to positively regulate EPHA2 mRNA and protein expression, while MEK inhibition by the compound U0126 has been shown to conversely inhibit EPHA2 expression (151).

EPHA2 receptor signaling in cancer

EPHA2 shares a degree of signaling similarity to other A class EPH RTKs in its ability to propagate forward signaling in both a ligand dependent and a ligand independent fashion. EPHA2 preferentially binds to the ephrinA1 ligand, although it can also bind to ephrinA2, ephrinA4, and ephrinA5 at a lower affinity (163). Upon ligand binding the EPHA2-ephrinA1 complex can oligomerize and initiate an autophosphorylation event starting with two tyrosine residues (Y587 and Y593) in the juxtamembrane domain of the receptor. This is followed by activation of two additional tyrosine residues in the kinase domain (Y734 and Y771) (137). Following these phosphorylation events a number of adaptor and signaling effector proteins such as SHC, SHP2, and GRB2 can bind to EPHA2 via the phosphorylated tyrosine residues. VAV GEFs can bind to EPHA2 at sites Y587 and Y593, and PI3K can bind to EPHA2 directly at sites Y734 and Y771 (137, 145). Internalization and degradation of EPHA2 typically follow its ligand mediated activation (166). Of note, EPHA2 also signals in a

ligand independent fashion, which is often the case in the disordered epithelium of tumor cells exhibiting EPHA2 overexpression. In these instances, EPHA2 often mediates signaling through interaction with another RTK, as has been evidenced by direct interactions with EGFR and HER2 (147, 149).

It appears that EPHA2 is capable of inducing signals through multiple effector pathways, and although it is not clear what drives EPHA2's pathway preference in a given tumor, it is possible that ephrin expression, tissue type, microenvironmental factors, and mutation status may contribute to the pathway selection process. Similar to the ERBB family member, EGFR, EPHA2 has been observed to signal through the RAS/MAPK, PI3K/AKT/mTOR, and RAC/RHO pathways. In concert with its ability to control cellular proliferation, EPHA2 has been shown to control MAPK signaling as measured by phosphorylation of ERK1/2 in breast cancer (143, 149, 151), prostate cancer (167), and mesothelioma (347). Additionally, work from our lab has indicated alternative cellular survival signaling pathways for EPHA2 in lung cancer, including regulation of the PI3K/AKT/mTORC1 pathway culminating in phosphorylation and inactivation of the pro-apoptotic protein, BAD, (153) as well as regulation of the JNK/C-JUN pathway (236). In lung cancer, EPHA2 has also been observed to modulate phosphorylation of a downstream component of the MAPK pathway, p90-RSK (153), which has been observed to not only regulate transcription but also regulate components of the PI3K/mTORC1 signaling axis through phosphorylation of TSC2, S6, and BAD (348-351).

In promotion of a migratory and invasive phenotype, EPHA2 has also been observed to regulate RHOA and RAC1. Activation of RHOA by EPHA2 has been noted in the context of its interactions with FAK (157, 158) as well as the HER2 receptor (149). Ligand stimulation of EPHA2 was found to activate RAC1 contributing to EPHA2 receptor endocytosis in a PI3K dependent manner (352).

Pharmacological inhibition of EPHA2

Because of its prominent overexpression and oncogenic profile in a large range of tumors, efforts to pharmacologically inhibit EPHA2 have been attempted for many years. Due to the ligand mediated signaling repression displayed by EPHA2, agonistic monoclonal antibodies were among the first therapeutics tested. Among the antibodies developed, a fully humanized mAb from MedImmune, 1C1, was able to induce EPHA2 phosphorylation and degradation although it was not able to reduce cell viability (262). Subsequent efforts to use this antibody conjugated to a chemotherapeutic payload (1C1-mc-MMAF) blocked tumor growth in vivo, but unfortunately did not pass phase I clinical trials due to drug related toxicities (263). Other studies have assessed the therapeutic potential of treating tumors with liposomes bearing EPHA2 siRNAs (238). Additional studies have assessed the efficacy of treating tumors with an infusion of soluble ephrinA1 fused to an Fc portion of an immunoglobulin (ephrinA1-Fc) (308) to silence EPHA2 by inducing receptor internalization and degradation. Issues of RNA and protein stability have made these various methods difficult, although currently the use of liposome encapsulated EPHA2 siRNAs is in phase I clinical trials.

Additionally, small molecule tyrosine kinase inhibitors have been developed for EPHA2. Due to a high level of conservation of EPHA2's kinase domain with the kinase domains of other EPH family members as well as other receptor tyrosine kinases, specific inhibition of EPHA2 has been challenging. Dasatinib has demonstrated potent activity against EPHA2, although it is a pan-kinase inhibitor also inhibiting SRC, ABL, PDGFR, KIT, EPHB1, EPHB2, and EPHB4 (280, 282). Another pan-kinase inhibitor, bafetinib, was shown to inhibit EPHA2 in addition to ABL, LYN, EPHA5, and EPHA8 (284). More recently, a type II EPHA2 kinase inhibitor, ALW-II-41-27, was developed with ability to bind to both to the ATP binding region of the kinase domain and also a secondary allosteric location to increase specificity for EPHA2 (153). This drug has

been tested in *KRAS* and *EGFR* mutant lung cancer in vitro and in vivo, and it will be discussed further in Chapters 2 and 3.

Thesis projects

Although a significant amount of progress has been made in the molecular diagnosis and treatment of lung cancer, this disease still accounts for approximately 160,000 deaths per year in the United States. Due to innate and acquired resistance to therapeutics as well as the lack of therapeutics available for even the most commonly observed mutations in lung cancer (e.g. *KRAS*), it is essential to evaluate novel targets for therapeutic intervention. The EPH family of receptor tyrosine kinases has long been implicated in cancer with the EPHA2 receptor overexpressed in many different tumor types including the lung. While previous studies have provided correlative data linking high EPHA2 levels to poor clinical outcomes in human lung cancer populations, the biology underlying these observations and translational potential of these correlations remained underexplored. This dissertation set out to determine the functional and mechanistic role of EPHA2 in lung cancer, particularly in relation to different genetic subtypes of lung cancer. To this end we integrated genetically engineered mouse models, RNAi-mediated silencing techniques, characterization and implementation of a small molecule inhibitor, data mining of clinical specimens, and staining of lung cancer patient tissue to systematically investigate the function of EPHA2 in lung cancer. The thesis projects presented here include several significant findings. We demonstrated that EPHA2 promotes cellular survival in a large panel of lung cancer cell lines most notably in those harboring activating *KRAS* and $EGFR^{T790M}$ mutations. We provided the first functional evidence that EPHA2 promotes tumor growth in vivo as evidenced by human lung cancer xenografts as well as two independent transgenic mouse models of lung cancer, $Kras^{G12D}$ (LA2) and Tet-O-$EGFR^{L858R+T790M}$. Mechanistically, we identified

that S6K1-dependent BAD phosphorylation is a key signaling event mediating the EPHA2-regulated cell survival pathway in lung cancer. Furthermore, we identified a selective EPHA2 kinase inhibitor, ALW-II-41-27, that suppressed cell viability in vitro and reduced tumor growth of both *KRAS* and *EGFR*^{T790M} mutant lung cancer xenografts in vivo, demonstrating the translational potential of targeting EPHA2 in lung cancer.

CHAPTER II

GENETIC AND PHARMACOLOGIC INHIBITION OF EPHA2 PROMOTES APOPTOSIS IN NSCLC

The work presented in this chapter is published with the same title in the *Journal of Clinical Investigation*, May 2014 [Volume 124, Number 5].

Abstract

Genome-wide analyses determined previously that the receptor tyrosine kinase (RTK) EPHA2 is commonly overexpressed in non–small cell lung cancers (NSCLCs). EPHA2 overexpression is associated with poor clinical outcomes; therefore, EPHA2 may represent a promising therapeutic target for patients with NSCLC. In support of this hypothesis, here we have shown that targeted disruption of *EphA2* in a murine model of aggressive *Kras*-mutant NSCLC impairs tumor growth. Knockdown of *EPHA2* in human NSCLC cell lines reduced cell growth and viability, confirming the epithelial cell autonomous requirements for EPHA2 in NSCLCs. Targeting *EPHA2* in NSCLCs decreased S6K1-mediated phosphorylation of cell death agonist BAD and induced apoptosis. Induction of *EPHA2* knockdown within established NSCLC tumors in a subcutaneous murine model reduced tumor volume and induced tumor cell death. Furthermore, an ATP-competitive EPHA2 RTK inhibitor, ALW-II-41-27, reduced the number of viable NSCLC cells in a time-dependent and dose-dependent manner in vitro and induced tumor regression in human NSCLC xenografts in vivo. Collectively, these data demonstrate a role for EPHA2 in the maintenance and progression of NSCLCs and

provide evidence that ALW-II-41-27 effectively inhibits EPHA2-mediated tumor growth in preclinical models of NSCLC.

Introduction

Genome-wide expression analyses of human lung cancer have identified a number of receptor tyrosine kinases (RTKs) as overexpressed and potentially representing drivers of non–small cell lung cancer (NSCLC) (217, 353-355). Among these RTKs was EPHA2, which belongs to the largest family of RTKs, the EPH family. EPH family proteins have been recognized increasingly as key regulators of both normal development and disease (reviewed in refs (123, 124, 126)). EPH molecules contain a single transmembrane-spanning domain and distinct domains for ligand binding, receptor clustering, and signaling. Binding of EPH receptors to their ligands, known as EPHRINS, induces receptor clustering and activation. In addition to ligand-induced receptor activities, EPH receptors can also be activated by other cell-surface receptors, such as EGFR and ERBB2 (147, 149). Multiple intracellular signaling pathways have been linked to EPH receptors, including RAS/RAF/MAPK, PI3K/AKT/mTOR, SRC, FAK, ABL, and RHO/RAC/CDC42 (reviewed in refs. (123, 124, 126)). An oncogenic role for EPHA2 has been suggested due to its overexpression in lung cancer as well as the correlation of high levels of EPHA2 with smoking, brain metastasis, disease relapse, and overall poor patient survival (224-226). However, the biological and clinical relevance underlying these observations remains poorly understood.

Similar to what is seen in lung cancers, EPHA2 is overexpressed in a number of other cancers, including breast cancer. Preclinical models provide compelling evidence that EPHA2 overexpression increases breast tumor formation, malignant progression, and therapeutic resistance to antitumor therapies (149, 231). Large-scale expression profiling for EPHA2 transcript levels in relation to clinical outcome revealed a negative

association between *EPHA2* transcript levels and overall survival in breast cancer (227). These findings are consistent with preclinical studies in genetically engineered mouse models of breast cancer, which revealed distinct roles for EPHA2 in the tumor epithelia, in which EPHA2 signaling drives tumor cell proliferation and survival, and in the tumor microenvironment, in which EPHA2 is required for tumor angiogenesis (149, 157, 249). Thus, therapeutic inhibition of EPHA2 in breast cancers may provide a dual benefit to the patient, targeting both the tumor cells and the tumor microenvironment. The role of EPHA2 in lung tumor growth and/or angiogenesis is not yet clear.

In this study, we used a genetically engineered mouse model of NSCLC driven by mutant *Kras* to demonstrate that gene targeting of *EphA2* decreased growth and progression of spontaneous NSCLCs. We found that RNAi-mediated silencing of *EPHA2* inhibited the number of viable tumor cells in a panel of human NSCLC cell lines in vitro. Targeting *EPHA2* in KRAS mutant NSCLCs decreased S6K1-mediated BAD phosphorylation and induced apoptosis. Using human NSCLC xenografts, we found that inducible loss of *EPHA2* from preexisting tumor cells decreased tumor growth. Furthermore, an ATP-competitive, small-molecule tyrosine kinase inhibitor for EPHA2 decreased tumor cell viability in vitro and tumor growth in vivo. Collectively, these studies identify EPHA2 as a promising therapeutic target for NSCLCs.

Methods

Tumor studies in mutant *Kras* knockin mice

$Kras^{LA2}$ mice harboring the $Kras^{G12D}$ mutation (47) were provided by Ambra Pozzi (Vanderbilt University). $Kras^{LA2}$ mice were crossed with *EphA2* heterozygous mice (245) on the C57BL/6 background to generate $Kras^{G12D}EphA2^{+/+}$ and $Kras^{G12D}EphA2^{-/-}$ mice. Age-matched $Kras^{G12D}EphA2^{+/+}$ and $Kras^{G12D}EphA2^{-/-}$ littermates were sacrificed at 3 different time points: 15, 20, and 25 weeks of age. Genotypes were confirmed for each

animal in the study 2 independent times by analyzing genomic DNA of both tail and ear tissues, respectively. *EphA2* primers were 5′-GGGTGCCAAAGTAGAACTGCG-3′ (forward), 5′-GACAGAATAAAACGCACGGGTG-3′ (Neo), and 5′-TTCAGCCAAGCCTATGTAGAAAGC-3′ (reverse) (245). *Kras* primers were 5′-TGCACAGCTTAGTGAGACCC-3′ (common forward), 5′-GACTGCTCTCTTTCACCTCC-3′ (wild-type reverse), and 5′-GGAGCAAAGCTGCTATTGGC-3′ (mutant reverse). Lungs removed for analysis were first perfused with 1× PBS followed by 10% buffered formalin (Fisher). Lungs were weighed after 24 hours of fixation in formalin. Lung tumor surface area was calculated by measuring a length (l) and width (w) of each surface tumor nodule and using the area calculation $([l + w]/4)^2 \times \pi$.

MRI

Mice were anesthetized via inhalation of 2%:98% isoflurane:oxygen. Animals were secured in a prone position in a 38-mm inner diameter radiofrequency coil and placed in a Varian 7T horizontal bore imaging system (Varian Inc.) for data collection. For each animal, multi-slice scout images were collected in all 3 imaging planes (axial, sagittal, and coronal) for subsequent localization of the lungs, using a gradient echo sequence with repetition time = 75 ms, echo time = 4 ms, slice thickness = 2 mm, flip angle = 30°, and an average of 4 acquisitions. Additional parameters include field of view = 32 mm × 32 mm and data matrix = 128 × 128. Following localization of the lungs, a respiratory-triggered T2-weighted fast-spin echo imaging sequence was used to acquire image slices in the axial plane, with field of view = 25.6 mm × 25.6 mm, slice thickness = 1 mm, repetition time = 2 seconds, effective echo time = 36 ms, data matrix = 256 × 256, and an average of 16 acquisitions, with a total acquisition time of approximately 25 minutes per animal. Following image acquisition, lung tumor volume measurements were performed using Matlab 2012a (The MathWorks Inc.). A region of

interest encompassing the entire lung was manually drawn for each slice, and a signal intensity threshold of 25 times the noise level (defined as the standard deviation of signal intensities in a region of the image background) was used to segment voxels within that region of interest as positive for tumor. Total lung tumor volume was then calculated as the sum of the number of voxels within the segmented tumor region multiplied by the volume of each voxel.

Immunohistochemistry

Whole lungs and tumors were harvested at the indicated time points and fixed in 10% buffered formalin (Fisher). Immunohistochemical staining for EPHA2 and PCNA was performed as described previously (248). A proliferation index was calculated as the average percentage of PCNA+ nuclei relative to total nuclei (4 fields of at least 5 tumors per genotype or treatment condition were assessed). Apoptosis assays were performed using the Apoptag Red In Situ Apoptosis Detection Kit per the manufacturer's protocol (Millipore). An apoptosis index was measured as the percentage of TUNEL+ nuclei relative to total nuclei (4 fields of at least 5 independent tumors per genotype or treatment condition were assessed). Immunofluorescence staining for vWF was performed as described previously (249). Tumor vessel density was determined by assessing the vWF+ vessels (pixels) in 4 fields per sample of at least 5 independent tumors per genotype or treatment condition. Antibodies against the following proteins were used: EPHA2 (Invitrogen; 347400), PCNA (BD Biosciences), vWF (Dako Cytomation), biotin goat anti-rabbit (BD Pharmingen), and anti-rabbit Cy3 (Jackson ImmunoResearch). Additionally, retrievagen A (pH 6.0) (BD Pharmingen, 550524), streptavidin peroxidase reagents (BD Pharmingen, 51-75477E), and the liquid 3,3′-diaminobenzidine tetrahydrochloride substrate kit (Zymed Laboratories) were used.

Cytoseal XYL (Richard Allan Scientific) or ProLong Gold antifade reagent with DAPI (Life Technologies) were used to mount slides.

Cell culture

The human NSCLC lines were provided by David Carbone, William Pao, and Pierre Massion (Vanderbilt University). 293T cells were purchased from the ATCC. All NSCLC cells were maintained in RPMI 1640 medium (Corning/Cellgro) supplemented with L-glutamine (2 mM), penicillin (100 U/ml), streptomycin (100 µg/ml), and 10% fetal bovine serum (Thermo Scientific, HyClone Laboratories Inc.). 293T cells were maintained in DMEM (Corning/Cellgro) supplemented with L-glutamine (2 mM), penicillin (100 U/ml), streptomycin (100 µg/ml), and 10% fetal bovine serum (Thermo Scientific, HyClone Laboratories Inc.). Authenticity of the cells was verified by DNA profiling, flow cytometry, or immunohistochemistry. Cells were grown in a humidified incubator with 5% CO_2 at 37°C. Stable cell lines generated with the pLKO.1 and pTRIPZ vectors were maintained in 1 to 2 µg/ml of puromycin containing complete media. For cells transduced with the pTRIPZ vector, production of shRNA was initiated with addition of 1 µg/ml DOX (Sigma-Aldrich) to the media, which was refreshed every 3 days. *EPHA2* ON-TARGETplus Human SMARTpool siRNA (L-003116-00-0005) and ON-TARGETplus Non-Targeting pool siRNA (D-001810-10-05) (Dharmacon/Thermo Scientific) were used at a concentration of 12.5 nM in conjunction with Lipofectamine RNAiMAX transfection reagent (Invitrogen) according to the manufacturer's protocol. Stable *EPHA2* knockdown cells lines were created by lentiviral transduction of a pLKO.1 vector containing *EPHA2*-specific shRNA constructs (sh*EPHA2* no. 1 mature sense 5′-CGGACAGACATATAGGATATT-3′ or sh*EPHA2* no. 2 mature sense 5′-GCGTATCTTCATTGAGCTCAA-3′). Plasmids were obtained from Open Biosystems.

Inducible sh*EPHA2* (5′-AAGGAGACTTTCAACCTCT-3′) and scrambled control plasmid constructs (pTRIPZ) from Open Biosystems were also used.

Cell viability assays

MTT assay. Cells were seeded in 100 µl media in 96-well plates at a density of 4,000 cells per well. On the final day of the assay, 20 µl of 5 mg/ml of thiazolyl blue tetrazolium bromide (MTT) (Sigma-Aldrich) in PBS was added and incubated at 37°C for 2 hours. The MTT solution was aspirated, and an isopropanol solution with 4 mM HCl and 0.1% Nonidet P-40 was added and incubated at room temperature for 10 minutes. The absorbance was read on a spectrophotometer (BioTEK) at 590 nm. All experimental points were set up with at least 6 replicates and were performed at least 2 independent times. Cell viability was presented as a percentage of cells transduced with an empty vector, transfected with scrambled siRNA, or treated with a vehicle alone.

Cell death ELISA. Cells were seeded along with RNAiMAX transfection reagent and appropriate siRNAs (12.5 nM final concentration). At 72 hours after transfection, cells were washed once with PBS and lysed as per the manufacturer's instructions (Cell Death Detection ELISA PLUS kit, Roche). Detection of histone-associated DNA fragments in the lysate was measured using biotin labeled anti-histone and peroxidase-conjugated anti-DNA antibodies. Signal was detected upon the addition of the peroxidase substrate ABTS, and the absorbance was measured at 405 nm wavelength.

TUNEL assay. TUNEL was used to assess apoptosis. Cells were seeded on 8-well chamber slides (Lab-Tek), and the Apoptag Red In Situ Apoptosis Detection Kit (Millipore) was used according the manufacturer's instructions. Four representative images were taken of the TUNEL staining, with corresponding DAPI staining, and the

number of TUNEL-positive nuclei relative to total nuclei per image was counted and calculated. Data are representative of at least 2 independent experiments.

Antibodies and immunoblotting

Antibodies against the following proteins were used: EPHA2 (D7, mouse monoclonal, 1:1,000, Millipore); phospho-tyrosine pY20 and pY99 (mouse monoclonal, 1:1,000, Santa Cruz Biotechnology); β-tubulin (mouse monoclonal, 1:2,000, Sigma-Aldrich); p-AKT (S473 and T308), AKT, p-ERK (T202/Y204), ERK, p-P90RSK (S380), RSK, p-S6K1 (T389), S6K1, p-S6 (S235/6), S6, p-BAD (S112), BAD (all rabbit monoclonal, 1:1,000, Cell Signaling Technology); cleaved caspase-3, caspase-3, and cleaved PARP (all rabbit, 1:500, Cell Signaling Technology). HRP-conjugated anti-mouse and anti-rabbit antibodies were used, respectively. For immunoblotting, cells were washed with 1x PBS and lysed on ice with RIPA buffer supplemented with a protease inhibitor cocktail (P8340) (Sigma-Aldrich) and phosphatase inhibitors (Roche Diagnostics). Lysates were subjected to SDS/PAGE followed by blotting with the indicated antibodies. Signal detection was achieved using Clarity Western ECL substrate (Bio-Rad).

Tumor xenograft

H358 cells (15×10^6 cells) containing a DOX-inducible scrambled or *EPHA2* knockdown sequence (pTRIPZ) were injected with Matrigel into opposing hind flanks of 6-week-old athymic nude mice ($Foxn1^{nu}$) (Harlan). When tumors reached approximately 150–250 mm^3, animals were randomized to receive either a DOX-containing diet (TD.00426, Harlan) or a standard mouse diet. Tumors were measured every 2 days using digital calipers. Volumes were calculated using the following formula: volume = length × $width^2$ × 0.52.

For inhibitor studies, 15×10^6 H358 cells were injected with Matrigel into the hind flanks of 6-week-old athymic nude mice ($Foxn1^{nu}$) (Harlan). Once tumors reached 150–250 mm^3, animals received either 15 mg/kg (Figure 2.11A) or 30 mg/kg (Figure 2.11I) of ALW-II-41-27 or NG-25 in 10% 1-methyl-2-pyrrolidinone and 90% PEG 300 or the vehicle alone. Mice were treated 2 times daily via intraperitoneal injection, and tumors were measured daily with digital calipers. Volumes were calculated using the following formula: volume = length × $width^2$ × 0.52.

Kinase inhibitor screen and analysis of drug-target interaction in vivo

ALW-II-41-27 and NG-25 were synthesized in the lab of Nathanael Gray. The inhibitors were dissolved in DMSO for all in vitro studies. In situ drug-target interaction in tumor xenografts was analyzed by a chemical proteomics platform, KiNativ, at ActivX Inc., as described previously (356, 357). Tumor lysate was incubated with ATP-biotin labeled probes to assess which kinases received protection from the drug binding via MS analysis. Based on the resulting data set, parent ions corresponding to each kinase were selected for targeting and were assembled into a time-segmented target list using the instrument control software XCalibur 2.2. All MS data were analyzed using custom software that was designed to extract and normalize signals from relevant probe-labeled peptides. Signals were normalized based on the average signal ratios of major parent ions throughout the run. For signal extraction/quantitation, typically up to 4 ions were selected based on their presence, intensity, and correlation to the reference MS/MS spectrum. The resulting chromatographic peaks from each run were then integrated, and the integrated peak areas were used to determine percent inhibition values relative to control runs. Enzymatic IC_{50} data in Supplemental Table 2 were generated by in vitro kinase assays that were conducted at Life Technologies using the SelectScreen Kinase Profiling Service.

Statistics

For animal studies, linear mixed models were used to estimate the effects of treatment and genotype on tumor volume change over time and to account for potential correlation of within subject measurement. Possible values of the variable are from round 1 or round 2 of the duplicated experiment. In addition to estimated effect sizes and information criteria, P values for fixed-effects terms were calculated for a better understanding of findings by performing a likelihood ratio test for each term and model. These analyses were performed using R 2.15.1. For other studies, 2-tailed Student's t test was used for comparisons between 2 groups, and ANOVA or Kruskal-Wallis tests were used for analysis with multiple comparisons. All tests of statistical significance were 2 sided, and P values of less than 0.05 were considered to be statistically significant.

Study approval

All animal experiments were conducted under guidelines approved by the AAALAC and Vanderbilt University Institutional Animal Care and Use Committee.

Results

EphA2 promotes tumor growth in a transgenic mouse model of spontaneous NSCLC.

Under physiological conditions, *EphA2*-deficient mice produced by gene targeting are viable, fertile, and healthy. However, previous studies demonstrated that *EphA2* loss decreases growth of transgenic mouse mammary tumors and decreases tumor angiogenesis (149, 249). We therefore used the *EphA2*-deficient mouse model to determine whether EPHA2 is required in a transgenic mouse model of NSCLC, encoding a latent $Kras^{G12D}$ allele knocked in at the endogenous *Kras* locus (47). In this model, lung cancers driven by the active mutant $Kras^{G12D}$ develop spontaneously within the innate tissue microenvironment, recapitulating human lung cancer pathology. To assess tumor burden in $Kras^{G12D}EphA2^{+/+}$ and $Kras^{G12D}EphA2^{-/-}$ mice, we measured total lung wet weight over a time course. We found that $Kras^{G12D}$ tumor-bearing lungs were heavier than tumor-free lungs lacking $Kras^{G12D}$ expression (Figure 2.1A), suggesting that lung weight correlates with tumor burden. A reduction in lung wet weight was observed in $Kras^{G12D}EphA2^{-/-}$ mice compared with that in $Kras^{G12D}EphA2^{+/+}$ controls. Importantly, tumor-free lungs harvested from $EphA2^{-/-}$ mice were similar in weight to those harvested from tumor-free $EphA2^{+/+}$ mice, indicating that the decreased lung weight seen in $Kras^{G12D}EphA2^{-/-}$ mice was due to reduced tumor burden. It is possible, however, that lung weight could be altered as a result of changes in interstitial fluid volume in the lung because of the known role of EPHA2 in angiogenesis. To distinguish between these possibilities, tumor burden was assessed by two additional methods. First, we measured the area of tumors on the surface of lungs harvested at 3 time points (Figure 2.1B), demonstrating a decreased burden of surface lung tumors in $Kras^{G12D}EphA2^{-/-}$ mice compared with that in $Kras^{G12D}EphA2^{+/+}$ mice. Additionally, lung cancer progression in

Kras^{G12D}*EphA2*$^{+/+}$ and *Kras*^{G12D}*EphA2*$^{-/-}$ mice was monitored using MRI, beginning at 15 weeks of age, when tumors were evident in both groups of mice (Figure 2.1C). *Kras*^{G12D}*EphA2*$^{-/-}$ lung tumors were smaller than tumors in *Kras*^{G12D}*EphA2*$^{+/+}$ mice at 15 weeks of age, and this difference became more pronounced at 20 and 25 weeks of age (Figure 2.1D).

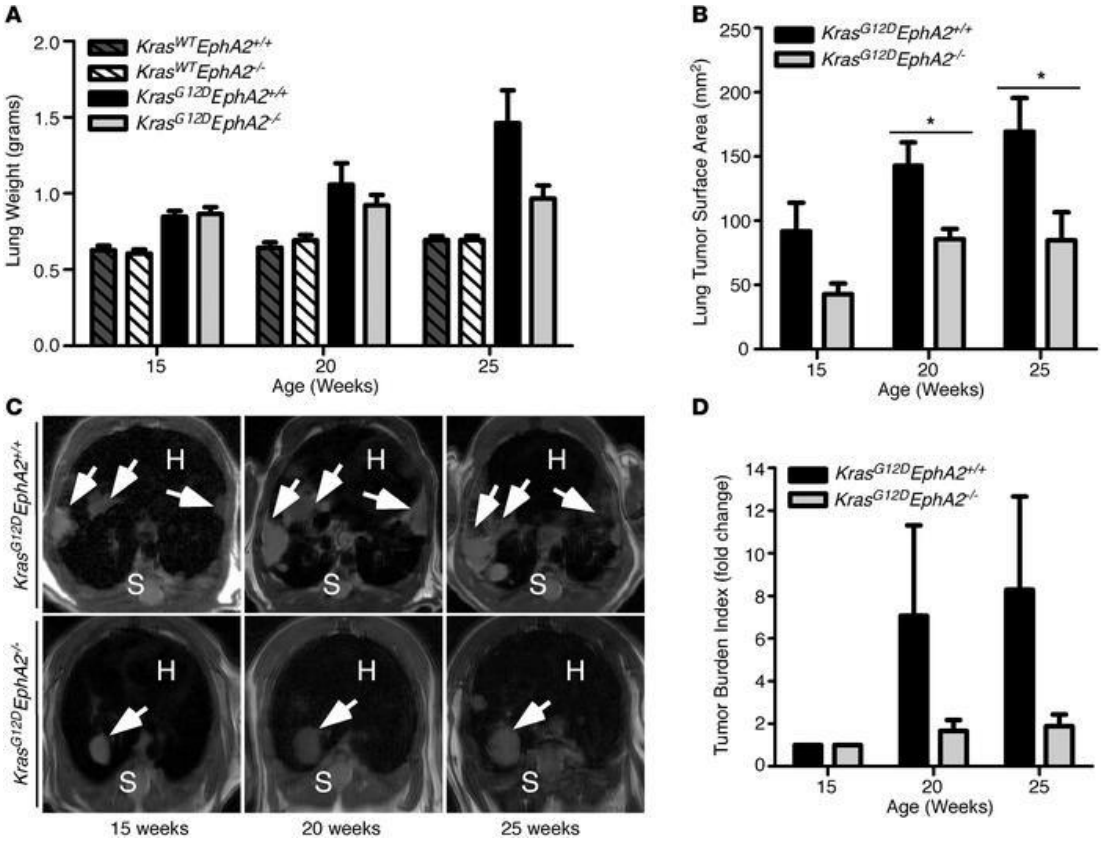

Figure 2.1 Loss of *EphA2* results in decreased tumor burden in a *Kras*^{G12D} knockin mouse model of spontaneous NSCLC. (A) Lungs of wild-type and *EphA2*-deficient mice were collected, and the total lung weight was measured at 15, 20, and 25 weeks of age to assess the additional mass contributed to the lungs by the tumor burden. Average lung weight ± SEM is shown (n = 10 per genotype). **(B)** Tumor area on the lung surface was measured by a digital caliper and presented as average lung tumor surface area ± SEM (n = 8 per genotype). **(C)** Wild-type and *EphA2*-deficient *Kras*^{G12D} mice were subjected to MRI at 15, 20, 25 weeks of age. T2-weighted MRI images were taken in the axial plane with slice thickness of 1 mm. Representative images at 15, 20, and 25 weeks are shown. White arrows indicate tumor tissue. H, heart; S, spine. **(D)** Tumor volumes were quantified as a composite of 10 serial MRI slices of the lung per mouse using Matlab software and were graphed as a tumor burden index relative to 15 weeks ± SEM (n = 5 per genotype). *P < 0.05.

Histological *analysis* of the lungs demonstrated the presence of tumors in both *Kras*^{G12D}*EphA2*$^{+/+}$ and *Kras*^{G12D}*EphA2*$^{-/-}$ mice and the absence of EPHA2 expression in *EphA2*-knockout mice (Figure 2.3, A and B, and Figure 2.2A). Tumors were less frequent and smaller in size in *Kras*^{G12D}*EphA2*$^{-/-}$ mice compared with those in *Kras*^{G12D}*EphA2*$^{+/+}$ mice. Tumor cell apoptosis, as measured by TUNEL staining, was significantly higher in *Kras*^{G12D}*EphA2*$^{-/-}$ tumors compared with that in *Kras*^{G12D}*EphA2*$^{+/+}$ tumors (Figure 2.3, C and D), whereas tumor cell proliferation, as measured by PCNA immunohistochemistry, was unchanged in *Kras*^{G12D}*EphA2*$^{-/-}$ tumors (Figure 2.3, E and

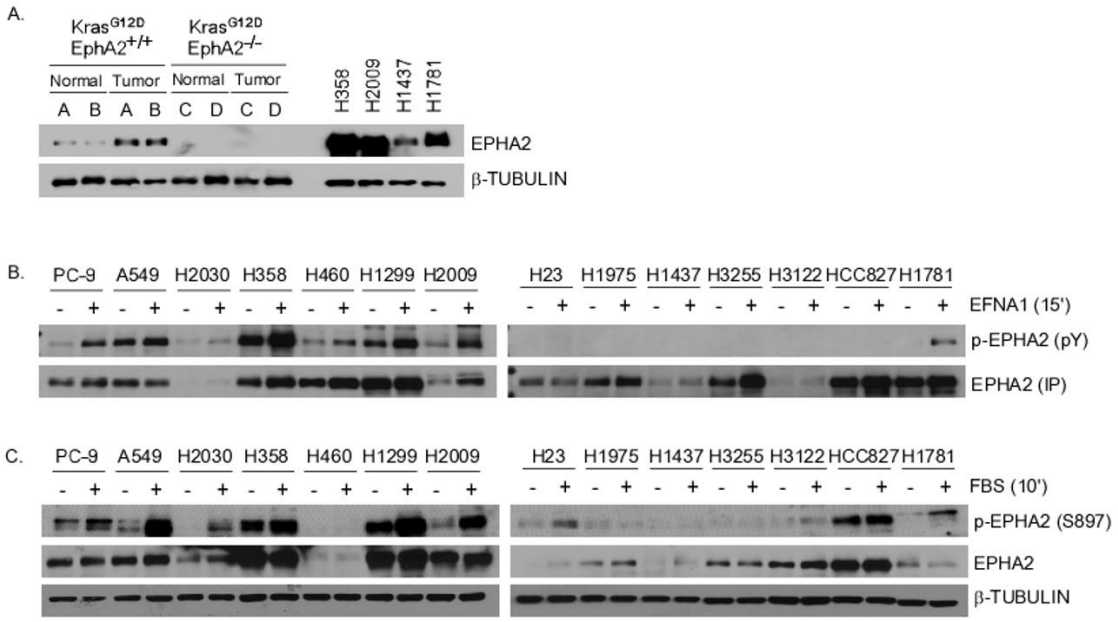

Figure 2.2 EPHA2 expression and activity in NSCLC. (A) EPHA2 expression was assessed in the lung tissue of a mutant *Kras* model of NSCLC by western blot analysis of paired tumor and normal lung tissue. Two representative mice were used per condition (*Kras*^{G12D}*EphA2*$^{+/+}$, A and B, and *Kras*^{G12D}*EphA2*$^{-/-}$, C and D). EPHA2 expression levels in mouse tumors were compared with those in human NSCLC lines. **(B)** Cells were serum starved overnight and stimulated with EPHRIN-A1 (EFNA1,100ng/mL) for 15 minutes before lysis. EPHA2 was immunoprecipitated, followed by immunoblotting for phospho-tyrosine (pY). **(C)** Total cell lysates of cells starved and stimulated with 10% FBS were probed for phosphorylated EPHA2 (S897). Relative levels of EPHA2 expression across the various cell lines are shown. β-TUBULIN expression was used as a loading control.

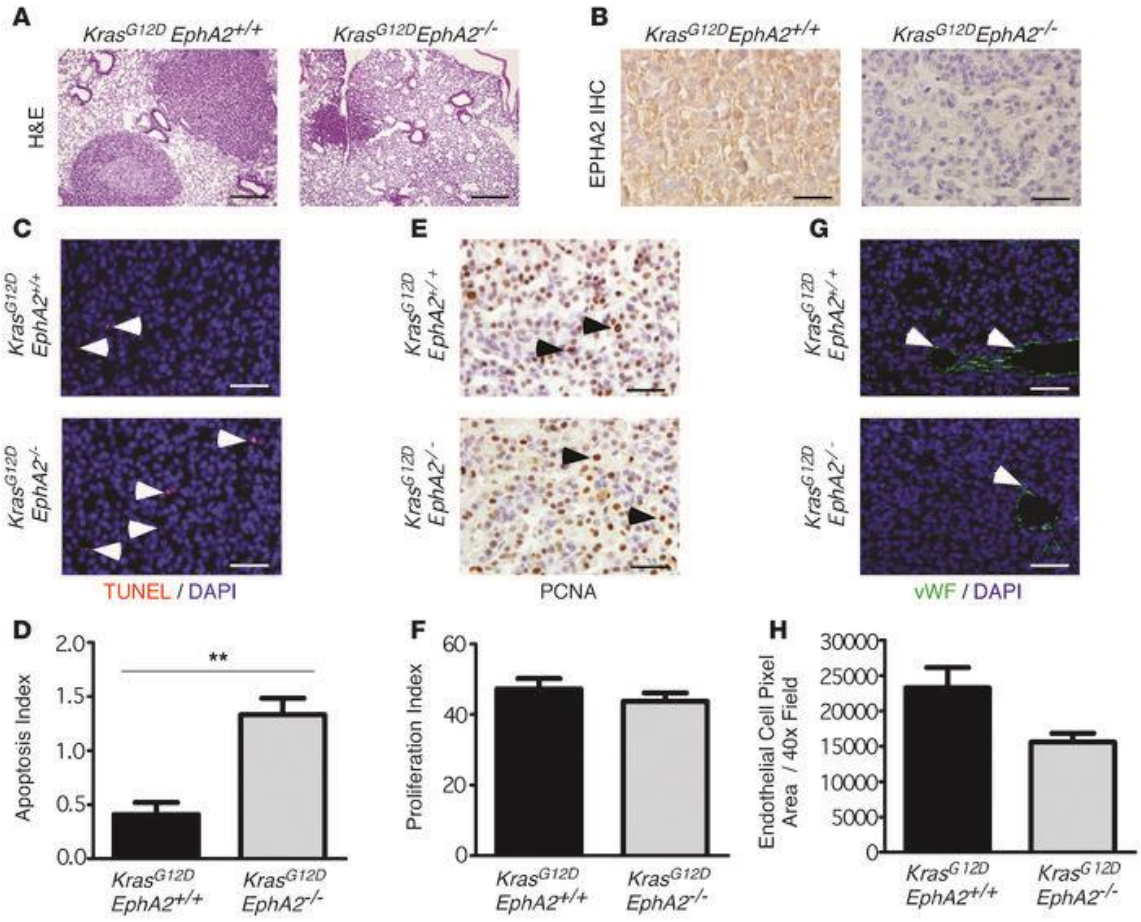

Figure 2.3 *EphA2* deficiency results in increased apoptosis in *Kras^{G12D}* tumors. (A) H&E-stained lung sections (25 weeks) showing tumors derived from *Kras^{G12D}EphA2$^{-/-}$* mice relative to those derived from *Kras^{G12D}EphA2$^{+/+}$* mice. Scale bar: 200 μm. **(B)** Loss of EPHA2 protein expression in tumors was confirmed by immunohistochemistry (IHC). Scale bar: 50 μm. **(C)** Apoptosis in tumor sections was measured by the TUNEL assay. TUNEL+ nuclei (red) are indicated with arrowheads. Scale bar: 50 μm. **(D)** Apoptosis was quantified as a percentage of TUNEL-positive nuclei relative to the total nuclei. Apoptosis index is presented as average percentage of TUNEL-positive nuclei per total nuclei ± SEM (n = 6 per genotype). **(E)** Tumor cell proliferation was assessed by PCNA immunohistochemistry. Arrowheads indicate representative proliferating nuclei. Scale bar: 50 μm. **(F)** Proliferation was quantified by assessing the total number of PCNA+ nuclei (brown) compared with the total nuclei. Proliferation index is presented as average percentage of PCNA-positive nuclei per total nuclei ± SEM (n = 6 per genotype). **(G)** Tumor vasculature was assessed by vWF immunofluorescence (green). Arrowheads indicate tumor microvessels. Scale bar: 50 μm. (H) Microvessels in the tumor were quantified by measuring vWF+ pixels in each tumor field ± SEM (P = 0.07) (n = 6 per genotype). **P < 0.01.

F). Because EPHA2 is known to promote tumor angiogenesis in breast cancer models (249), we assessed tumor microvessels in situ using immunofluorescence detection of vWF to visualize endothelial cells. These studies revealed a modest decrease in vWF-positive tumor vessels in *Kras*^{G12D}*EphA2*$^{-/-}$ tumors compared with that in *Kras*^{G12D}*EphA2*$^{+/+}$ tumors (Figure 2.3, G and H). Collectively, these results show that EPHA2 promotes progression of NSCLCs within their native microenvironment, such that genetic ablation of *EphA2* limited progression of this aggressive NSCLC tumor model.

Epithelial EPHA2 is required to maintain viable NSCLC cells.

EPHA2 is overexpressed across all major histological subtypes of human NSCLC, and this overexpression is associated with poor clinical outcomes (224-226). Using a lentiviral-based shRNA strategy to silence *EPHA2* expression in a panel of 14 human NSCLC cell lines (Table 2.1), we assessed the number of viable cells in culture 3 days after plating in media supplemented with 10% serum (Figure 2.4A). In 8 of 14 cell lines tested, *EphA2* shRNA (sh*EphA2*) reduced the number of viable tumor cells by more than 25% compared with cells treated with control shRNA (sh*Control*). Of these 8 NSCLC cell lines, 6 harbored activating *KRAS* mutations, 1 harbored an activating *NRAS* mutation, and 1 harbored an oncogenic *EGFR* mutation, highlighting EPHA2 as a potential therapeutic target across several NSCLC genetic subtypes, even the difficult-to-treat *KRAS* subtype. Western blot analysis performed in parallel with the MTT assays showed a substantial loss of EPHA2 protein expression in sh*EPHA2*-infected cells (Figure 2.4B). By 5 days after plating, sh*EPHA2*-infected cells that showed initial sensitivity to *EPHA2* inhibition demonstrated a further reduction in the number of viable tumor cells, with decreases ranging from 50% to 80% compared with that in sh*Control*-infected cells (Figure 2.4C, top 6 graphs).

Cell Line	*KRAS*	*EGFR*	Other Mutations
A549	G12S		
H2009	G12A		
H2030	G12C		
H23	G12C		
H358	G12C		
H460	Q61H		
H1975		L858R; T790M	
H3255		L858R	
HCC827		Δ 19	
PC-9		Δ 19	
H1299			*NRAS*
H1437			*MEK1*
H1781			*HER2*
H3122			*EML4-ALK*

Table 2.1. Lung cancer cell lines with respective driver mutations.

Cell lines most sensitive to *EPHA2* inhibition demonstrated higher EPHA2 receptor phosphorylation upon stimulation with either EPHRIN-A1 or serum (Figure 2.2, B and C), suggesting that EPHA2 receptor activity drives an increase in viable NSCLC cells. While these data do not rule out the contribution of EPHA2 in the NSCLC microenvironment, this observation supports the hypothesis that targeting EPHA2 may be a feasible therapeutic approach for NSCLCs with heightened EPHA2 phosphorylation.

EPHA2 increases NSCLC tumor cell survival.

To determine whether EPHA2 is required for NSCLC cellular survival, we assessed apoptosis in cells transfected with *EPHA2* siRNA (si*EPHA2*) sequences compared to that in those transfected with scrambled siRNA sequences. At 3 days after transfection, EPHA2 expression was reduced in the 6 cell lines transfected with si*EPHA2* as compared with that in those transfected with a scrambled siRNA sequence (Figure 2.5D and data not shown). Increased frequency of tumor cell death was observed in all 6 NSCLC cell lines transfected with si*EPHA2*, as measured by TUNEL analysis (Figure 4A) and cleavage of caspase-3 and PARP (Figure 2.5B). These results were confirmed using a cell death ELISA to detect histone-associated DNA fragmentation (Figure 2.5C), again revealing that si*EPHA2* increased apoptosis in each of the 6 cell lines. At the same time point, we collected cell lysates from serum-starved H2009 and H358, 2 cell lines with high EPHA2 receptor phosphorylation levels. Signaling studies in these cells revealed decreased basal phosphorylation levels of S6 kinase and its substrate ribosomal protein S6 (Figure 2.5D), while many pathways, including AKT and ERK, were not significantly affected by EPHA2 loss in the absence of serum. EPHA2-deficient cells stimulated for 10 minutes with 10% serum showed no alteration in the phosphorylation of ERK. However, serum-induced phosphorylation of p90-RSK, and AKT at a lesser extent, was reduced in si*EPHA2* cells, suggesting that EPHA2 is required to stimulate acute growth factor signaling from p90-RSK to S6 kinase and S6. Phosphorylation of the pro-apoptotic BH3-only protein BAD, which results in BAD inhibition and tumor cell survival, is another target of the p90-RSK/S6 kinase signaling pathway (358, 359). Interestingly, loss of *EPHA2* in si*EPHA2*-transfected cells caused a decreased level of BAD phosphorylation in serum-stimulated conditions, consistent with the increased levels of cell death seen in si*EPHA2*-transfected cells. Together, these data indicate that

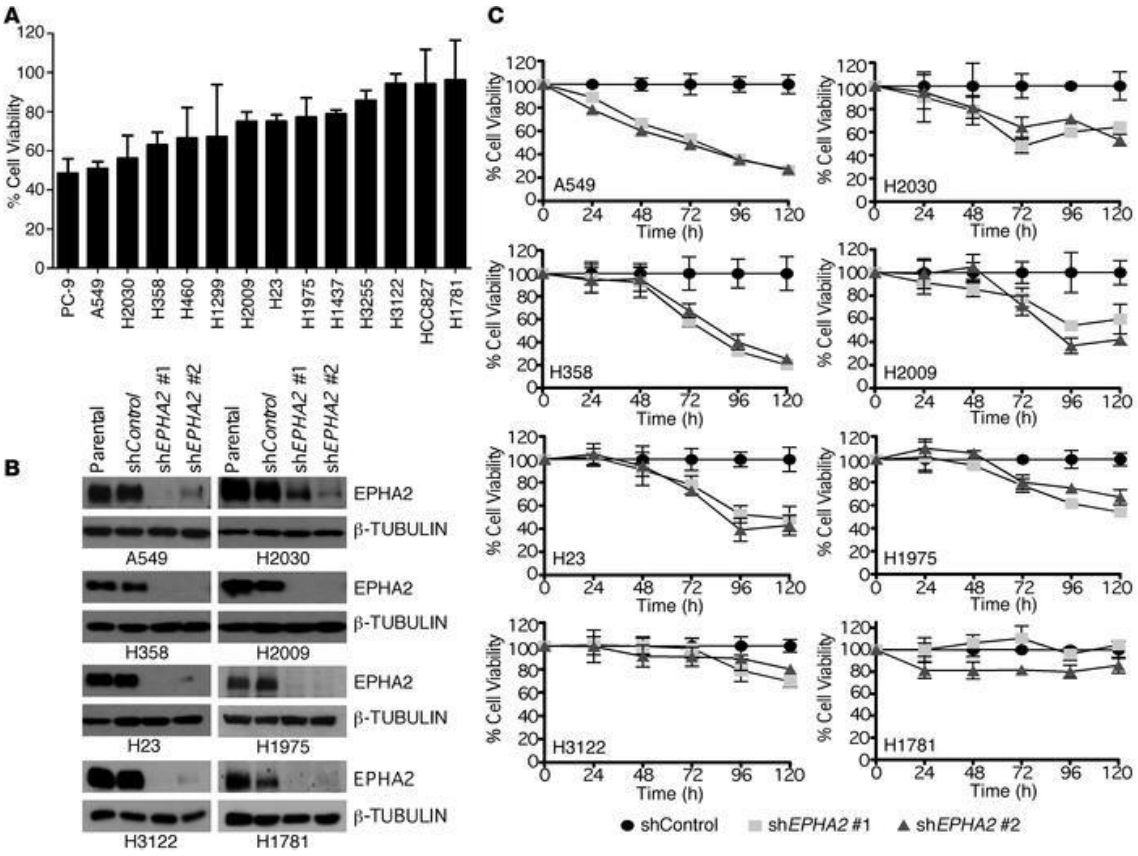

Figure 2.4 Effects of knockdown of *EPHA2* on a panel of NSCLC cell lines. (A) 14 NSCLC cell lines were transduced with lentiviruses containing either sh*EPHA2* or a pLKO.1 vector control. The resulting cell populations were selected in 1 to 2 μg/ml puromycin for 5 days. Cell viability was analyzed by the MTT assay at 72 hours after puromycin selection. Experiments were repeated twice with 6 replicates per experiment. Data were pooled and are presented as viability of sh*EPHA2* knockdown cells relative to that of the vector control cells ± SEM. **(B)** Immunoblotting for EPHA2 expression confirmed knockdown in 8 NSCLC cell lines. β-Tubulin expression was used as a loading control. **(C)** Cells were treated as in A, and cell viability was assessed over 5 days. Experiments were repeated twice, and data were pooled and are presented as shRNA knockdown relative to the vector control cells ± SEM.

EPHA2 signaling is required within the tumor epithelial compartment of NSCLCs to maintain tumor cell survival.

EPHA2 knockdown in the tumor epithelial compartment decreases NSCLC growth in vivo.

To assess the therapeutic potential of targeting EPHA2 in the context of pre-existing NSCLC tumors, we transduced H358 cells with a lentivirus encoding doxycycline-inducible (DOX-inducible) shRNA sequences against *EPHA2* or a scrambled control sequence. DOX treatment of H358-sh*EPHA2* cells in culture resulted in decreased EPHA2 protein expression compared with that in untreated H358-sh*EPHA2* cells and DOX-treated H358-sh*SCRAMBLED* cells (Figure 2.6A). Similar to what was seen with stable shRNA-mediated *EPHA2* knockdown, DOX-induced knockdown of *EPHA2* decreased the number of viable cells by 70% of the number seen in untreated H358-sh*EPHA2* cells or DOX-treated H358-sh*SCRAMBLED* controls after 9 days in culture (Figure 2.6B). H358-sh*EPHA2* and H358-sh*SCRAMBLED* cells were injected into the left and right flanks of each mouse, respectively, to generate matched pairs of subcutaneous tumor xenografts. Once the tumor volume reached 200 mm^3, DOX was delivered in the mouse chow ad libitum. DOX-treated H358-sh*EPHA2* tumor growth was significantly inhibited compared with what was seen in DOX-treated H358-sh*SCRAMBLED* xenografts (Figure 2.6C), resulting in a 30% decrease in tumor volume after 35 days of DOX treatment ($P < 0.0001$). Western blot analysis using tumor lysates derived at the end of the study revealed a persistent decrease of EPHA2 protein levels in DOX-treated tumors (Figure 2.6D). Similar to previous data, a significant increase of apoptosis was observed in DOX-treated H358-sh*EPHA2* cells compared with that in untreated H358-sh*EPHA2* cells and DOX-treated H358-sh*SCRAMBLED* cells (Figure 2.6, E and F). PCNA immunohistochemical analysis of tumor sections indicated no

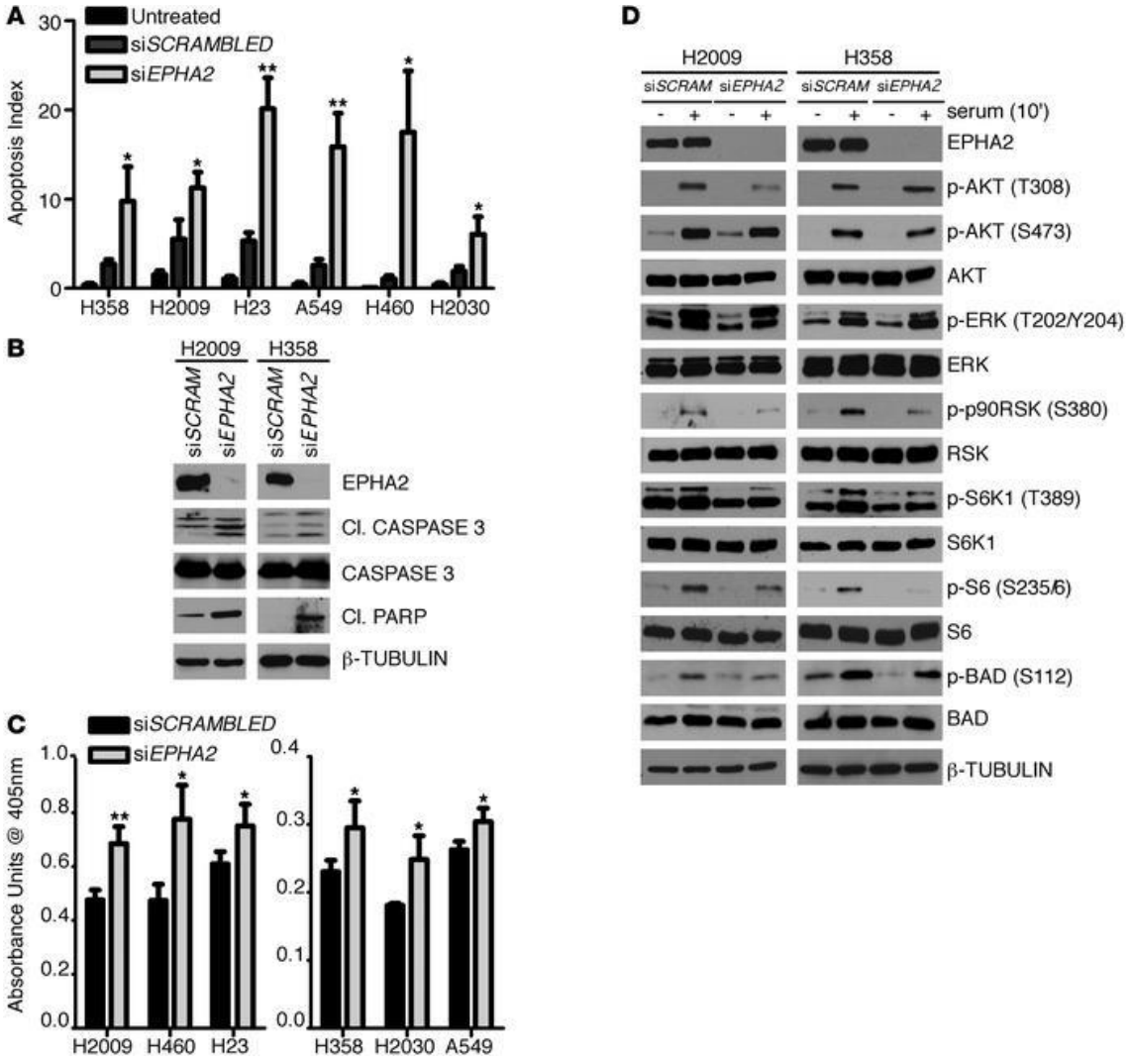

Figure 2.5 *EPHA2* knockdown leads to an increase in apoptosis in NSCLC cell lines. **(A)** Cells were treated with scrambled or *EPHA2*-specific siRNA for 72 hours. Apoptosis was detected via the ApopTag TUNEL assay. Graph represents 3 independent experiments, and data are presented as the percentage of TUNEL-positive nuclei of total nuclei ± SEM. **(B)** Western blotting of H2009 and H358 cells treated with scrambled or si*EPHA2* for 72 hours with 5 μg/ml TRAIL added during the final 24 hours after transfection. Cl. cleaved (caspase-3 or PARP). **(C)** Apoptosis was measured by quantifying histone-associated DNA fragments using a Cell Death ELISA Kit. Cells were treated with scrambled or si*EPHA2* for 72 hours before the assay. All 6 cell lines exhibited a statistically significant increase in apoptosis in the cells treated with si*EPHA2* compared with the scrambled controls. Experiments were repeated 3 times, and data are presented as average absorbance unit (AU) ± SEM. **(D)** H2009 and H358 cells were treated with scrambled or si*EPHA2* for 72 hours. Cells were starved for 24 hours and stimulated with 10% serum for 10 minutes before lysis. Shown are representative immunoblots in which phosphorylation levels of signaling molecules were detected using anti-phospho antibodies and EPHA2 expression was detected by an anti-EPHA2 antibody. *P < 0.05, **P < 0.01.

change in the proliferation of H358-sh*EPHA2* cells relative to H358-sh*SCRAMBLED* cells (Figure 2.6, G and H). No statistically significant change was observed in tumor blood vessels in any of the treatment conditions (Figure 2.6, I and J). These results demonstrate that inhibition of EPHA2 within the established tumor epithelium is capable of decreasing growth of NSCLCs in vivo.

An EPHA2 kinase inhibitor suppresses growth of NSCLC in vitro and in vivo.

We tested more than 50 small molecules predicted to inhibit EPHA2 tyrosine kinase activity, revealing that the compound ALW-II-41-27 had the most potent effect on tumor cell viability (data not shown). ALW-II-41-27 is a type II small-molecule inhibitor that targets the ATP-binding pocket of the kinase domain as well as an allosteric site next to the “DFG” motif in the receptor (refs (279, 360) and Figure 2.7A). A compound with similar structure, NG-25 (361), was used as a control, because it possessed a very similar profile of kinase targets as that of ALW-II-41-27, with EPHA2 being a notable exception. ALW-II-41-27 inhibits EPHA2 with an enzymatic IC_{50} of 11 nM compared with an IC_{50} of 770 nM for NG-25, as measured by an in vitro kinase assay (Table 2.2). In lung cancer cells, 1 μM ALW-II-41-27 impaired tyrosine phosphorylation of the EPHA2 receptor in H358 cells within 15 minutes and continued to inhibit EPHA2 tyrosine phosphorylation through 6 hours of treatment (Figure 2.7B). In contrast, NG-25 showed no effect on EPHA2 phosphorylation at the same concentration. ALW-II-41-27 also inhibited ligand-induced EPHA2 phosphorylation in a dose-dependent manner (Figure 2.7C). Furthermore, depletion of *EPHA2* by RNAi rendered NSCLC cell lines much less sensitive to the effects of ALW-II-41-27 relative to undepleted controls, consistent with EPHA2 being a functionally important target of the compound (Figure 2.7, D and E).

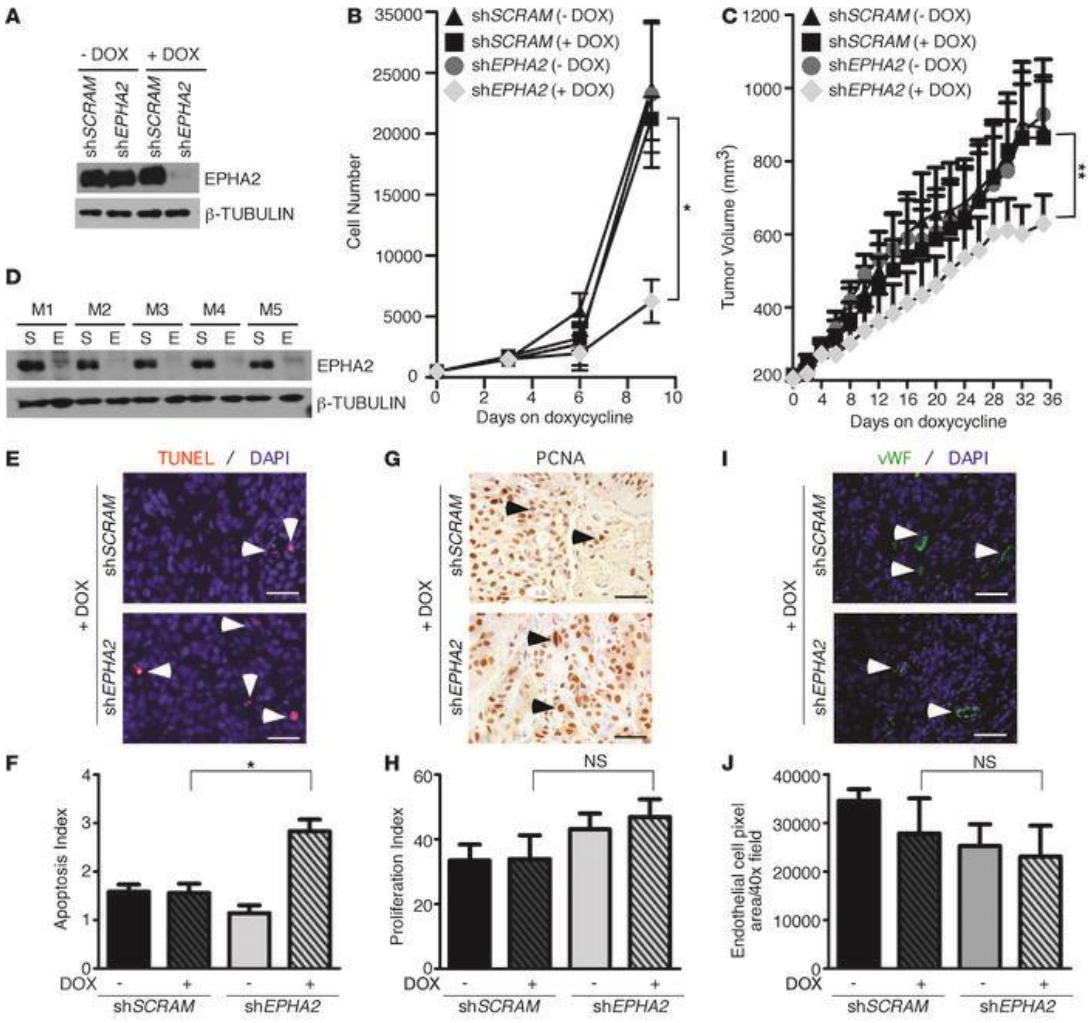

Figure 2.6 Inducible knockdown of *EPHA2* reduces cell viability in vitro and mitigates tumor growth in vivo. (A and B) Cells were transduced with lentiviruses carrying either DOX-inducible sh*EPHA2* or scrambled shRNA (sh*SCRAM*). **(A)** Cells were treated with 1 μg/ml DOX for 9 days. Expression of EPHA2 was determined by immunoblotting, and **(B)** cell viability was determined by enumerating live cells over a time course. Shown are average cell numbers ± SEM. **(C)** H358 cells containing DOX-inducible *EPHA2* or scrambled shRNA were injected into the left or right flank in the same nude mouse subcutaneously. Tumors were allowed to grow to 200 mm^3 before administering DOX-containing food pellets or regular mouse chow. Data are presented as the mean tumor volumes ± SEM (n = 5 per group). Differences among the 4 treatment groups were analyzed statistically using linear mixed model fit by REML. **(D)** Loss of EPHA2 expression was confirmed in mice fed DOX via immunoblotting of whole tumor lysates harvested at the end of experiment. S, sh*Scrambled*; E, sh*EPHA2*. **(E and F)** Apoptosis was determined by TUNEL staining. Apoptosis index is presented as average percentage TUNEL+ nuclei (arrowheads) per total nuclei ± SEM (n = 5 tumors per condition). **(G and H)** Proliferation was measured by PCNA staining. Proliferation index is presented as the average percentage of PCNA+ nuclei (arrowheads) per total nuclei ± SEM (n = 5 tumors per condition). **(I and J)** Tumor vasculature was quantified and presented as the mean of vWF+ pixels (arrowheads) per section ± SEM. (n = 5 tumors per condition). Scale bar: 50 μm. *P < 0.05, **P < 0.01. n.s., not significant.

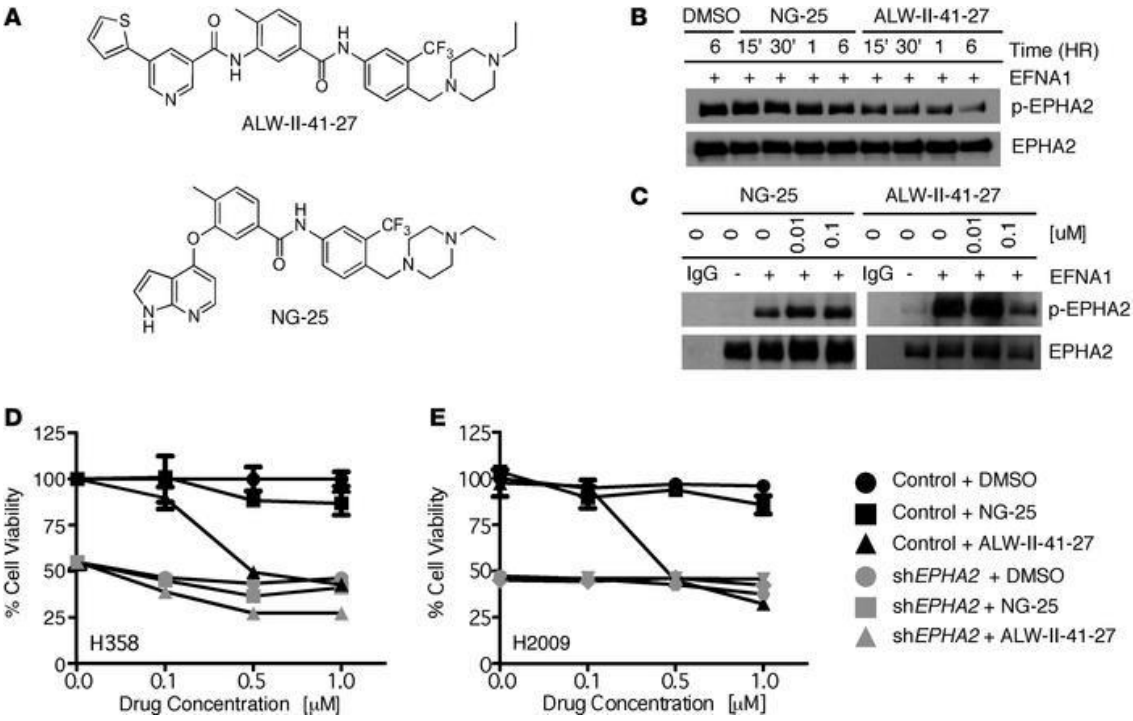

Figure 2.7 Structure and properties of ALW-II-41-27, a small-molecule kinase inhibitor of EPHA2. (A) Chemical structures for ALW-II-41-27 and its structural analog, NG-25. **(B)** H358 cells were treated with 1 μM NG-25 or ALW-II-41-27 over a time course, and cells were stimulated with EPHRIN-A1 ligand (EFNA1, 100 ng/ml) for the last 15 minutes of treatment. EPHA2 was immunoprecipitated, and tyrosine phosphorylation of EPHA2 was determined by Western blot analysis. **(C)** Dose-dependent effect of ALW-II-41-27 on EPHA2 phosphorylation. Cells were treated with inhibitors for 72 hours, including a 15-minute stimulation with EFNA1 at the end of the incubation. Tyrosine phosphorylation of EPHA2 was determined as in B. **(D and E)** H358 or H2009 cells transduced with lentiviruses containing an empty vector or an EPHA2-specific shRNA were treated with ALW-II-41-27, NG-25, or DMSO, and the percentage of viable cells was assessed at 72 hours via the MTT assay. Cells with wild-type levels of *EPHA2* exhibited a marked loss of cell viability in the presence of ALW-II-41-27, while *EPHA2* knockdown cells displayed minimal decrease in cell viability upon ALW-II-41-27 treatment. Data are presented as average percent of cell viability ± SEM.

Next, we assessed cell viability in NSCLC cells treated with ALW-II-41-27. H358 cells treated over a 72-hour time course with 1 μM ALW-II-41-27 displayed a time-dependent decrease in the number of viable tumor cells compared with cells treated with 1 μM NG-25 (Figure 2.8A). Five additional NSCLC lines were also tested, and a 40%–80% reduction in the number of viable tumor cells after 72 hours in the presence of 1 μM ALW-II-41-27 as compared with treatment with 1 μM NG-25 was observed (Figure 2.9A, top 6 graphs). Two cell lines (H3122 and H1781) that were resistant to EPHA2 knockdown were also less sensitive to ALW-II-41-27. Cell death was increased in response to ALW-II-41-27 in H358 cells (Figure 2.8B), suggesting that pharmacologic EPHA2 inhibitors reproduce the effects obtained using genetic methods of EPHA2 inhibition and may be therapeutically advantageous in the treatment of NSCLC. To assess the intracellular consequences of targeting EPHA2 by ALW-II-41-27, cell lysates were collected from serum-starved H2009 and H358 cells treated with ALW-II-41-27 or DMSO for 6 hours. Western signaling analysis revealed decreases in both the basal and serum-stimulated phosphorylation of S6K1, S6, and BAD (Figure 2.9B), which is similar to the results seen in *EPHA2* knockdown experiments. These data suggest that ALW-II-41-27 inhibits EPHA2 signaling pathways necessary to maintain cell survival in NSCLC.

To assess the efficacy of the EPHA2 inhibitor in vivo, we treated 200 mm^3 H358 xenograft tumors with ALW-II-41-27, NG-25, or the vehicle alone. Initial pharmacokinetic analysis of ALW-II-41-27 following intravenous (1 mg/kg) and oral administration (10 mg/kg) revealed a relatively short half-life ($t_{1/2}$ = 0.83 hour), low plasma exposure (AUC = 333.7 nM/l), and low oral bioavailability (bioavailability = 24.6%). To compensate for this poor pharmacokinetic profile, mice were treated twice daily with 15 mg/kg ALW-II-41-27 via intraperitoneal injection.

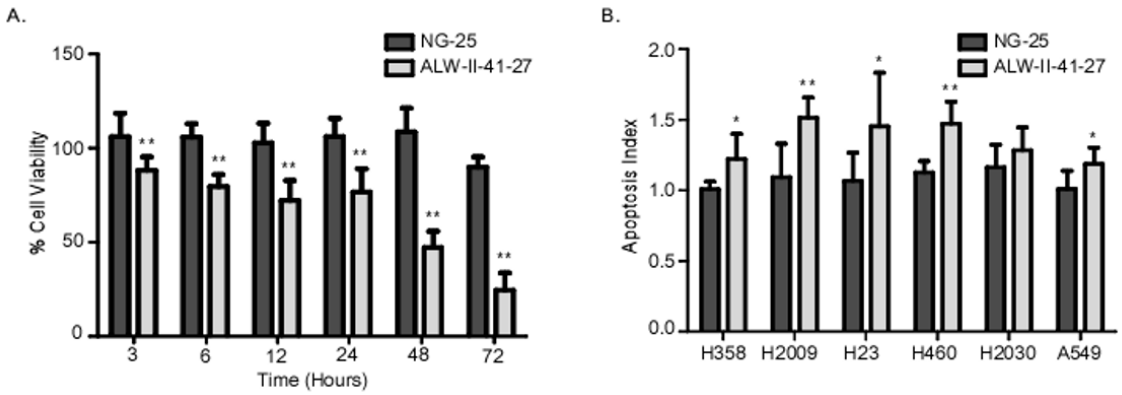

Figure 2.8. ALW-II-41-27 inhibits cell viability and promotes apoptosis. (A) H358 cells were treated with 1μM NG-25 or ALW-II-41-27 over a time course and cell viability was determined via the MTT assay. Experiments were repeated three times and data are presented as the percentage of viable cells after NG-25 or ALW-II-41-27 treatment relative to DMSO treatment + SEM. **(B)** Cells were treated with 1μM of indicated drug for 6 hours, and apoptosis was assessed by quantifying the histone associated DNA fragments via a cell death ELISA Kit (Roche). Data was normalized to respective DMSO controls. * $p<0.05$, ** $p<0.01$.

Administration of ALW-II-41-27 to tumor-bearing animals for 14 days significantly inhibited tumor growth of H358 tumors (Figure 2.11A). Toxicity was assessed by weighing the mice daily and by histopathologic examination of vital organs (hearts, kidneys, and livers) at the end of the studies. Mice treated with ALW-II-41-27 did not experience significant weight loss during the course of the study, and no significant histopathologic differences were seen in the heart, liver, or kidney tissue among the various treatment groups (Figure 2.10 and Figure 2.11B).

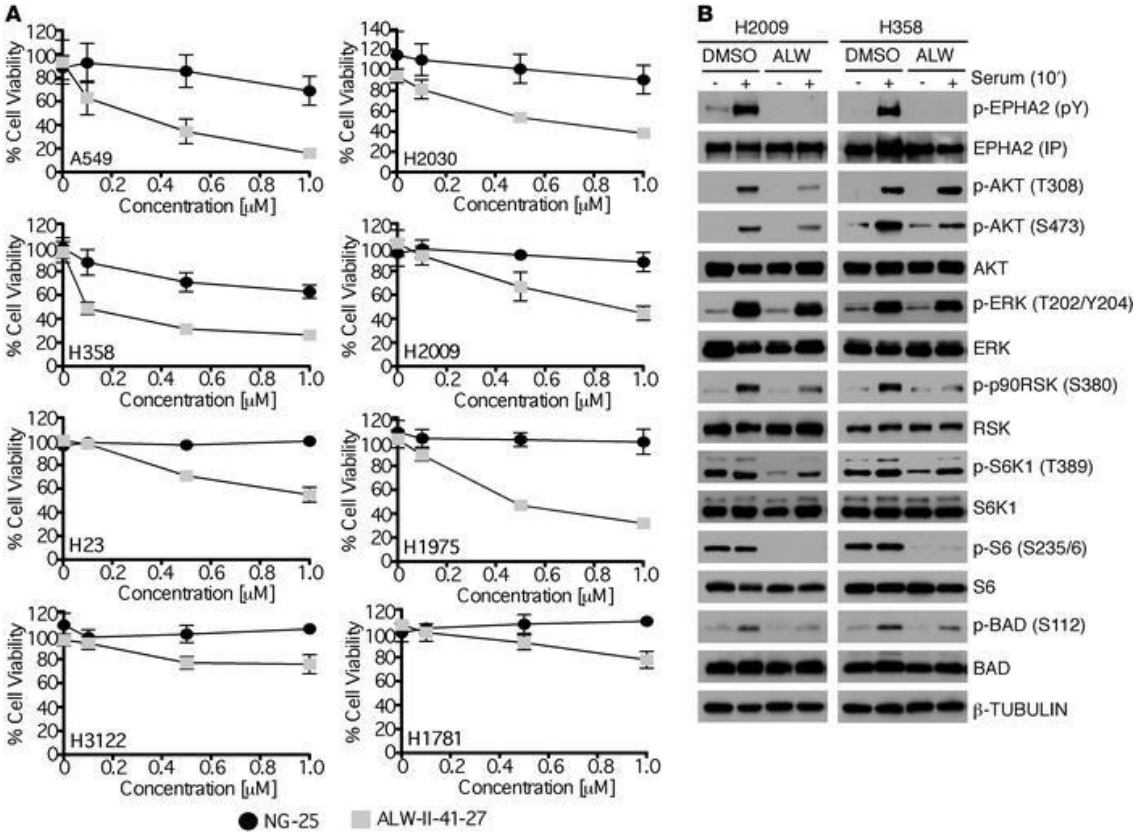

Figure 2.9 ALW-II-41-27 treatment leads to decreased cell viability in NSCLC cell lines. (A) NSCLC cell lines were treated with ALW-II-41-27, NG-25, or DMSO for 72 hours, and cell viability was assessed by the MTT assay. Shown are percentages of cell viability ± SEM in drug treatment groups relative to a DMSO control group. **(B)** H2009 and H358 cells were treated with 1 μM ALW-II-41-27 or DMSO for 6 hours. Cells were starved 24 hours and stimulated with 10% serum-containing media 10 minutes before lysis. EPHA2 was pulled down in immunoprecipitation and immunoblotted for pY99 and pY20 (represented here as p-EPHA2 [pY]). Phosphorylation of other signaling molecules was determined by Western blot analyses using anti-phospho or anti-total protein antibodies as indicated. Shown are blots representative of 2 to 3 independent experiments for each signaling molecule.

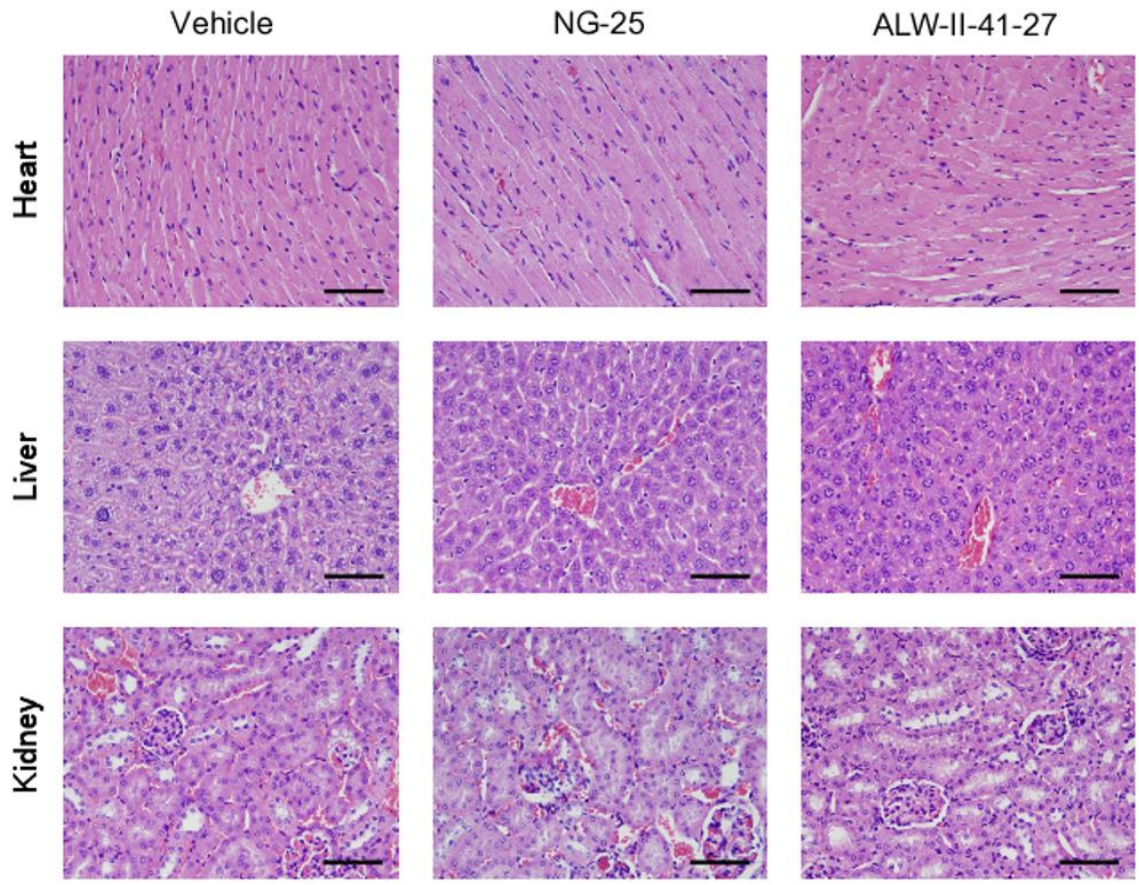

Figure 2.10. Histopathologic analysis of vital organs in mice treated with ALW-II-41-27, NG-25, or the vehicle. H358 cells were engrafted in nude mice and treated with 15mg/kg of ALW-II-41-27, NG-25, or the vehicle twice daily for 14 days, as in Figure 2.11A. Heart, liver, and kidney were harvested at the end of studies and tissue sections were stained with H&E. Scale bars indicate 100 µm.

Histological analysis of tumors treated with ALW-II-41-27 showed a significant increase in apoptosis compared with tumors treated with NG-25 or the vehicle alone (Figure 2.11, C and D), similar to what was seen upon genetic ablation of EPHA2. No significant differences were observed in proliferation or tumor vessel density in ALW-II-41-27–treated tumors compared with NG-25– or vehicle-treated tumors, as measured by PCNA and vWF staining, respectively (Figure 2.11, E–H). Remarkably, administration of an increased dose of ALW-II-41-27 (30 mg/kg) to tumor-bearing animals resulted in

tumor regression (Figure 2.11I), although some toxicity was observed at this concentration. These data suggest that efforts in further development of EPHA2 inhibitors should focus on increasing efficacy and selectivity while preventing off-target side effects.

To investigate the drug-tumor interaction in vivo, tumors from drug-treated animals were analyzed for an interaction between ALW-II-41-27 and EPHA2 in situ using the chemical proteomics platform, KiNativ (356), wherein the extent to which a biotinylated ATP probe covalently binds to the kinase's ATP-binding pocket is measured by mass spectrometry (MS). These studies revealed that the majority of the ATP probe (>95%) was unable to bind EPHA2 in tumors from mice treated with 30 mg/kg ALW-II-41-27, suggesting that the majority of the EPHA2 receptor located on the tumor cells was bound by the EPHA2 inhibitor in vivo. In contrast, other EPH family receptors, such as EPHB2 and EPHB3, retained the ATP probes, leaving 52% and 45% of the ATP probe unbound, thus confirming specificity of ALW-II-41-27 for EPHA2 above other EPH family RTKs. Additionally, ALW-II-41-27 had a low affinity in vivo for other kinases, such as EGFR, ERK, HER2, and PIK3CA (Figure 2.11J and Table 2.2).

ALW-II-41-27 can potently bind to several intracellular kinases, including ABL, p38, ZAK, and several SRC-family kinases, but these targets were also engaged by the structural analog, NG-25, which did not inhibit tumor growth in vivo (Table 2.2). Collectively, EPHA2 is the most dramatically distinct target engaged by ALW-II-41-27 as compared with NG-25, which is consistent with EPHA2 being a functionally important target of ALW-II-41-27 in NSCLC.

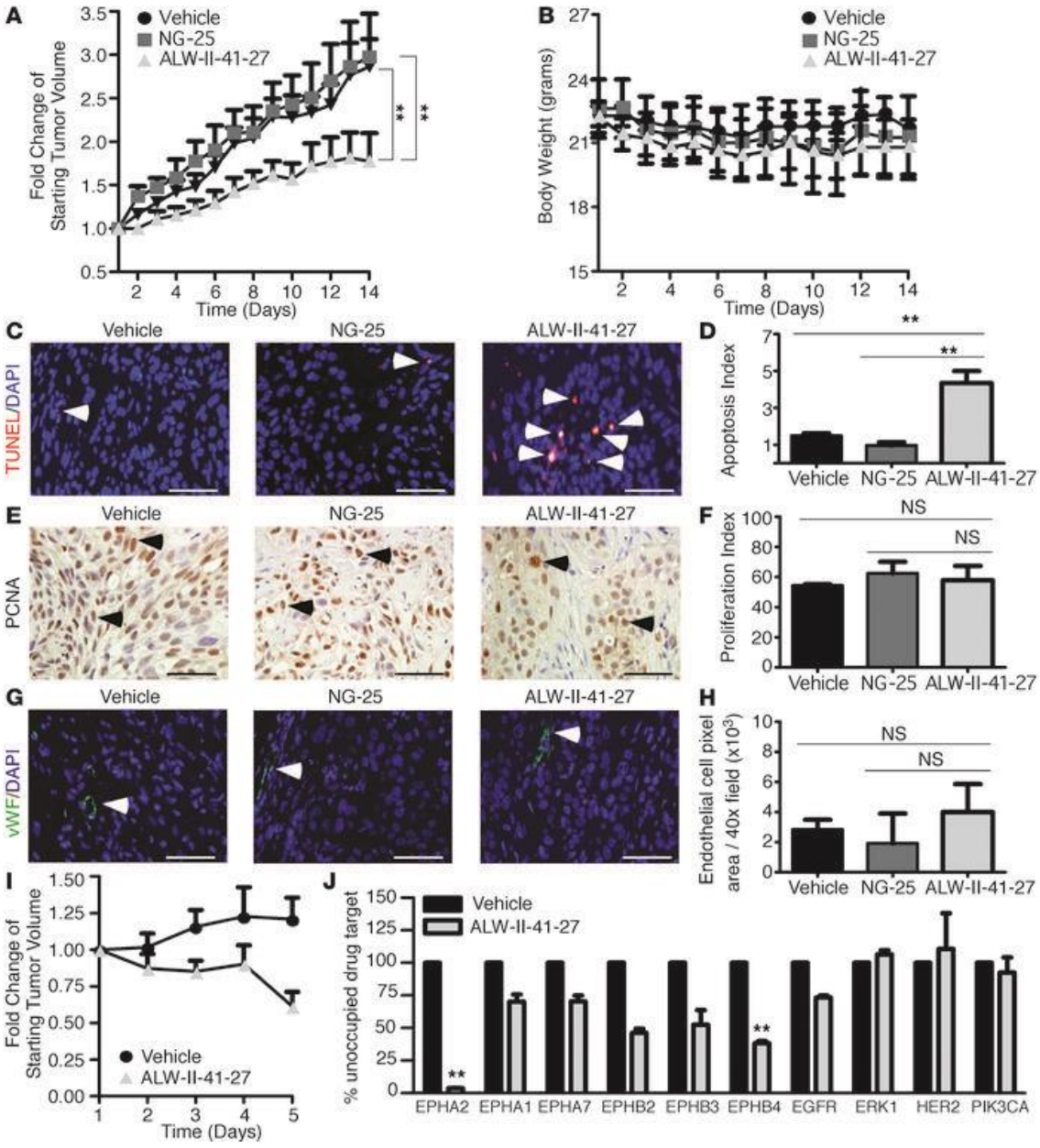

Figure 2.11 ALW-II-41-27 inhibits NSCLC tumor growth in vivo. (A) 15×10^6 H358 cells were injected subcutaneously into the dorsal flanks of nude mice. Tumors were allowed to grow to 200 mm^3 before administration of 15 mg/kg NG-25, ALW-II-41-27, or vehicle alone via intraperitoneal injection twice daily. Tumor size was measured every day with a digital caliper, and tumor volumes were calculated. Data are presented as the fold change of starting tumor volumes ± SEM (n = 5 per condition). **(B)** No statistical difference in body weight was detected among any of the treatment groups during the course of treatment. Data are presented as average body weight ± SEM. (C and D) Tumors were harvested at the termination of the study, and apoptosis was assessed via TUNEL staining. An apoptosis index of the tumor sections is presented as TUNEL-positive nuclei (arrowheads) per total nuclei ± SEM. **(E and F)** Proliferation in tumors treated with NG-25, ALW-II-41-27, or vehicle alone was quantified as the total number of

PCNA-positive nuclei (arrowheads) relative to the total nuclei ± SEM. **(G and H)** No change in tumor vessel density (arrowheads) was detected by vWF staining. Data are presented as average endothelial cell pixel area ± SEM. **(I)** Tumor regression was observed when H358 xenografts (as in A) were treated with an increased dose of ALW-II-41-27 (30 mg/kg) over 5 days (n = 5 per condition). Data are presented as percent of change in tumor volume ± SEM. **(J)** Drug-target interaction in xenograft tumors in situ was determined by the chemical proteomics platform KiNativ (see Methods). Shown are percentages of drug targets unoccupied by ALW-II-41-27 relative to vehicle control. Data are presented as percent of unoccupied drug target ± SEM. **P < 0.01, Student's t test (n = 5 tumors per group). Scale bar: 50 μm.

Kinases	Sequence	Labeling Site	KiNativ Inhibition Percentage					** Enzymatic IC_{50} (nM)	
			ALW-II-41-27			NG-25			
			* H358 Xenograft	A375					
				5.0 μM	0.5 μM	5.0 μM	0.5 μM	ALW-II-41-27	NG-25
ABL,ARG	LMTGDTYTAHAGAKFPIK	ACT	>98.2	>95	>95	> 98	> 98	7.7	75.2
ABL,ARG	YSLTVAVKTLKEDTMEVEEFLK	Lys1	>95.9	>90	>90	86.8	85.5		
GAK	DLKVENLLLSNQGTIK	Lys2	>95.2	N.D	N.D	N.D	N.D		
LYN	VAVKTLKPGTMSVQAFLEEANLMK	Lys1	>94.8	N.D	N.D	> 95	90.5	0.8	12.9
ZAK	WISQDKEVAVKK	Lys1	>93.6	>98	>98	98.1	93.0	40.2	698
p38a	QELNKTIWEVPER	Other	98.5	97.7	98.1	53.3	51.9	55.6	102
EPHA2	VLEDDPEATYTTSGGKIPIR	ACT	95.1	98.3	97.5	57.7	27.9	11	773
p38b	QELNKTVWEVPQR	Other	91.6	38.7	44.2	-241.6	-228.7	138	194
FRK	HEIKLPVK	ACT	91.6	N.D	N.D	N.D	N.D	17.3	144
CSK	VSDFGLTKEASSTQDTGKLPVK	ACT	87.7	99.4	95.0	78.2	36.5	13.9	56.4
FYN,SRC,YES	QGAKFPIKWTAPEAALYGR	ACT	87.2	93.4	85.4	89.6	36.5	14.4	113
p38a	DLKPSNLAVNEDCELK	Lys2	62.9	65.3	71.7	21.9	20.2	55.6	102
EPHB4	FLEENSSDPTYTSSLGGKIPIR	ACT	61.4	N.D	N.D	-4.2	39.2	13.1	999
HER3/ErbB3	GVWIPEGESIKIPVCIKVIEDK	Lys1	56.7	-43.1	-14.3	27.3	22.8		
EPHB2	FLEDDTSDPTYTSALGGKIPIR	ACT	52.2	>85	12.2	21.6	-2.2	14.4	672
EPHB3	FLEDDPSDPTYTSSLGGKIPIR	ACT	45.1	N.D	N.D	N.D	N.D	119	3710
BRAF	DLKSNNIFLHEDLTVK	Lys2	44.0	>80	>80	66.8	22.5	1280	>10000
BTK	YVLDDEYTSSVGSKFPVR	ACT	40.3	N.D	N.D	N.D	N.D		
JAK1 domain2	IGDFGLTKAIETDKEYYTVK	ACT	37.9	83.7	48.7	95.4	20.8		
PRP4	CNILHADIKPDNILVNESK	Lys2	37.8	-15.4	-4.3	-33.5	-34		
YSK1	EVVAIKIIDLEEAEDEIEDIQQEITVLSQCDSPYITR	Lys1	37.5	N.D	N.D	N.D	N.D		
EPHA1	LLDDFDGTYETQGGKIPIR	ACT	31.4	N.D	N.D	N.D	N.D		
EPHA7	VIEDDPEAVYTTTGGKIPVR	ACT	28.3	N.D	N.D	N.D	N.D		
EGFR	LLGAEEKEYHAEGGKVPIK	ACT	24	84.7	31.3	0.7	4.8		
PI3KCA	RPLWLNWENPDIMSELLFQNNEIIFKNGDDLRQDMLTLQIIR	ATP	-0.8	N.D	N.D	28.3	21.9		
ERK1	DLKPSNLLINTTCDLK	Lys2	-11.5	0.3	7.4	-49.9	-31.9		
HER2/ERBB2	GIWIPDGENVKIPVAIKVLR	Lus1	-22.5	97.1	70.9	-19.4	-60.4		

Table 2.2 Drug-target interaction in xenograft tumors in situ. *H358 xenograft tumors treated with 30mg/kg ALW-II-41-27 for five days (n=5/group) (as in Figure 8I) were analyzed for drug-target interaction by chemical proteomics platform, KiNativ. Tumor lysate was incubated with ATP-biotin labeled probes to assess which kinases received protection from the drug binding. Percent inhibition of kinase labeling by the ATP-biotin probes is shown with the larger numbers representing a stronger interaction between the inhibitor and the kinase. Additionally, A375 cells were tested in a similar manner in vitro by treatment with 5μM and 0.5μM ALW-II-41-27 or NG-25 (control compound). Colors indicate the level of inhibition of ATP binding to the respective kinase: Brown (90% inhibition), Red (90-75% inhibition), Orange (75-50% inhibition), Yellow (50-35% inhibition), and Green (no change). ACT = Activation loop; Lys1 = Conserved Lysine 1; Lys2 = Conserved Lysine 2; Other = Labeling of residue outside of the protein kinase domain; N.D. = Not detected. ** The in vitro IC_{50} of ALW-II- 41-27 and NG-25 was determined by in vitro kinase assay using the SelectScreen™ Kinase Profiling Service (Life Technologies).

Discussion

Genome-wide analyses identified overexpression of the RTK EPHA2 in NSCLCs. While previous studies have provided correlative data linking high EPHA2 levels to poor clinical outcome in human lung cancer populations (224-226), the biology underlying these observations and translational potential of these correlations remain underexplored. Here, we show the first functional evidence that EPHA2 promotes tumor growth and survival in a large panel of NSCLC lines, in human tumor xenografts, and in a transgenic mouse model of aggressive *Kras*-mutant lung cancer. We show that S6K1-dependent BAD phosphorylation is one of the key signaling events mediating the EPHA2-regulated cell survival pathway. We also identified an EPHA2 kinase inhibitor, ALW-II-41-27, that suppresses cell viability in vitro and induces tumor regression of human NSCLC xenografts in vivo, demonstrating the translational potential of targeting EPHA2 in lung cancer.

To assess the subtypes of lung cancer most sensitive to EPHA2 inhibition, we analyzed a panel of 14 NSCLC cell lines carrying the 6 most common mutations present in patients with lung cancer. Knockdown of EPHA2 expression inhibits tumor cell viability in the majority of cell lines tested, most dramatically affecting cell lines bearing *KRAS* mutations. However, sensitivity to EPHA2 inhibition does not correlate strictly with *KRAS* mutation status. Rather, EPHA2 receptor phosphorylation levels appeared to be important in determining whether a given tumor cell line is sensitive to *EPHA2* knockdown (Figure 2.2, B and C). Therefore, although targeting EPHA2 is effective in *KRAS* mutant NSCLC, it is not exclusive to *KRAS* mutant NSCLC. The utility of targeting EPHA2 in *KRAS* mutant NSCLC is further supported by our in vivo data, which show that either genetic or pharmacologic inhibition of EPHA2 in *KRAS* mutant lung tumors promotes apoptosis and inhibits tumor growth. Because there is currently no effective

targeted therapy for treating *KRAS* mutant lung cancer, EPHA2 provides a promising alternative target for this subtype of lung cancer.

Previous studies have shown that RAS/MAPK signaling induces EPHA2 expression and ligand-stimulated EPHA2 forward signaling in turn attenuates growth factor–induced RAS activity, forming a negative feedback loop in normal epithelial cells (151). An escape from the negative effects of this interaction has been suggested to be important in the development of cancer (151). Indeed, our lab and others demonstrated that ligand-independent EPHA2 signaling and cross-talk with other oncogenic pathways serve to promote tumor cell proliferation and motility in breast cancer and glioma (147, 149, 168). Consistent with these findings, the tumor promotion role of EPHA2 in lung cancer appears to be ligand-independent, as exogenous EPHRIN-A1 stimulation inhibits tumor cell proliferation (362). In this study, we showed that genetic and pharmacologic inhibition of EPHA2 induces apoptosis in lung cancer. Interestingly, loss of EPHA2 does not appear to significantly affect the activities of ERK but rather inhibits cell survival by modulating mitochondrial apoptosis through p90-RSK/S6K1-induced inactivation of the pro-apoptotic protein BAD. These studies suggest that EPHA2 could serve as an attractive target for therapeutic intervention in lung cancer.

The effect of systemic loss of *EPHA2* through gene targeting on tumor growth may be due to loss of EPHA2 in the tumor epithelia and within the tumor microenvironment. In support of an epithelial-autonomous role for EPHA2 in NSCLCs, inducible shRNA-mediated *EPHA2* knockdown in NSCLC xenografts showed reduced tumor progression but to a lesser extent than systemic genetic knockout (Figures 2.1 and 2.3) or systemic pharmacologic inhibition (Figure 2.11). These studies are consistent with previous reports that EPHA2 expressed in endothelial cells promotes tumor angiogenesis (248, 249, 363). Because EPHA2 is important in both tumor cells

and their microenvironment, inhibition of EPHA2 may provide a dual benefit toward eradicating cancers.

This study identified a type II kinase inhibitor, ALW-II-41-27, that inhibits EPHA2 kinase activity and causes NSCLC tumor regression in vivo. As is true for most kinase-targeted drugs, ALW-II-41-27 also inhibits other targets. Four lines of evidence indicate that EPHA2 is a functionally important target of ALW-II-41-27. First, NG-25, a structural analog with a similar target spectrum as ALW-II-41-27, but which does not inhibit the EPHA2 RTK, displayed limited effects on cell viability in vitro and tumor growth in vivo. Second, signaling studies in cells treated with ALW-II-41-27 recapitulated what was observed in *EPHA2* knockdown cells, suggesting that EPHA2 is a major target of the compound. Third, depletion of *EPHA2* by RNAi rendered NSCLC cells much less sensitive to the effects of ALW-II-41-27, relative to the undepleted controls, consistent with EPHA2 being a functionally important target of the compound. Finally, in situ drug-tumor interaction studies using “KiNativ” MS demonstrated the selectivity of ALW-II-41-27 for EPHA2 within the EPH receptor family as well as among other kinases.

To assess whether EPHA2 inhibition has the potential to affect patient outcomes, we compared the effectiveness of ALW-II-41-27 with erlotinib in 4 cell lines carrying mutant *KRAS* (H2009 and H358), *EGFR* (PC-9), or *MEK-1* (H1437). As expected, erlotinib is only efficacious in PC-9 cells expressing mutant *EGFR*, whereas ALW-II-41-27 also inhibits cell viability in 2 cell lines carrying *KRAS* mutations (Figure 2.12). In PC-9 cells, erlotinib is approximately 5-fold more potent than ALW-II-41-27. However, the approximately 500 nM anti-proliferative IC_{50} of ALW-II-41-27 represents a good starting point for further medicinal chemistry efforts to yield a compound with suitable properties for clinical evaluation.

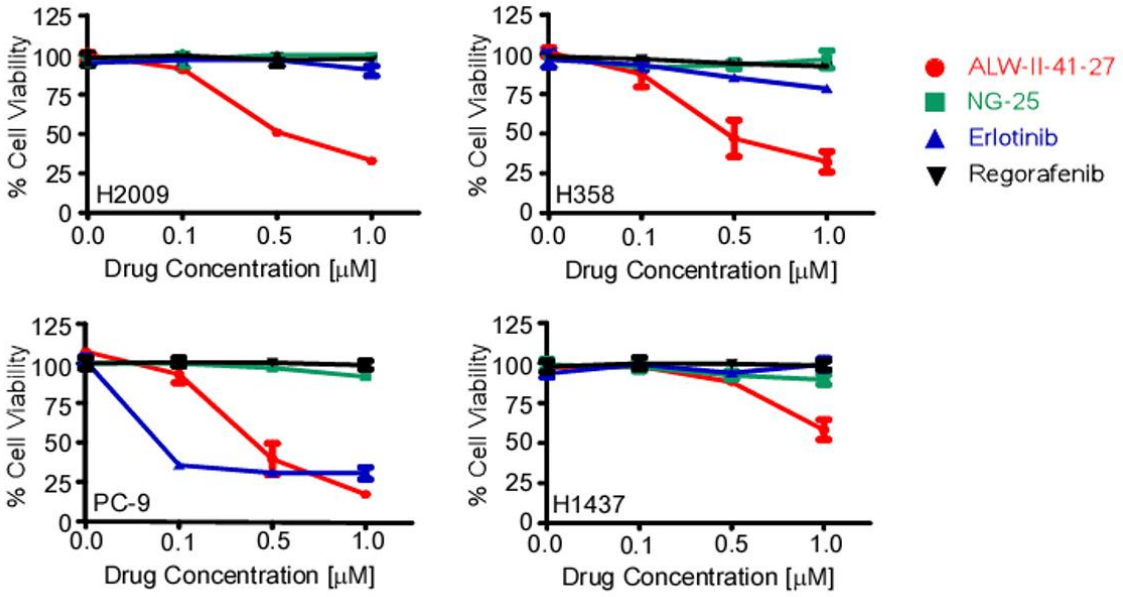

Figure 2.12 Comparison of the efficacy of tyrosine kinase inhibitors relative to ALW-II-41-27 in NSCLC cell lines. Cells were treated for 72 hours with the indicated TKIs before measuring viability by the MTT assay. H2009 and H358 cells contain a mutation in *KRAS*. PC-9 and H1437 cells carry a mutation in EGFR and a mutation in MEK-1, respectively.

In addition, although targeting EPHA2 does not exclusively affect mutant *KRAS* tumors, EPHA2 inhibitors provide promise for treating *KRAS* mutant lung cancer, as there is currently no effective targeted therapy for treating this subtype of lung cancer.

In summary, we have provided genetic, functional, mechanistic, and pharmacologic evidence that EPHA2 signaling promotes the progression and survival of NSCLC. Furthermore, this study identified a new category of EPHA2 kinase inhibitors that hold promise for therapeutics in NSCLCs, even for those driven by activating *KRAS* mutations.

CHAPTER III

EPHA2 INHIBITION OVERCOMES ACQUIRED RESISTANCE TO EGFR TYROSINE KINASE INHIBITORS IN LUNG CANCER

Abstract

Despite the success of treating *EGFR* mutant lung cancer patients with EGFR tyrosine kinase inhibitors (TKIs), all patients eventually acquire resistance to these therapies. Although various resistance mechanisms have been described, there are currently no FDA-approved therapies to treat lung tumors with acquired resistance to first-line EGFR TKI agents. Here we found that EPHA2 is overexpressed in EGFR TKI resistant tumor cells. Loss of EPHA2 reduced the viability of erlotinib resistant tumor cells harboring $EGFR^{T790M}$ mutations in vitro and inhibited tumor growth and progression in an inducible $EGFR^{L858R+T790M}$ mutant lung cancer model in vivo. Targeting EPHA2 in erlotinib resistant cells decreased S6K1-mediated phosphorylation of cell death agonist BAD, resulting in reduced tumor cell proliferation and increased apoptosis. Furthermore, pharmacologic inhibition of EPHA2 by the small molecule inhibitor, ALW-II-41-27, decreased both survival and proliferation of erlotinib resistant tumor cells and inhibited tumor growth in vivo. Collectively, these data define a role for EPHA2 in the maintenance of erlotinib resistant *EGFR* mutant lung cancer and indicate that EPHA2 may serve as a useful therapeutic target in TKI resistant tumors.

Significance

In this study we demonstrate that EPHA2 regulates cell viability in lung cancers with acquired resistance to selective EGFR inhibitors, and we show that both genetic and pharmacologic inhibition of EPHA2 is effective in mitigating erlotinib resistant cell

survival. These studies demonstrate the promise and utility of targeting EPHA2 in EGFR TKI resistant lung cancer.

Introduction

Lung cancer remains the leading cause of cancer-related deaths in the United States despite a significant number of advancements in the molecular diagnosis and treatment of this disease (364). One of the most extensively studied molecular subset in lung cancer is those harboring activating mutations in the epidermal growth factor receptor (*EGFR*) gene. These mutations, most commonly a point mutation in exon 21 (L858R) or a deletion in exon 19 (LREA) (365), are activating mutations that result in enhanced EGFR kinase activity (366) as well as exquisite sensitivity to first-generation EGFR-specific tyrosine kinase inhibitors (TKIs), such as erlotinib (66-68). Unfortunately, approximately a year after commencing treatment all patients treated with EGFR TKIs acquire resistance to these therapies (77, 78). Sequencing efforts have revealed that tumors with acquired resistance to EGFR TKIs commonly gain an additional mutation, T790M, in the gatekeeper position of the kinase domain of EGFR (79, 80). Currently, there are limited options for the treatment of first-generation EGFR TKI (erlotinib) resistant tumors, although some success has been observed with administration of second (83, 84) and third (85, 86) generation EGFR TKIs or combining antibody therapy targeting EGFR with second generation inhibitors (87). Risks of persistent and/or mutation-specific targeting of EGFR include likely development of alternative mechanisms of TKI resistance distinct from further mutations in *EGFR* (85), including oncogene addiction to other kinases. Such “bypass” RTK signaling is a well-documented mechanism of EGFR TKI resistance as evidenced by compensatory activation of MET, HER2, AXL, IGF1R, and FGFR in the context of EGFR TKI acquired

resistance (99-105). Identifying bypass pathways responsible for mediating TKI resistance may provide novel targets needed for therapeutic intervention.

EPHA2 is overexpressed in lung cancer, correlating to poor patient outcomes (224-226). EPHA2 belongs to the largest family of RTKs, the EPH RTKs, which have been implicated in the regulation of a wide array of pathological conditions including cancer (123, 124, 126, 216, 367). Upon binding to their ligands, EPHRINS, EPH RTKs oligomerize and are capable of activating multiple downstream signaling pathways including RAS/MAPK, PI3K/AKT, and RHO/RAC (123, 124, 126). We previously reported that targeting EPHA2 in ERBB2 driven murine mammary tumor models resulted in impaired tumor initiation and metastatic progression, and that heightened levels of EPHA2 were sufficient to mediate resistance to ERBB2 TKI therapy in human breast cancer cell lines (149, 231). In lung cancer, genetic and pharmacologic inhibition of EPHA2 results in increased tumor cell death in vitro and decreased tumor burden in vivo (224). However, the role of EPHA2 in resistance to EGFR TKIs in lung cancer remains undefined.

Because targeted inhibition of EPHA2 has proven useful in lung cancer subtypes with constitutive MAPK signaling and because EPHA2 expression positively correlates to TKI resistance of a known ERBB family member in breast cancer, we hypothesized that it would be an effective target for the treatment of EGFR TKI resistant lung cancer. In this study, we found that EPHA2 is overexpressed in erlotinib resistant lung cancer cells compared to erlotinib sensitive lung cancer cells. Genetic ablation of *EPHA2* in $EGFR^{T790M}$ mutant, erlotinib resistant cells led to both increased apoptosis and decreased proliferation. Gene targeting of *EphA2* in an inducible, genetically engineered mouse model of EGFR TKI resistance led to decreased tumor growth and progression. Treatment of erlotinib resistant cells with an ATP-competitive, small molecule tyrosine kinase inhibitor of EPHA2, ALW-II-41-27, decreased cell viability in vitro and tumor

growth in vivo. Collectively, these studies demonstrate the promise and utility of targeting EPHA2 in EGFR TKI resistant lung cancer.

Methods

Microarray analysis

Data from 58 matched lung tumor specimens and adjacent normal lung (116 total samples) with annotated mutation status were downloaded from Gene Expression Omnibus (GSE32863) (368). Normalized gene expression data for EPHA2 were extracted and compared between normal and tumor tissue in all patients or by the presence or absence of the *EGFR* genotype. A paired-sample student's t-test was used to compare normal versus tumor for each group, using patient-specific matching.

For microarray experiments, RNA was extracted from erlotinib sensitive and resistant cell lines in the absence of erlotinib for 72 hours (369). Microarray profiling was performed using U133 Plus chips (Affymetrix). Normalized expression data were analyzed in R3.1.1. Hierarchical clustering was performed using the complete linkage algorithm. Distances for clustering were calculated as 1-r, where r represents the correlation coefficient value. All tests are significant at two-sided 5% level, false-discovery-rate (FDR) corrected p-values were reported for multiple comparisons.

Tumor biopsy samples

All patient tumor biopsy samples were obtained under Institutional Review Board (IRB) approved protocols (Vanderbilt University IRB# 050644). Written informed consent was obtained from all patients. All samples were de-identified and protected health information was reviewed according to the Health Insurance Portability and Accountability Act (HIPAA) guidelines.

Cells and cell culture

EGFR mutant PC-9 and HCC827 (ΔE746-A750) and PC-9/ER, PC-9/ERC15, PC-9/ERC16, and HCC827/ER (ΔE746-A750; T790M) cells were provided by Dr. William Pao (Vanderbilt University). EGFR TKI resistant cells were derived as described and characterized (370). Cell lines were authenticated and sequenced for signature mutations (370). EGFR TKI resistant lines were maintained in the presence of 1μM erlotinib (Cell Signaling Technology) throughout the study (refreshed every 72 hours) although experiments were routinely conducted after a 72 hour drug holiday. ALW-II-41-27 and NG-25 were generously provided by Nathanael Gray (Dana-Farber Cancer Institute, Harvard Medical School). 293T cells used for lentivirus production were purchased from ATCC.

All lung cancer cell lines were cultured in RPMI-1640 medium (Corning/Cellgro) supplemented with L-glutamine (2mM), 10% fetal bovine serum (FBS) (Thermo Scientific, HyClone Laboratories Inc.), penicillin (100U/mL), and streptomycin (100μg/mL). 293T cells were grown in DMEM (Corning/Cellgro) supplemented with L-glutamine (2mM), and 10% FBS. All cells were grown in a humidified incubator with 5% CO_2 at 37°C.

EPHA2 knockdown cell lines were created by lenti-viral transduction of a pLKO.1 vector containing *EPHA2* specific shRNA constructs (sh*EPHA2* #1 mature sense 5'-CGGACAGACATATAGGATATT-3' or sh*EPHA2* #2 mature sense 5'-GCGTATCTTCATTGAGCTCAA-3') obtained from Open Biosystems. Cell lines generated with pLKO.1 vectors were selected for 5 days in 1.5μg/mL of puromycin containing complete RPMI-1640 media before initiation of the assay. EPHA2 ON-TARGETplus Human SMARTpool siRNA (L-003116-00-0005) and ON-TARGETplus Non-Targeting pool siRNA (D-001810-10-05) (Dharmacon/Thermo Scientific) were used at a concentration of 12.5nM in conjunction with Lipofectamine

RNAiMAX transfection reagent (Invitrogen) according to the manufacturer's protocol. 72 hours after transfection, cells were subjected to western blot analysis.

Cell viability assays

MTT assay. Cells were seeded at a density of 1,500 cells per well in 100 µl media in 96-well plates. Upon conclusion of the experiment, 20 µl of 5 mg/ml of thiazolyl blue tetrazolium bromide (MTT) (Sigma-Aldrich) in PBS was added and incubated at 37°C for 2 hours. After incubation the MTT containing media was aspirated, and an isopropanol solution containing 4 mM HCl and 0.1% Nonidet P-40 was added to each well and maintained at room temperature for 10 minutes. The absorbance was read at 590nm on a spectrophotometer (BioTEK). Each assay was designed to include at least 6 replicates and was repeated at least 3 independent times. Cell viability was presented as a percentage of cells transduced with an empty vector or treated with a vehicle alone.

BrdU incorporation assay. Proliferation was assessed by labeling cells with 5-bromo-2'-deoxyuridine (BrdU) and assaying the level of incorporation of this pyrimidine analog into the cellular DNA per the manufacturer's instructions (BrdU Cell Proliferation Assay kit, Cell Signaling Technology). In short, cells were seeded (~1500 cells/well). Two hours prior to the conclusion of the study 10µM BrdU was added to each well of cells for a final concentration of 1µM BrdU. Cells were then fixed and DNA was denatured. Detection of BrdU incorporation was measured using a mouse mAb against BrdU followed by a peroxidase linked anti-mouse secondary antibody. Signal was detected by using the substrate TMB, and the absorbance was measured at 450 nm wavelength.

Cell death ELISA. To assess the level of apoptosis in a given cell population, treated cells were washed once with PBS and lysed as per the manufacturer's instructions (Cell

Death Detection ELISA PLUS kit, Roche). Biotin labeled anti-histone and peroxidase-conjugated anti-DNA antibodies were used to detect histone-associated DNA fragments in the lysate. Signal was detected upon the addition of the peroxidase substrate ABTS, and the absorbance was measured at 405 nm wavelength.

Murine tumor studies

TetO-*EGFR*$^{L858R+T790M}$ and *CCSP-rtTA* mice were provided by Dr. William Pao (Vanderbilt University) and have been described previously (371, 372). Genotypes were confirmed twice for each animal by analyzing genomic DNA isolated from both tail and ear tissues. TetO-*EGFR*$^{L858R+T790M}$ primers were 5'-ACTGTCCAGCCCACCTGTGT-3' and 5'-GCCTGCGACGGCGGCATCTGC-3'. *CCSP-rtTA* primers were 5'-ACTGCCCATTGCCCAAACAC-3' and 5'-AAAATCTTGCCAGCTTTCCCC-3'. *EphA2* primers were 5'-GGGTGCCAAAGTAGAACTGCG-3′ (forward), 5′-GACAGAATAAAACGCACGGGTG-3′ (Neo), and 5′-TTCAGCCAAGCCTATGTAGAAAGC-3′ (reverse). Doxycycline was administered at the time of weening (3 weeks old) by feeding the mice doxycycline containing food pellets (625 ppm) (Harland-Tekland) to induce lung specific expression of mutant *EGFR*$^{L858R+T790M}$.

Lungs removed for gross and histological analysis were first perfused with 1× PBS followed by 10% buffered formalin (Fisher). After 24 hours of fixation in formalin lungs were weighed to determine a total wet weight. MRI imaging analysis was performed at both 10 and 15 weeks of age following the initiation of doxycycline administration at weening as described previously (153). Tumor volumes were calculated using Matlab 2012a (The MathWorks Inc.) as described previously (153).

All animal experiments were conducted under guidelines approved by the AAALAC and Vanderbilt University Institutional Animal Care and Use Committee.

Immunohistochemistry

Immunohistochemical staining (IHC) on tumor sections was performed as described previously (248, 249, 373), using antibodies against EPHA2 (Life Technologies; #347400), $EGFR^{L858R}$ (Cell Signaling Technology, #3197S), PCNA (BD Pharmingen, #555567), and vWF (DakoCytomation, #A0082). PCNA+ staining was quantified as the average percentage of PCNA+ nuclei relative to total nuclei (proliferation index). Four fields of at least 5 tumors per genotype or treatment condition were assessed. Apoptosis assays were performed using the Apoptag Red In Situ Apoptosis Detection Kit per the manufacturer's protocol (Millipore). TUNEL+ staining was quantified as the percentage of TUNEL+ nuclei relative to total nuclei (apoptotic index). Four fields of at least 5 independent tumors per genotype or treatment condition were assessed. Tumor vessels were quantified by assessing the vWF+ vessels (pixels) in 4 fields per sample of at least 5 independent tumors per genotype or treatment condition. Biotin goat anti-rabbit (BD Pharmingen), anti-rabbit Cy3 (Jackson ImmunoResearch), retrievagen A (pH 6.0) (BD Pharmingen, #550524), streptavidin peroxidase reagents (BD Pharmingen, #51-75477E), and the liquid 3,3′-diaminobenzidine tetrahydrochloride substrate kit (Zymed Laboratories) were used for IHC. Cytoseal XYL (Richard Allan Scientific) or ProLong Gold antifade reagent with DAPI (Life Technologies) were used to mount slides.

Antibodies and immunoblotting

Antibodies against the following proteins were used: EPHA2 (D7, mouse monoclonal, 1:1,000, Millipore); β-tubulin (mouse monoclonal, 1:2,000, Sigma-Aldrich,

T4026); p-AKT (S473 and T308), AKT, p-ERK (T202/Y204), ERK, p-P90RSK (S380), RSK, p-S6K1 (T389), S6K1, p-S6 (S235/6), S6, p-BAD (S112), BAD, (all rabbit, 1:1,000, Cell Signaling Technology); cleaved caspase-3, caspase-3, and cleaved PARP (all rabbit, 1:500, Cell Signaling Technology). Secondary antibodies used were HRP-conjugated anti-mouse and anti-rabbit antibodies (Promega). For immunoblotting, cells were washed with 1x PBS and lysed on ice with RIPA buffer supplemented with a protease inhibitor cocktail (P8340) (Sigma-Aldrich) and phosphatase inhibitors (Roche). Clarified lysates were subjected to SDS-PAGE and transferred onto nitrocellulose membranes. Membranes were blocked for 30 minutes in 5% nonfat dry milk in TBS-T buffer followed by incubation with the indicated primary antibodies. Horseradish peroxidase conjugated secondary antibodies were used subsequently. Clarity Western ECL substrate (Bio-Rad) was used for signal detection.

Tumor xenograft

HCC827/ER ($2.5x10^6$) were injected with Martigel into the hind flanks of 6-week-old athymic nude mice ($Foxn1^{nu}$) (Harlan). Once tumors reached approximately 200 mm^3, mice were randomized by body weight and tumor volume into treatment groups (n=5 per group) to receive 15mg/kg of either erlotinib, ALW-II-41-27, or the vehicle alone (10% 1-methyl-2-pyrrolidinone and 90% PEG 300) twice daily via intraperitoneal injection. Tumors were measured daily with digital calipers and tumor volumes were calculated by using the formula; volume = length x $width^2$ x 0.52. Additionally, to monitor the toxicity of the given drugs, body weight was measured daily.

Results

EPHA2 is overexpressed in *EGFR* mutant lung cancer with further overexpression upon development of acquired resistance to EGFR TKIs.

EPHA2 is overexpressed in lung cancer patient tumor samples irrespective of the histological subtype (224). To investigate whether EPHA2 expression correlates with any molecular subtypes of lung cancer, we analyzed a dataset of 58 matched normal and lung tumor tissue samples. In all patients (n=58), levels of EPHA2 expression were significantly higher (p=0.003) in the tumor tissue compared to the adjacent normal lung tissue (Figure 3.1A), consistent with previous studies (224-226). In *EGFR* mutant lung cancer, EPHA2 expression was also markedly increased compared to adjacent normal tissue (Figure 3.1A).

Given the known role of EPHA2 in promoting lung cancer growth and survival (153, 224) and its contribution to drug resistance in breast cancer (231), we investigated if EPHA2 is upregulated in *EGFR* mutant lung cancer cells with $EGFR^{T790M}$ mediated, acquired resistance to erlotinib. The erlotinib resistant, *EGFR* mutant lung cancer cell lines, PC-9/ER and HCC827/ER, were generated post completion of a drug escalation protocol (370). The resulting resistant cell lines tolerated erlotinib concentrations more than ten times the IC_{50} of their parental, TKI sensitive counterparts (Figure 3.1B). Microarray analysis of PC-9 and PC-9/ER cells revealed that three EPH receptors, *EPHA2, EPHB2, and EPHB4*, were overexpressed in the erlotinib resistant PC-9/ER cells, compared to erlotinib sensitive PC-9 parental cells (Figure 3.1C).

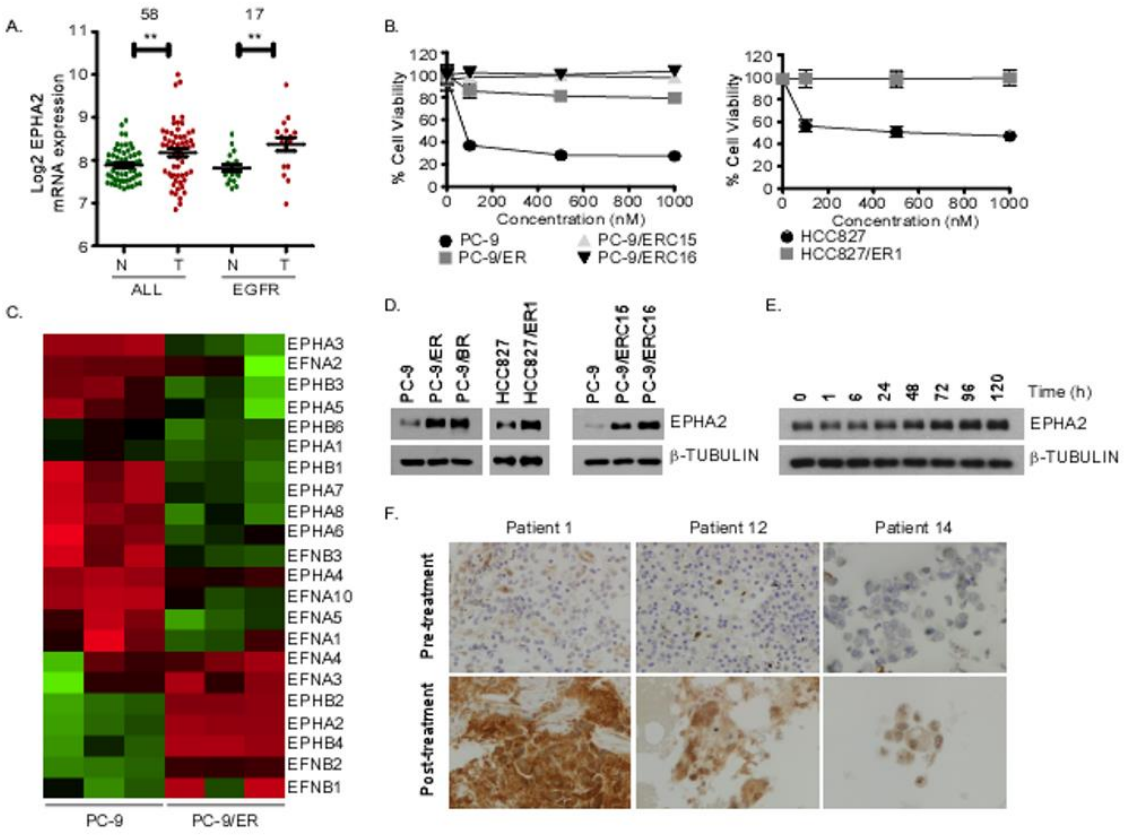

Figure 3.1 EPHA2 expression in erlotinib sensitive and resistant *EGFR* mutant lung cancer. **(A)** Comparison of EPHA2 expression in 58 paired lung cancer patient samples between tumor and adjacent normal tissue (GSE32863) (368). Statistical analysis with patient-specific matching was performed using a paired student's t-test. ALL, all tumor samples; *EGFR*, tumor samples harboring *EGFR* mutations; N, normal (green); T, tumor (red). **p $\leq$ 0.005. **(B)** PC-9 erlotinib resistant cells (PC-9/ER), erlotinib resistant clones (PC-9/ERC15 and PC-9/ERC16), and HCC827 erlotinib resistant cells (HCC827/ER) were assessed for resistance to erlotinib. **(C)** Heatmap showing the mRNA expression profiles of EPH RTKs and EPHRIN ligands comparing PC-9 and PC-9 cells with acquired resistance to erlotinib (PC-9/ER). **(D)** EPHA2 protein expression levels were assessed via western blot analysis in erlotinib resistant cell lines (ER) and afatinib resistant cell lines (BR) harboring $EGFR^{T790M}$ and their parental cells. **(E)** EPHA2 expression in PC-9/ERC16 cells was measured over time after erlotinib was removed from culture media. **(F)** Immunohistochemistry showed increased EPHA2 levels in EGFR TKI resistant tumor samples compared to pre-treatment tumor specimens from 3 patients.

To validate these findings, we assessed EPHA2 protein levels in the same isogenic, paired cell lines (PC-9 and PC-9/ER) as well as an independent erlotinib sensitive and resistant cell line pair, HCC827 and HCC827/ER. EPHA2 was overexpressed in all of the erlotinib resistant cell lines (Figure 3.1D), as well as in two independent single-cell *EGFR*^{T790M} containing clones derived from the PC-9/ER cell line (Figure 3.1D) confirming observations from our gene expression analysis. Interestingly, we found that EPHA2 expression could be regulated by the presence of erlotinib, and EPHA2 expression increased in a time-dependent manner post erlotinib withdrawal in PC-9/ERC16 cells (Figure 3.1E), consistent with a previous observation that EPHA2 expression is regulated by MAPK signaling (151).

Lastly, we assessed the EPHA2 expression in samples from patients with *EGFR* mutations pre- and post-development of resistance to EGFR TKIs. In 4 samples with matched pre-treatment and post-relapse tumor sections, we detected higher EPHA2 protein levels by immunohistochemistry in 3 of the post-relapse tumor samples (Figure 3.1F). Overall, we determined that EPHA2 is overexpressed in *EGFR* mutant lung cancer cells harboring *EGFR*^{T790M} mediated resistance to erlotinib compared to *EGFR* mutant lung cancer cells with sensitivity to EGFR inhibitors, suggesting a possible correlation between EPHA2 expression and EGFR TKI sensitivity both in vitro and in the clinical setting.

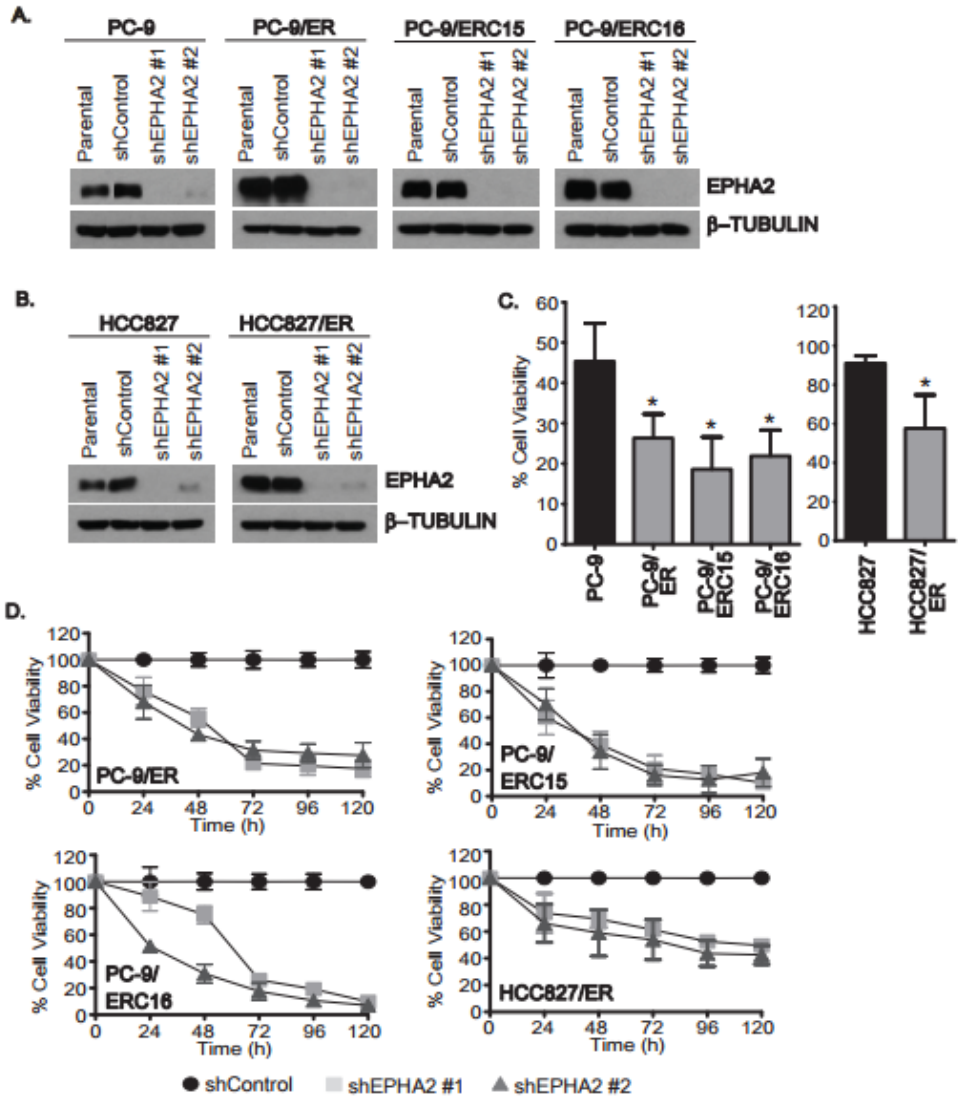

Figure 3.2 EPHA2 is required for cell viability in erlotinib resistant lung cancer cells. Erlotinib sensitive and resistant cell lines were transduced with lentiviruses containing either sh*EPHA2* or a pLKO.1 vector control. The resulting cell populations were selected in 1.5µg/ml puromycin for 5 days. Shown are immunoblots for EPHA2 expression in PC-9 cells and PC-9 cells with acquired resistance to erlotinib (PC-9/ER) and erlotinib resistant clonal cell populations (PC-9/ERC15 and PC-9/ERC16) **(A),** as well as HCC827 cells and HCC827 cells with acquired resistance to erlotinib (HCC827/ER) 3 days after completion of puromycin selection **(B)**. β-Tubulin expression was used as a loading control. **(C)** Erlotinib sensitive and resistant cell lines were treated as in (A&B), and cell viability was analyzed by the MTT assay at 72 hours after puromycin selection. Experiments were repeated three times with 6 replicates per experiment. Data is presented as the mean viability of sh*EPHA2* knockdown cells relative to that of the sh*Control* cells ± SEM. *$p < 0.05$ **(D)** Cells were treated as in **C**, and cell viability was assessed over 5 days. Experiments were repeated three times, and the mean sh*EPHA2* knockdown relative to the vector control cells ± SEM was presented.

EPHA2 promotes the cell viability of erlotinib resistant lung cancer.

To determine if EPHA2 was required for cellular survival in EGFR TKI resistant lung cancer, we knocked down the expression of *EPHA2* using a lenti-viral based shRNA strategy in four erlotinib resistant and two erlotinib sensitive lung cancer cell lines. Both of the two independent shRNAs against *EPHA2* (sh*EPHA2*) silenced EPHA2 protein expression and reduced cell viability when tested three days after puromycin selection (Figure 3.2A and 3.2B). Although sh*EPHA2* reduced cell viability in both erlotinib sensitive and resistant cell lines, erlotinib resistant cells displayed a greater dependence on *EPHA2* for cell survival compared to erlotinib sensitive cell lines. For example, 72 hours after puromycin selection, *EPHA2*-deficient, erlotinib resistant PC-9/ER and HCC827/ER cells displayed 20% and 40% cell viability, respectively, while erlotinib sensitive PC-9 and HCC827 cells maintained 45% and 90% cell viability (Figure 3.2C). We next performed a time course to monitor cell viability after *EPHA2* knockdown in these cells. The results showed that by five days post puromycin selection, *EPHA2*-deficient, erlotinib resistant cells displayed a further reduction in the number of viable tumor cells, in some cases with only 10% overall cell viability (Figure 3.2D). These data suggests that TKI resistant lung cancer cells are dependent upon EPHA2 RTK for survival.

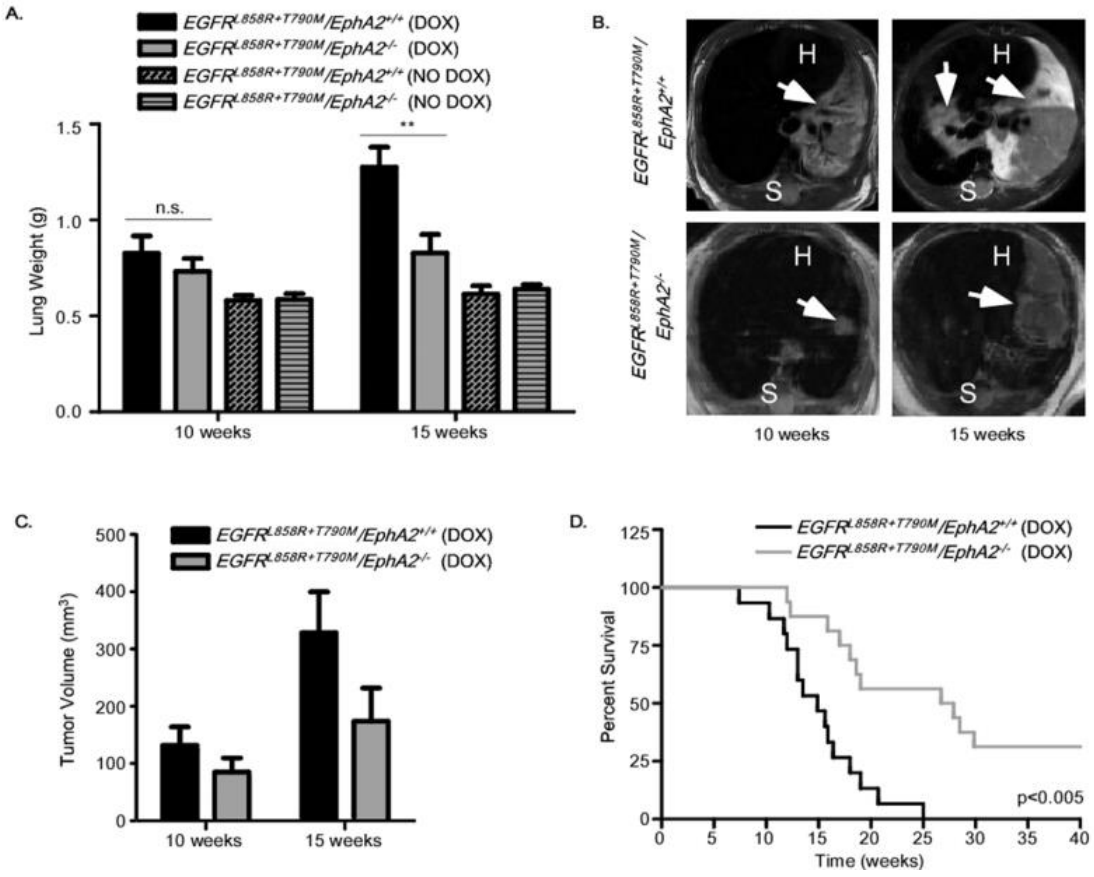

Figure 3.3 Loss of *EphA2* results in decreased tumor burden and increased survival in a TKI resistant *EGFR*$^{L858R+T790M}$ transgenic model. (A) Lungs of *EGFR*$^{L858R+T790M}$ mice from wild-type (*EphA2*$^{+/+}$) or knockout (*EphA2*$^{-/-}$) of *EphA2* were collected, and total lung wet weight was measured at 10 and 15 weeks of age to assess the additional mass contributed to the lungs by the tumor burden. Average lung weight $\pm$ SEM is shown (n = 10 per time point per genotype). **(B)** Wild-type and *EphA2* deficient mice were subjected to MRI analysis at 15 and 20 weeks of age. T2-weighted MRI images were taken in the axial plane with slice thickness of 1mm. Representative images at 15 and 20 weeks are shown. White arrows indicate tumor tissue. H, heart; S, spine. **(C)** Tumor volumes were quantified as a composite of 10 serial MRI slices of the lung per mouse using Matlab software and were graphed as an average tumor volume (mm^3) $\pm$ SEM (n $\geq$ at least 5 mice per genotype). **(D)** Kaplan-Meier survival curves for *EGFR*$^{L858R+T790M}$ mice with or without *EphA2*. Mutant *EGFR* gene expression was induced by doxycycline at 3 weeks of age. *p < 0.005

EPHA2 promotes tumor growth in an inducible transgenic model of *EGFR*$^{L858R+T790M}$ mutant lung cancer in vivo.

To assess the contribution of EPHA2 to EGFR TKI resistant lung cancer in vivo, we crossed *EphA2* deficient animals with an inducible *EGFR*$^{L858R+T790M}$ mutant lung cancer transgenic model (87, 245). In this model, expression of the mutant *EGFR* (TetO-*EGFR*$^{L858R+T790M}$*; CCSP-rtTA)* is induced upon doxycycline administration and resulting tumors are resistant to erlotinib. To assess tumor burden in lungs of *EGFR*$^{L858R+T790M}$/*EphA2*$^{+/+}$ and *EGFR*$^{L858R+T790M}$/*EphA2*$^{-/-}$ mice, we measured the lung wet weight over a time course as described previously (153, 374). A significant reduction in lung weight was observed in doxycycline-treated, *EGFR*$^{L858R+T790M}$/*EphA2*$^{-/-}$ mice compared to doxycycline-treated, *EGFR*$^{L858R+T790M}$/*EphA2*$^{+/+}$ mice or compared to tumor-free mice not fed doxycycline (Figure 3.3A). Because no changes in lung weight were observed between *EGFR*$^{L858R+T790M}$/*EphA2*$^{-/-}$ and *EGFR*$^{L858R+T790M}$/*EphA2*$^{+/+}$ mice that were not fed doxycycline, we attribute the differences seen in mice fed doxycycline to a reduction in tumor burden. To further quantify tumor burden, we monitored mice by MRI imaging when tumors had developed in both groups at 10 weeks of age and again at 15 weeks of age (Figure 3.3B). As expected, tumors did not develop in any of the mice not fed doxycycline. Quantification of the MRI images revealed that doxycycline-fed *EGFR*$^{L858R+T790M}$/*EphA2*$^{-/-}$ mice had a lower overall tumor burden than *EGFR*$^{L858R+T790M}$/*EphA2*$^{+/+}$ mouse counterparts, which became more evident as the mice aged (Figure 3.3C). *EphA2* deficiency also correlated to significantly longer overall survival in this model of TKI resistant *EGFR*$^{L858R+T790M}$ mutant lung cancer. *EphA2*$^{+/+}$ mice did not surviving more than 25 weeks of age, whereas more than 25% the *EphA2*$^{-/-}$ mice surviving greater than 1 year on doxycycline (Figure 3.3D).

Histological analysis of the lungs confirmed the presence of tumors and *EGFR*$^{L858R+T790M}$ expression in doxycycline treated animals as well as the absence of

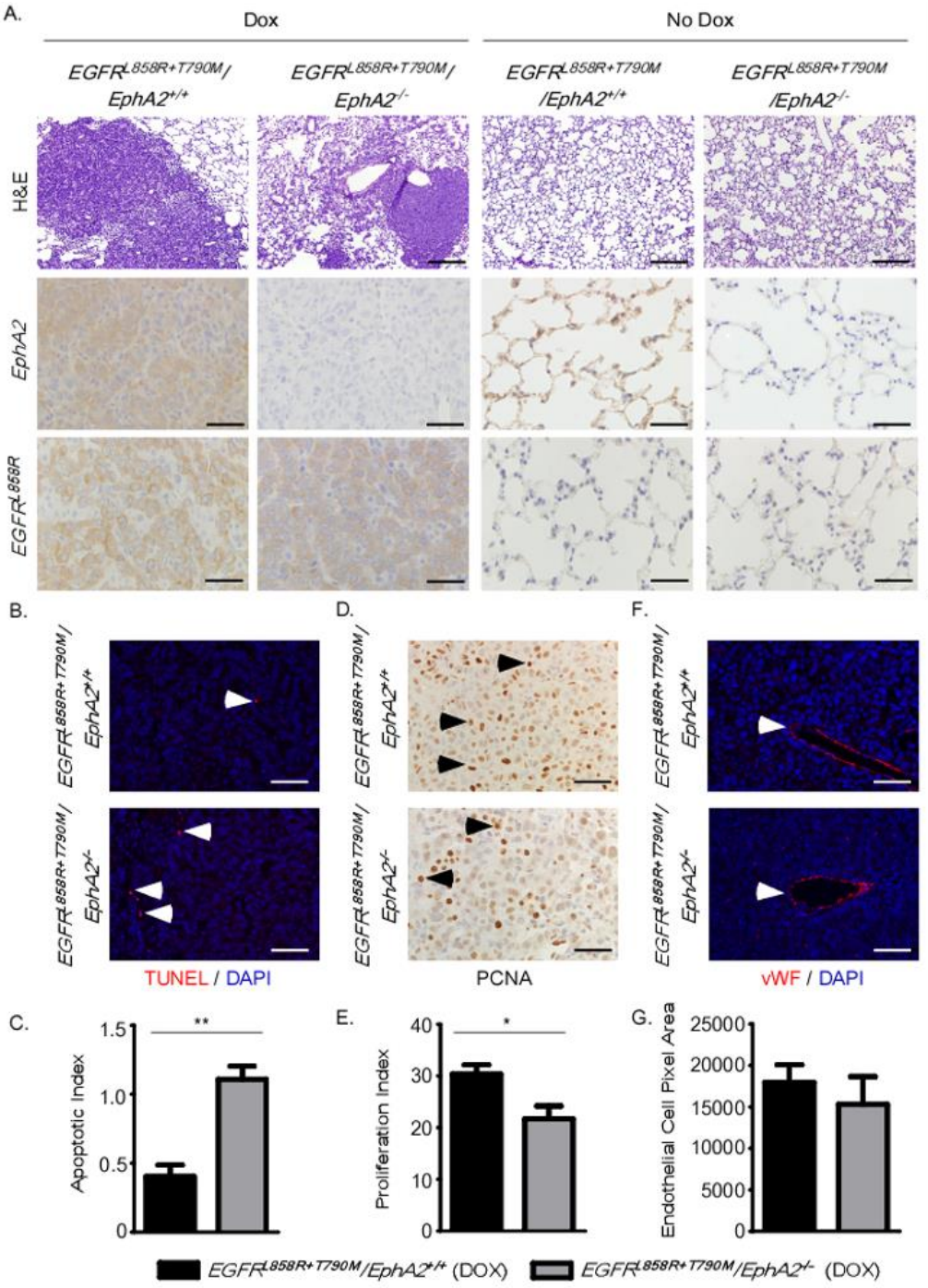

Figure 3.4 *EphA2* deficiency results in decreased proliferation and increased apoptosis in *EGFR*$^{L858R+T790M}$ tumors. (A) H&E stained lung sections (20 weeks) from *EGFR*$^{L858R+T790M}$*EphA2*$^{+/+}$ and *EGFR*$^{L858R+T790M}$*EphA2*$^{-/-}$ mice in the presence or absence of doxycycline. Scale bar: 200µm. Loss of EPHA2 protein expression and the presence of *EGFR*$^{L858R+T790M}$ mutant protein expression were confirmed by immunohistochemistry. Scale bar: 50µm. **(B)** Apoptosis in tumor sections was measured by the TUNEL assay. TUNEL positive nuclei (red) are indicated with arrowheads. Scale bar: 50µm. **(C)**

Apoptosis was quantified as a percentage of TUNEL positive nuclei relative to the total nuclei. An apoptosis index is presented as average percentage of TUNEL positive nuclei per total nuclei ± SEM. (n = 5 per genotype). **(D)** Tumor cell proliferation was assessed by PCNA immunohistochemistry. Arrowheads indicate representative proliferating nuclei. Scale bar: 50µm. **(E)** Proliferation was quantified by assessing the total number of PCNA positive nuclei (brown) compared with the total nuclei. A proliferation index is presented assessed as PCNA positive nuclei per total nuclei ± SEM. **(F)** The presence of tumor microvessels was assessed by vWF immunofluorescence staining (red, indicated by arrowheads). Scale bar: 50µm. **(G)** Microvessels in the tumor were quantified by measuring vWF positive pixels in each tumor field ± SEM (n = 5 per genotype). *p<0.05

EPHA2 expression in *EphA2* knockout animals (Figure 3.4A). In doxycycline fed, tumor-bearing mice, relative levels of apoptosis, proliferation, and tumor microvessels were quantified. Apoptosis was significantly higher in the tumors of $EGFR^{L858R+T790M}/EphA2^{-/-}$ mice, compared to tumors of $EGFR^{L858R+T790M}/EphA2^{+/+}$ mice, as measured by TUNEL staining (Figure 3.4B and 3.4C). Tumor cell proliferation was measured by staining tumor sections for proliferating cell nuclear antigen (PCNA) (Figure 3.4D). Proliferation was significantly decreased in $EGFR^{L858R+T790M}/EphA2^{-/-}$ tumors compared to tumors of mice with wild-type levels of EPHA2 (Figure 3.4E). Because previous murine studies in breast cancer have indicated that EPHA2 can function to support tumor vasculature (249), we assessed tumor microvessels by Von Willebrand factor (vWF) immunohistochemistry. No significant differences in vWF staining were seen in the tumor tissue between $EGFR^{L858R+T790M}/EphA2^{+/+}$ and $EGFR^{L858R+T790M}/EphA2^{-/-}$ mice (Figure 3.4F and 3.4G). Together, these data indicate that EPHA2 is required for the maintenance and progression of EGFR TKI resistant lung cancer in their intrinsic setting and microenvironment, such that deletion of *EphA2* limited proliferation and induced apoptosis in this tumor model.

EPHA2 regulates cell viability in erlotinib resistant cells through up-regulation of proliferation and inhibition of apoptosis.

To dissect the mechanism by which EPHA2 is required for cell viability in erlotinib resistant lung cancer cells, we quantified both proliferation and apoptosis after silencing *EPHA2* (sh*EPHA2*) by using a BrdU incorporation assay and a Cell Death ELISA, respectively. Upon *EPHA2* knockdown, we observed a decrease in proliferation of approximately 73.5 percent compared to sh*Control* cells, while cell lines sensitive to erlotinib displayed only a 22.4 percent decrease in proliferation (Figure 3.5A). Consistent with this effect, loss of *EPHA2* in erlotinib resistant cells resulted in a 3.4 fold increase in cellular apoptosis, compared to an only 2.0 fold increase in cells undergoing apoptosis from *EPHA2* knockdown in erlotinib sensitive cells (Figure 3.5B). Knockdown of *EPHA2* also increased cleavage of caspase 3 and PARP (Figure 3.5C), confirming elevated apoptosis in erlotinib resistant cells. Signaling analysis from two independent cell lines that contain $EGFR^{T790M}$ mediated erlotinib resistance (PC-9/ERC16 and HCC827/ER) revealed that loss of *EPHA2* decreased phosphorylation of p90-RSK, S6 kinase 1, and the pro-apoptotic BH3-only protein BAD, whereas other effector proteins, including AKT and ERK, were not significantly affected by *EPHA2* loss (Figure 3.5D). These results consistently suggest a mechanism by which EPHA2 expression maintains cell viability in cells with acquired resistance to erlotinib by promoting both survival and proliferation pathways.

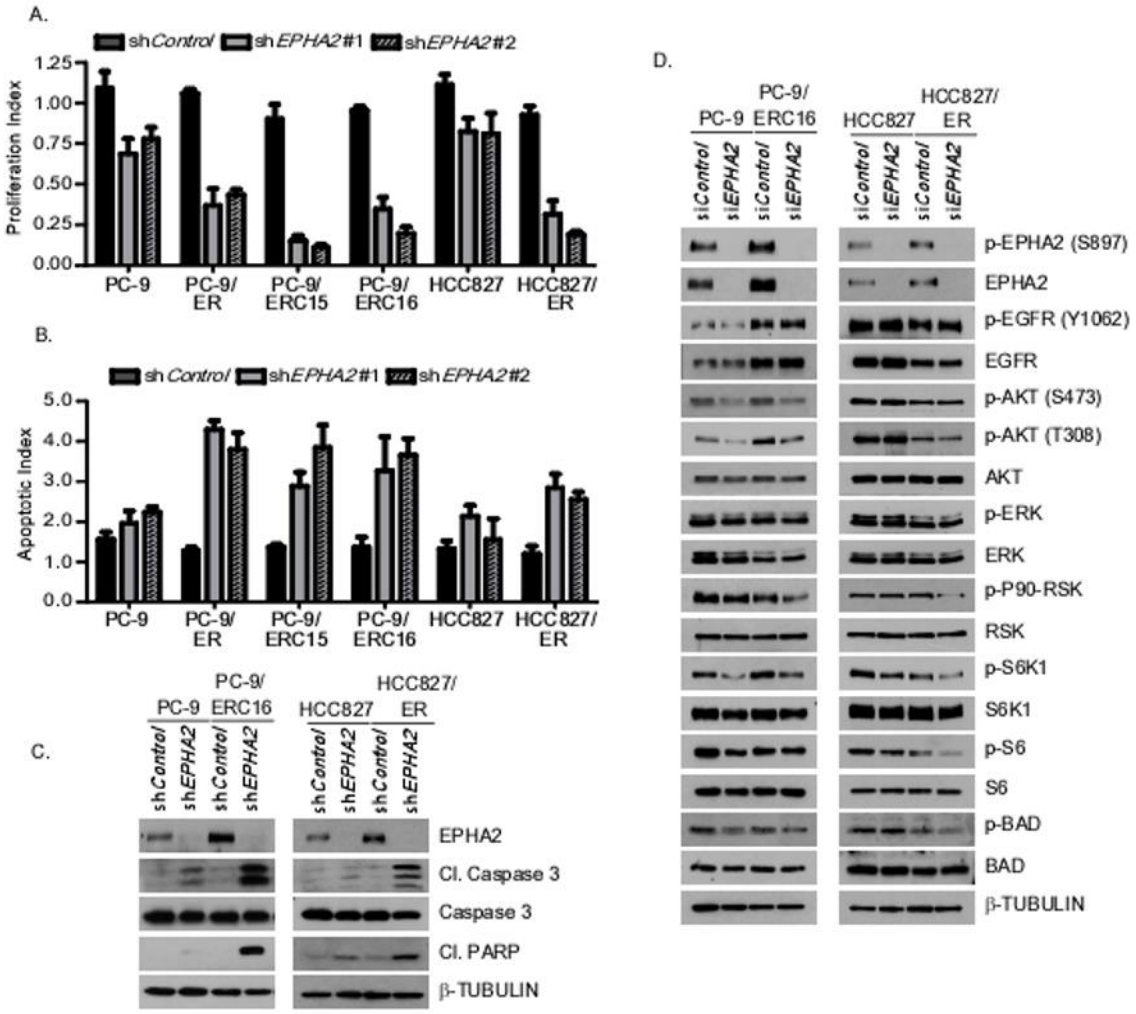

Figure 3.5 EPHA2 regulates cell signaling that promotes proliferation and survival. **(A)** Erlotinib sensitive and resistant cell lines were transduced with lentiviruses containing either sh*EPHA2* or a pLKO.1 vector control. The resulting cell populations were selected in 1.5µg/ml puromycin for 5 days. Proliferation was measured by quantifying incorporation of BrdU into the cellular DNA using the BrdU Cell Proliferation Assay kit. Experiments were repeated 3 times, and data are presented as a proliferation index relative to the sh*Control* ± SEM. **(B)** Apoptosis was measured by quantifying histone-associated DNA fragments using a Cell Death ELISA kit (Roche). Experiments were repeated 3 times, and data are presented as an apoptotic index relative to the sh*Control* ± SEM. **(C)** Western blot analysis for cleaved (Cl.) caspase 3 or PARP in lysates from erlotinib sensitive or resistant cells that had been treated with control (sh*Control*) or EPHA2 specific (sh*EPHA2*) shRNA. Lysates were collected 72 hours post-puromycin selection. **(D)** Signaling analysis on cell lysates from two pairs of isogenic erlotinib sensitive and resistant cell lines were treated with si*Control* or si*EPHA2* for 72 hours. Shown are representative immunoblots in which signaling molecules were detected with the indicated antibodies.

Pharmacologic inhibition of EPHA2 decreases cell survival of erlotinib resistant lung cancer cells in vitro and tumor growth in vivo.

To assess the value of pharmacological inhibition of EPHA2 in lung cancer subsets with acquired resistance to first-generation EGFR TKIs, we treated cells with an EPHA2 small molecule inhibitor, ALW-II-41-27, that was recently characterized for EPHA2 target engagement and specificity in the context lung cancer and melanoma both in vitro and in vivo (153, 233). NG-25, a structural analog that possesses a similar profile of kinase targets but does not inhibit EPHA2, was used as a control. We first assessed the effects of pharmacological inhibition of EPHA2 via ALW-II-41-27 on four cell lines with acquired resistance to erlotinib. TKI resistant cells treated with 1μM ALW-II-41-27 displayed a time-dependent decrease in the number of viable tumor cells with an average reduction of cell viability of 60% at 72 hours after drug treatment, whereas there was no significant change in the viability of cells treated with NG-25 at the same dose (Figure 3.6A). Additionally, treatment with 1μM ALW-II-41-27 decreased cell proliferation (Figure 3.6B) and increased apoptosis (Figure 3.6C) in erlotinib resistant cell lines. ALW-II-41-27-induced apoptosis was accompanied by the cleavage of caspase 3 and PARP as well as decreased expression of anti-apoptotic proteins BCL-xL and MCL-1 (Figure 3.6D). To assess the acute signaling consequences of targeting EPHA2 via ALW-II-41-27 treatment, cell lysates were collected from erlotinib sensitive and resistant lung cancer cells after treatment with 1μM ALW-II-41-27 for 6 hours. Signaling studies revealed decreased phosphorylation of key effector proteins such as p90-RSK, S6K1, S6, and BAD (Figure 3.6E), recapitulating the effects observed in *EPHA2* knockdown experiments. These data suggest that ALW-II-41-27 inhibits EPHA2 signaling pathways necessary to maintain proliferation and survival in erlotinib resistant *EGFR* mutant lung cancer cells.

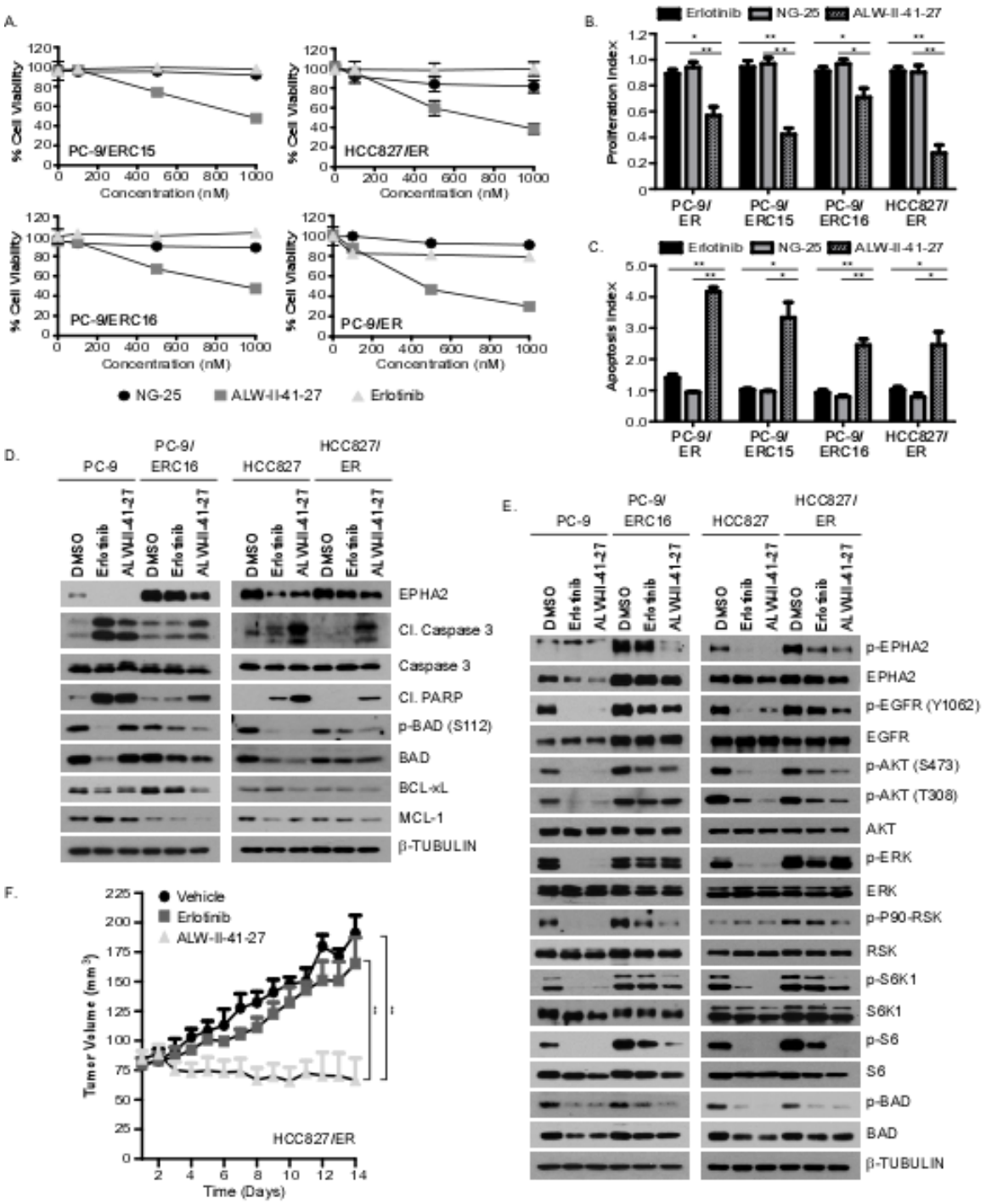

Figure 3.6 A selective EPHA2 small molecule inhibitor decreases cell survival of erlotinib resistant lung cancer cells in vitro and tumor growth in vivo. (A) Four cell lines with acquired resistance to erlotinib were treated with ALW-II-41-27, NG-25, erlotinib, or DMSO for 72 hours, and cell viability was assessed by the MTT assay. Shown are percentages of cell viability in drug treatment groups relative to a DMSO control group. **(B)** Cells were treated with 1μM ALW-II-41-27, NG-25, or erlotinib for 72 hours, and BrdU was added 2 hours prior to the commencement of the assay. Proliferation was measured by quantifying incorporation of BrdU into the cellular DNA

using the BrdU Cell Proliferation Assay kit. Experiments were repeated 3 times, and data are presented as a proliferation index relative to DMSO ± SEM. **(C)** Cells were treated as in B and apoptosis was measured by quantifying histone-associated DNA fragments using a Cell Death ELISA kit. Experiments were repeated 3 times, and data are presented as an apoptotic index relative to the DMSO ± SEM. **(D)** Immunoblotting for proteins involved in the apoptosis pathway from lysates of cells treated with 1μM ALW-II-41-27, 1μM erlotinib, or DMSO for 24 hours. **(E)** Pairs of erlotinib sensitive and resistant cells were treated with 1μM ALW-II-41-27, 1μM erlotinib, or DMSO for 6 hours. Phosphorylation of signaling molecules was determined by western blot analysis using anti-phospho and anti-total protein antibodies as indicated. **(F)** $2.5x10^6$ HCC827/ER cells were injected into the dorsal flanks of nude mice subcutaneously. Tumors were allowed to grow to ~$100mm^3$ before administration of 15mg/kg ALW-II-41-27, erlotinib, or vehicle alone via intraperitoneal injection twice daily. Tumors were measured every day with a digital caliper, and tumor volumes were calculated. (n = 5/treatment group). Data is presented as the mean body weight ± SEM.

To assess the utility and efficacy of ALW-II-41-27 on tumors with acquired resistance to erlotinib in vivo, we treated xenografted tumor cells (HCC827/ER) with ALW-II-41-27, erlotinib, or the vehicle alone twice a day at 15mg/kg via intraperitoneal injection. After 14 days of the treatment regimen, ALW-II-41-27 significantly inhibited the growth of the erlotinib resistant tumors (Figure 3.6F). Toxicity as measured by body weight was not significantly changed by any of the drugs compared to the vehicle over the course of this study (data not shown). These data indicate that pharmacological inhibition of EPHA2 may be advantageous in lung cancers with acquired resistance to erlotinib as inhibition of this receptor is able to mitigate key survival signaling pathways and induce an apoptotic phenotype.

Discussion

EGFR mutant lung tumors acquire resistance to TKIs through a variety of mechanisms, including secondary mutations within *EGFR* at position T790 (80), mutations in EGFR effector proteins (99, 375), histologic transformation (99), and upregulation of parallel RTKs (e.g. MET, HER2, and AXL) (101, 102, 105, 376). Here we have demonstrated that EPHA2 overexpression serves as an additional novel

mechanism of drug resistance particularly in *EGFR*^{T790M} mutant lung cancer. We found that knockdown of *EPHA2* resulted in decreased proliferation and increased apoptosis in erlotinib resistant cells with *EGFR*^{T790M} mutations. Genetic targeting of *EphA2* significantly inhibited *EGFR*$^{L858R+T790M}$ mutant lung tumor progression and prolonged overall survival in vivo. Furthermore, an EPHA2 small molecule inhibitor, ALW-II-41-27, mitigated viability of erlotinib resistant cells and reduced tumor growth in a xenograft model. These data suggest that pharmacological inhibition of EPHA2 may represent a viable, alternative strategy for treating *EGFR*^{T790M} mutant lung cancers harboring resistance to first-line EGFR TKI therapies.

The ability of EPHA2 to maintain cell viability in the context of tumorigenesis does not go without precedence. EPHA2 overexpression has been observed to contribute to tumorigenesis in a variety of tissues including breast, ovary, skin, brain, and lung (226, 227, 237, 377). Studies from our lab have demonstrated that EPHA2 has a distinct role in tumor promotion in the epithelial component of both breast and lung tumors as evidenced by targeted inhibition of EPHA2 in murine models of these tumor types (149, 153). Although the EPHA2 receptor has previously been shown to regulate RAS/MAPK signaling in breast cancer cells (149, 151), in *EGFR*^{T790M} mutant lung cancer loss of EPHA2 does not appear to significantly affect the activities of ERK, but rather modulates phosphorylation levels of p90-RSK, S6K1 (a known signaling component of mTORC1), and the pro-apoptotic protein BAD. These results are consistent with the recent findings that activation of mTORC1 is associated with acquired resistance of *EGFR* mutant lung cancer to combined EGFR inhibition via a TKI and cetuximab (88). mTORC2 has also been implicated in the maintenance of EGFR TKI resistant lung cancer (89), however the degree to which mTORC2 plays a role in EPHA2-mediated maintenance of cell viability in erlotinib resistant cells remains to be determined.

Targeting EPHA2 in EGFR TKI resistant lung tumors represents a unique opportunity for mitigating cell viability, as our studies have demonstrated that erlotinib resistant cells are more dependent on EPHA2 for cell viability than erlotinib sensitive cells (Figure 3.5A and 3.5B). Knockdown of *EPHA2* induced a greater than 3 fold increase in cell death and greater than 3 fold reduction in proliferation in erlotinib resistant cells relative to their parental, erlotinib sensitive counterparts. These data indicate a distinct addiction of $EGFR^{T790M}$ mutant lung tumors to EPHA2 for survival, and it may illuminate why RNAi-mediated EPHA2 knockdown experiments as well as pharmacologic inhibition of EPHA2 appear to be remarkably effective without the combination of other inhibitors. It is, however, possible that combination of an EPHA2 inhibitor in this context with inhibitors of other kinases such as EGFR, MEK, ERK, or IGF-1R, could further diminish cell survival. Additional investigation is needed to assess whether the EPHA2 signaling addiction observed is specific to the erlotinib-mediated development of $EGFR^{T790M}$ or if it is a universal feature of $EGFR^{T790M}$ resistance acquired in the presence of any EGFR TKI. Preliminary data from our lab indicates that cells with acquired resistance to two, unique second generation EGFR inhibitors, afatinib or XL-647, also display overexpression of EPHA2 compared to cells sensitive to these inhibitors and are highly sensitive to EPHA2 inhibition (Figure 3.1D and data not shown). Studies to characterize the role of EPHA2 in viability maintenance of *EGFR* mutant cells with acquired resistance to second and third generation EGFR TKIs is currently under investigation.

Although strategies to overcome $EGFR^{T790M}$ mediated TKI resistance are rapidly evolving, including but not limited to the development of $EGFR^{T790M}$ mutant-specific EGFR inhibitors (85) and the combination of second generation EGFR TKIs with antibodies against EGFR such as cetuximab (87), persistent treatment of a single target (e.g. EGFR) may make tumors more likely to engage in alternative, non-EGFR-related

bypass escape mechanisms (85). Recent studies indicate that optimizing the dose and sequence of TKI treatment may be an essential component in the effective treatment of *EGFR*^{T790M} disease (370, 378). We have observed that EPHA2 expression in *EGFR*^{T790M} mutant cells increases in a time-dependent fashion after being withdrawn from erlotinib (Figure 3.1E). Interestingly, there have been several clinical reports of patients with *EGFR*^{T790M} mutant lung tumors that exhibited a flare of tumor growth post TKI withdrawal (379-382). This could be due in part to the surge in EPHA2 expression we observe upon EGFR TKI withdrawal. It is quite possible that EPHA2 inhibition may be most efficacious in *EGFR*^{T790M} mutant tumors during an EGFR TKI "holiday", when EPHA2 levels are at their highest. Because EPHA2 inhibition preferentially eliminates EGFR TKI resistant cells over EGFR TKI sensitive cells (Figure 3.5A), it is reasonable to hypothesize that after a regimen of EPHA2 inhibition the tumor may be repopulated with more EGFR TKI sensitive cells and may re-respond to first-line EGFR TKIs. Thus, it may be possible in the future to treat *EGFR*^{T790M} mutant tumors with cycles of sequential EGFR TKIs followed by EPHA2 inhibitors with the ultimate goal of eradicating the both EGFR TKI sensitive and TKI resistant disease. Although the specificity and functional importance of the EPHA2 pharmacological inhibitor, ALW-II-41-27, has already been characterized previously in the context of lung cancer (153), further compound iterations are in development to enhance target specificity and pharmacodynamics in vivo.

In summary, we show that EPHA2 overexpression is required for survival of erlotinib resistant lung cancer, and that both genetic and pharmacologic inhibition of EPHA2 results in decreased survival and proliferation of cells with *EGFR*^{T790M} mediated, erlotinib resistance. These studies not only present evidence for the utility of EPHA2 inhibitors in the treatment of erlotinib resistant tumors, but also provide rationale for optimizing the sequence of treatment with existing first-generation EGFR inhibitors to maximize patient benefit.

CHAPTER IV

CONCLUSIONS AND FUTURE DIRECTIONS

Conclusions

In the last decade, considerable progress has been made to identify and characterize mutations, amplifications, deletions, and rearrangements that function to drive tumorigenesis in the lung epithelium. Although advancements have been made in translating these findings into therapeutic interventions, challenges still remain in developing effective and sustainable pharmacological inhibition in tumors with the most commonly observed mutations in lung cancer, *KRAS* and *EGFR*. To address these concerns and to identify novel targets for treatment, genome-wide expression analyses were completed to identify RTKs that were overexpressed and could represent potential drivers of lung cancer. Among the targets identified was the receptor tyrosine kinase, EPHA2. EPHA2 belongs to the EPH family of receptor tyrosine kinases which have been implicated in both normal and neoplastic development. In cancer, the role of EPH RTKs is variable and is largely dependent on the specific EPH receptors and ephrin ligands expressed, their relative concentrations on the cell surface, as well as the cell, tissue, and organ contexts. Therefore investigating EPH RTKs in specific tissue and disease contexts is essential for an informed understanding of the functional and mechanistic contributions of these receptors. EPHA2 has been found to be overexpressed in a large variety of cancers, including that of the lung. Although correlative data exists linking high EPHA2 expression with lower overall survival in lung cancer patients, a functional and mechanistic understanding underlying this relationship was nonexistent. The data in this thesis represents a step forward in understanding the contribution of EPHA2 in malignancies of the lung epithelium. Using a combination of in

vitro and in vivo models, we have demonstrated that EPHA2 promotes tumor cell survival and progression of both *KRAS* and *EGFR*^{T790M} mutant lung cancers. Moreover, we demonstrated the efficacy of a first-in-class, ATP competitive, small molecule EPHA2 tyrosine kinase inhibitor, ALW-II-41-27, both in vitro and in vivo. Together our finding have provided genetic, functional, mechanistic, and pharmacological evidence to define the role of EPHA2 in lung tumorigenesis. This work provides a basis for the continued investigation of EPHA2 in lung cancer in order to ultimately facilitate the translation and development of EPHA2 targeted therapeutics for clinical use.

Future Directions

Completion of the work described herein has contributed significantly to the understanding of the role of EPHA2 in lung cancer, particularly those harboring *KRAS* and *EGFR*^{T790M} mutations. At the same time it has raised many new questions regarding the mechanistic properties of EPHA2 and the therapeutic potential of using it as a drug target in cancer. A selection of these questions will be discussed below as a starting point for new avenues of discovery in the future.

<u>How is EPHA2 signaling regulated by the presence of different driver mutations in lung cancer?</u>

Previous studies have identified that EPHA2 is often overexpressed in tumor cells with ERBB pathway mutations (e.g. HER2, EGFR, RAS, and RAF), and that tumor cells of these genetic subtypes are often extraordinarily sensitive to EPHA2 inhibition (Chapter 3, (149, 153, 233)) as evidenced in breast, lung, and skin cancers, respectively. In these tumors, EPHA2 was found to regulate cell viability through modulation of the MAPK or PI3K/AKT pathways in a ligand independent manner. It is apparent that not all molecular subtypes in lung cancer maintain the same level of

dependency on EPHA2 for cell viability as evidenced by a lack of sensitivity to EPHA2 silencing in lung cancer cell lines with HER2 mutations and EML4-ALK rearrangements (Figure 2.4A). Understanding the underlying molecular mechanisms that confer dependency on EPHA2 expression and signaling will be essential for the effective use of EPHA2 as a therapeutic target and for effectively predicting clinical responses to EPHA2 targeting agents. The spectrum of dependency on EPHA2 for cell survival across known molecular subtypes of lung cancer is indicative of the diversity of signaling networks that these subtypes represent.

One mechanism by which EPHA2 acquires enhanced control of cell viability in certain genetic subtypes of lung cancer is through direct interaction with the oncogenic drivers. This has been evidenced by the ability of EPHA2 to directly interact with HER2 and amplify its signaling pathway in breast cancer (149). Although EGFR and EPHA2 have been observed to interact in previous studies (147), a direct interaction has not been assessed in *EGFR* mutant lung cancer cells. It is possible, however, that EPHA2 may interact directly with EGFR to promote and amplify its signaling in *EGFR* mutant lung tumors to enhance proliferation and survival. The ability of EPHA2 to interact with other common molecular drivers of lung cancer such as KRAS, FGFR, ALK, HER2, and MET is also an area which requires further investigation.

Another mechanism by which the dependency on EPHA2 may be controlled in the various molecular subtypes of lung cancer is through regulation of EPHA2 expression. It has been previously demonstrated that high EPHA2 expression correlates to poor overall survival outcomes in patients with lung cancer, although the means by which EPHA2 expression is regulated in the presence of various different genetic driver mutations in lung cancer is not entirely known. EPHA2 can be transcriptionally regulated by a number of factors such as EGFR, C-MYC, and p53 as has been evidenced previously (147, 151, 342, 343). In support of these findings, our lab has demonstrated

that EPHA2 expression increases in the presence of constitutive EGFR activation as evidenced by EGFR TKI resistance in lung cancer (Figure 3.1D). Additionally, another group found a similar phenomenon of elevated EPHA2 expression in the presence of BRAF TKI resistant melanoma (233). We also demonstrated that the removal of EGFR TKIs from erlotinib resistant cells could enhance EPHA2 expression in a time dependent manner, further corroborating the role of this pathway in regulating EPHA2 expression (Figure 3.1E). Further studies are needed to identify additional mechanisms by which EPHA2 expression can be regulated in different genetic subtypes of lung cancer to better define its role mechanistically and clinically in these contexts.

How does EPHA2 control cell viability in *KRAS* and *EGFR* mutant lung cancer?

As previously mentioned, although overexpression of EPHA2 had been established previously in lung cancer, its function and signaling capabilities in lung tumors were largely unstudied. Utilizing both RNAi-mediated silencing techniques and pharmacological inhibition, we determined that EPHA2 promotes signaling of both *KRAS* and $EGFR^{T790M}$ mutant lung tumors by promoting the activation of mTORC1 signaling pathway effectors such as p70-S6K1, S6, and BAD, which are known regulators of protein synthesis and cell survival (153). Although the contribution of mTORC1 signaling has been defined in *KRAS* and $EGFR^{T790M}$ mutant lung cancer, it is well established that the serine/threonine kinase, mTOR, can function in two distinct complexes, mTORC1 and mTORC2 to propagate signals (90, 91). Both mTOR complexes have been implicated in tumorigenesis and are known to regulate distinct activities and effectors. The predominant effectors of mTORC2 are AKT (S473), SGK1, and PKCα, which are known regulators of cell proliferation, survival, and cytoskeletal organization (91, 96-98). Although the work of this thesis has established the contribution of mTORC1 in *KRAS* and $EGFR^{T790M}$ mutant lung cancer, the relative contribution of mTORC2 to EPHA2

signaling remains to be investigated. Preliminary data reported in this thesis demonstrates that upon RNAi-mediated silencing of EPHA2, AKT phosphorylation at S473 is not significantly decreased in *KRAS* or *EGFR*^{T790M} mutant lung cancers (Figure 2.5D and Figure 3.5D). It remains to be investigated whether SGK1 or PKCα contribute to the EPHA2 mediated cell survival phenotype. To more clearly assess the relative influences of both mTOR complexes on EPHA2 mediated cell survival in *KRAS* and *EGFR*^{T790M} mutant lung cancer, studies silencing the mTORC1 subunit (Raptor) and the mTORC2 subunit (Rictor) may be useful.

In addition to the mTORC1 pathway, we also determined as a part of this thesis that EPHA2 could control phosphorylation of p90-RSK, a direct downstream effector of ERK, in both the *KRAS* and *EGFR*^{T790M} molecular subtypes of lung cancer. Currently, the mechanism by which EPHA2 regulates p90-RSK phosphorylation has not been fully elucidated, as its classical upstream effector, ERK, displayed no decrease in phosphorylation upon EPHA2 silencing (Figure 2.5D and Figure 3.5D). One possibility for this effect is that although p90-RSK may be primed for activation by ERK phosphorylation at Ser-369 and Thr-577, it is not able to be fully activated by subsequent PDK1 phosphorylation due to abrogated signals that result from EPHA2 inhibition (383). Determining the mechanism by which p90-RSK signaling is regulated downstream of EPHA2 would illuminate another key piece of this signaling network.

An additional signaling mechanism that remains to be explored involves the contribution of wild-type RAS isoforms to EPHA2 signaling particularly in *RAS* mutant lung cancer. Previous studies in rhabdomyosarcoma and bladder cancer identified that ligand mediated EPHA2 stimulation reduced GTP loading of wild-type RAS isoforms, while no change was detected in the GTP loading of mutant RAS (384). Additionally, the same study demonstrated that mutant, oncogenic *RAS* preferentially controlled basal MAPK signaling, while wild-type RAS proteins were primarily responsible for growth

factor induced signaling (384). Currently, it is not evident whether these signaling observations are universal to all *RAS* mutant cancers or *RAS* mutant cancers of the lung. Although these studies were performed in a ligand dependent model system, EPHA2 signaling is thought to occur in a ligand independent fashion in the endogenous lung tumor environment (362). It is therefore possible that the RAS signaling effects observed from these studies may not accurately represent relevant contributions of the RAS isoforms in EPHA2 signaling as displayed in lung tumors. Inducible, RNAi mediated silencing or pharmacological inhibition of EPHA2 may provide a more precise depiction of the extent to which EPHA2 regulates the activation of the various RAS isoforms in the context of lung tumorigenesis. To test this experimentally, RAS activity can be measured in various *RAS* mutant lung cancer cell lines by assessing the relative GTP loading in both wild-type and mutant *RAS* isoforms after EPHA2 inhibition. Understanding how EPHA2 regulates the activation and distinct roles of wild-type and mutant *RAS* isoforms may reveal novel vulnerabilities useful for enhancing the efficacy of EPHA2 targeted therapy in this difficult-to-treat molecular subset of lung cancer.

How does EPHA2 inhibition affect the lung tumor architecture?

A unique feature of EPH-ephrin signaling complexes is the necessity of cell-cell contact for ligand mediated receptor activation due to the membrane bound nature of both the receptor and ligand. In lung cancer, a combination of cellular disorganization and EPHA2 receptor overexpression, greatly limits the interactions between EPHA2 and its preferential ligand, ephrinA1, making the majority of EPHA2 signaling that occurs ligand independent. Currently, the extent to which inhibiting EPHA2 either genetically or pharmacologically can restore cellular adhesion, polarity, and organization of lung tumor cells has not been studied, although transgenic animal models of lung cancer with $EPHA2^{+/+}$ and $EPHA2^{-/-}$ would be ideal for this investigation. As mentioned above a key

component in EPHA2 mediated cellular organization involves proximity of the ligand, ephrinA1, to the EPHA2 receptor. Future studies should include investigation of the contribution of ephrinA1 expression and reverse signaling in lung tumorigenesis and tissue organization both in the presence and absence of EPHA2 expression and activity.

How does EPHA2 inhibition affect the lung tumor microenvironment?

The studies described in this dissertation have largely focused on the role of EPHA2 in the tumor epithelium, but the contribution of this receptor in the microenvironment should not be overlooked. Although EPHA2 has been found to be expressed at low levels in the developing and quiescent adult vasculature, studies performed in breast cancer discovered that EPHA2 was highly expressed in the tumor vasculature and could contribute to angiogenesis. To investigate the role of EPHA2 in lung tumor vasculature, we assessed the tumor microvasculature in two independent murine models of lung cancer (e.g. $Kras^{G12D}$ and $EGFR^{L858R+T790M}$) with EPHA2 depletion ($EphA2^{-/-}$) as measured by von Willebrand factor staining. Although a mild decrease in tumor microvessels was observed in the context of EPHA2 silencing, this result was not statistically significant in either murine model of lung cancer.

Other components of the tumor microenvironment such as the immune cells have not been assessed in the context of EPHA2 inhibition in lung cancer. As inhibitors are further developed to target EPHA2 in the clinical setting, it will be important to understand the immunological consequences of blocking this receptor on both epithelial cells and immune cells. It is well established that $CD8^+$ T cells are critical in regulating the host immune response to tumor malignancies. Furthermore, immune evasion by tumors is achieved through an intrinsic mechanism to downregulate T cell effector functions in a process termed exhaustion (385-390). This impairment of the $CD8^+$ T cell response is driven by the presence of multiple inhibitory receptors expressed on the

surface of T cells and their interaction with ligands on tumor tissue as well as in the tumor microenvironment. Upon EPHA2 inhibition, either genetically or pharmacologically, the expression of T cell inhibitory ligands such as PD-L1 and PD-L2, CD80, and MHCII on tumor cells as well as on antigen presenting cells (APC) at the tumor site, should be assessed to determine the extent to which EPHA2 signaling is capable of regulating the expression of these proteins (391, 392).

In addition to measuring the expression of inhibitory ligands on the surface of tumor cells, the effects of inhibiting EPHA2 on tumor-infiltrating $CD8^+$ T cells should also be investigated. Initially, EPHA2 expression and activity in $CD8^+$ T cells should be assessed upon treatment with a specific EPHA2 inhibitor to determine this cell type's level of dependency on EPHA2. Next, the effect of EPHA2 inhibition on $CD8^+$ T cell proliferation should be quantified using proliferative markers, such as Ki67. Additionally, tumor-specific $CD8^+$ T cell quantity and functionality could be measured by using fluorescently conjugated MHC class I tetramers loaded with peptides specific for tumor tissue (393, 394) in tandem with intracellular cytokine staining to assess the expression of effector molecules, such as IFNγ and TNFα (395), as well as markers of degranulation, like CD107a, in these cells (396). In a clinical setting, treatment with an EPHA2 inhibitor will occur after priming and maturation of a tumor-specific $CD8^+$ T cell response, so even if EPHA2 negatively affects T cell proliferation an increase in T cell functionality could still significantly impair tumor progression. In addition to assays to test T cell functionality as mentioned above, it will also be useful to determine the level of T cell exhaustion in the context of EPHA2 inhibition, by measuring expression of markers such as PD1, CTLA4, TIM3, LAG3, and 2B4. These markers of exhaustion progressively increase in expression as chronic stimulation with tumor antigens continues, and they actively induce negative signals to inhibit T cell receptor activation (392). The expression of these markers on tumor antigen specific as well as bulk $CD8^+$

T cells can be measured over the course of EPHA2 inhibition using flow cytometry. Depending on the contribution of EPHA2 in the regulation of the T cell exhaustion phenotype, it may be advantageous to use sequential or combination treatment of an EPHA2 inhibitor with blockade of these inhibitory receptors to enhance T cell functionality and increase the efficacy of EPHA2 targeted agents.

Can better biomarkers be defined to predict sensitivity to EPHA2 inhibition?

Although this dissertation has focused exclusively on targeting EPHA2 in lung cancer, overexpression of EPHA2 is found in a variety of other tumor types and may be a useful target for inhibition in those cancer types as well. As discovered in lung cancer, total EPHA2 expression does not directly correlate with sensitivity to EPHA2 inhibition, therefore other markers are essential in predicting sensitivity (Figure 2.2B and Figure 2.2C). It is possible that sensitivity to EPHA2 may positively correlate to specific genetic subtypes both in lung cancer and other cancers. As we discovered in lung cancer, EPHA2 sensitivity positively correlated to phosphorylated levels of EPHA2 as well as *KRAS* mutations and $EGFR^{T790M}$ mutations. Sensitivity to EPHA2 inhibition should be evaluated in tumors of other tissue types that also harbor high levels of EPHA2 phosphorylation, *KRAS* mutations, or *EGFR* mutations to assess if these dependencies are universal or if they are genotype or tissue specific. If sensitivity to EPHA2 targeting is genotype specific, it is likely that other tumors harboring constitutive MAPK signaling may benefit from EPHA2 inhibition such as *KRAS* mutant pancreatic and colon cancers.

Additionally, EPHA2 overexpression in a variety of TKI resistant tumor tissues including those resistant to trastuzumab, vemurafenib, and erlotinib, correlates with sensitivity to EPHA2 inhibition. Identifying if EPHA2 overexpression is a universal mechanism contributing to acquired resistance to TKIs or if is a MAPK-centric

mechanism of acquired resistance will help predict sensitivity by determining which molecular subtypes of cancer will be sensitive to EPHA2 inhibition.

Can the efficacy of the EPHA2 inhibitor, ALW-II-41-27, be enhanced?

Although the development of a first-in-class, type II, ATP-competitive, small molecule inhibitor of EPHA2 (ALW-II-41-27) has been developed, pharmacokinetic analysis of ALW-II-41-27 following intravenous (1 mg/kg) and oral administration (10 mg/kg) revealed a relatively short half-life ($t_{1/2}$ = 0.83 hour), low plasma exposure (AUC = 333.7 nM/l), and low oral bioavailability (bioavailability = 24.6%). Efforts to overcome these challenges have begun with the development of new iterations of this inhibitor to try to improve the pharmacokinetics. Compound development is currently underway.

In addition to drug development, combining therapy with ALW-II-41-27 may be useful in enhancing the efficacy of this small molecule inhibitor. In lung cancer combination of MEK (trametinib) or EGFR (erlotinib, afatinib, AZD9291) inhibitors with the EPHA2 inhibitor (ALW-II-41-27) may be useful in promoting an additive or synergistic therapeutic response in the most common molecular subtypes of lung cancer, *KRAS* and *EGFR* mutant, respectively. Alternatively, because MAPK pathway activation is known to transcriptionally regulate EPHA2 expression, co-treatment with an EGFR TKI or RAS pathway inhibitor may also limit therapeutic potential as these compounds downregulate EPHA2 expression theoretically shifting the dependence away from EPHA2 for viability and survival. Future studies are needed to assess the effects of EPHA2 therapy combinations.

Recent studies indicate that optimizing the dose and sequence of TKI treatment may be an essential component in the effective treatment of $EGFR^{T790M}$ disease (370, 378). We have observed that EPHA2 expression in $EGFR^{T790M}$ mutant cells increases in

a time-dependent fashion after being withdrawn from erlotinib (Figure 3.1E). Interestingly, there have been several clinical reports of patients with *EGFR*^{T790M} mutant lung tumors that exhibited a flare of tumor growth post TKI withdrawal (379-382). This could be due in part to the surge in EPHA2 expression we observe upon EGFR TKI withdrawal. It is quite possible that EPHA2 inhibition may be most efficacious in *EGFR*^{T790M} mutant tumors during an EGFR TKI "holiday", when EPHA2 levels are at their highest. Because EPHA2 inhibition preferentially eliminates EGFR TKI resistant cells over EGFR TKI sensitive cells (Figure 3.2C), it is reasonable to hypothesize that after a regimen of EPHA2 inhibition the tumor may be repopulated with more EGFR TKI sensitive cells and may re-respond to first-line EGFR TKIs. Thus, it may be possible in the future to treat *EGFR*^{T790M} mutant tumors with cycles of sequential EGFR TKIs followed by EPHA2 inhibitors with the ultimate goal of eradicating both EGFR TKI sensitive and TKI resistant disease.

Concluding remarks

The results reported in this thesis have made a significant step forward in the understanding of the functional and mechanistic contributions of EPHA2 in *KRAS* and *EGFR*^{T790M} mutant lung cancer. At the same time, much work still remains in the understanding of how this receptor is regulated by different genetic drivers and in the development and optimization of EPHA2 inhibitors for clinical use. With emerging technology and the accumulation of knowledge regarding the role of EPH family members as well as genetic drivers in lung cancer, further mechanistic understanding of EPHA2 along with clinical translation of these findings are imminent.

REFERENCES

1. Siegel RL, Miller KD, Jemal A. Cancer statistics, 2015. CA: a cancer journal for clinicians. 2015;65:5-29.

2. The Health Consequences of Smoking: A Report of the Surgeon General. In: Services USDoHaH, editor. US Department of Health and Human Services, Centers for Disease Control and Prevention, National Center for Chronic Disease Prevention and Health Promotion, Office on Smoking and Health2004.

3. McDonald JC, McDonald AD. Asbestos and carcinogenicity. Science. 1990;249:844.

4. Samet JM. Radon and lung cancer. Journal of the National Cancer Institute. 1989;81:745-57.

5. Wada S, Miyanishi M, Nishimoto Y, Kambe S, Miller RW. Mustard gas as a cause of respiratory neoplasia in man. Lancet. 1968;1:1161-3.

6. Redmond CK. Cancer mortality among coke oven workers. Environmental health perspectives. 1983;52:67-73.

7. Pasternack BS, Shore RE, Albert RE. Occupational exposure to chloromethyl ethers. A retrospective cohort mortality study (1948-1972). Journal of occupational medicine : official publication of the Industrial Medical Association. 1977;19:741-6.

8. Alderson MR, Rattan NS, Bidstrup L. Health of workmen in the chromate-producing industry in Britain. British journal of industrial medicine. 1981;38:117-24.

9. Doll R. Nickel exposure: a human health hazard. IARC scientific publications. 1984:3-21.

10. Pershagen G. Lung cancer mortality among men living near an arsenic-emitting smelter. American journal of epidemiology. 1985;122:684-94.

11. Abeloff MDA, J.O.; Niederhuber, J.E.; Kastan, M.B.; McKenna, W.G. Clinical Oncology 3rd Edition. Philadelphia: Elsevier; 2004.

12. Kantarjian HMW, R.A.; Koller, C.A. The MD Anderson Manual of Medical Oncology 2nd Edition. New York: McGraw-Hill Medical; 2011.

13. Kumar VA, A.K.; Aster J.C. Robbins and Cotran Pathologic Basis of Disease. Philadelphia: Elsevier Saunders; 2015.

14. Hansen HH, Selawry OS, Simon R, Carr DT, van Wyk CE, Tucker RD, et al. Combination chemotherapy of advanced lung cancer: a randomized trial. Cancer. 1976;38:2201-7.

15. Weinstein IB. Cancer. Addiction to oncogenes--the Achilles heal of cancer. Science. 2002;297:63-4.

16. Lovly CM, L. H, W. P. Molecular Profiling of Lung Cancer. My Cancer Genome. 2014; Available from: http://www.mycancergenome.org/content/disease/lung-cancer/

17. Tam IY, Chung LP, Suen WS, Wang E, Wong MC, Ho KK, et al. Distinct epidermal growth factor receptor and KRAS mutation patterns in non-small cell lung cancer patients with different tobacco exposure and clinicopathologic features. Clinical cancer research : an official journal of the American Association for Cancer Research. 2006;12:1647-53.

18. Gealy R, Zhang L, Siegfried JM, Luketich JD, Keohavong P. Comparison of mutations in the p53 and K-ras genes in lung carcinomas from smoking and nonsmoking women. Cancer epidemiology, biomarkers & prevention : a publication of the American Association for Cancer Research, cosponsored by the American Society of Preventive Oncology. 1999;8:297-302.

19. Husgafvel-Pursiainen K, Hackman P, Ridanpaa M, Anttila S, Karjalainen A, Partanen T, et al. K-ras mutations in human adenocarcinoma of the lung: association with smoking and occupational exposure to asbestos. International journal of cancer Journal international du cancer. 1993;53:250-6.

20. Westra WH. Early glandular neoplasia of the lung. Respiratory research. 2000;1:163-9.

21. Miller VA, Kris MG, Shah N, Patel J, Azzoli C, Gomez J, et al. Bronchioloalveolar pathologic subtype and smoking history predict sensitivity to gefitinib in advanced non-small-cell lung cancer. Journal of clinical oncology : official journal of the American Society of Clinical Oncology. 2004;22:1103-9.

22. Weinberg RA. The Biology of Cancer. New York: Garland Science; 2007.

23. Schlessinger J. Cell signaling by receptor tyrosine kinases. Cell. 2000;103:211-25.

24. Ahearn IM, Haigis K, Bar-Sagi D, Philips MR. Regulating the regulator: post-translational modification of RAS. Nature reviews Molecular cell biology. 2012;13:39-51.

25. Marshall CJ. Specificity of receptor tyrosine kinase signaling: transient versus sustained extracellular signal-regulated kinase activation. Cell. 1995;80:179-85.

26. Gavin AC, Nebreda AR. A MAP kinase docking site is required for phosphorylation and activation of p90(rsk)/MAPKAP kinase-1. Current biology : CB. 1999;9:281-4.

27. Chen RH, Abate C, Blenis J. Phosphorylation of the c-Fos transrepression domain by mitogen-activated protein kinase and 90-kDa ribosomal S6 kinase. Proceedings of the National Academy of Sciences of the United States of America. 1993;90:10952-6.

28. Xing J, Ginty DD, Greenberg ME. Coupling of the RAS-MAPK pathway to gene activation by RSK2, a growth factor-regulated CREB kinase. Science. 1996;273:959-63.

29. Waskiewicz AJ, Flynn A, Proud CG, Cooper JA. Mitogen-activated protein kinases activate the serine/threonine kinases Mnk1 and Mnk2. The EMBO journal. 1997;16:1909-20.

30. Deak M, Clifton AD, Lucocq LM, Alessi DR. Mitogen- and stress-activated protein kinase-1 (MSK1) is directly activated by MAPK and SAPK2/p38, and may mediate activation of CREB. The EMBO journal. 1998;17:4426-41.

31. Gupta P, Prywes R. ATF1 phosphorylation by the ERK MAPK pathway is required for epidermal growth factor-induced c-jun expression. The Journal of biological chemistry. 2002;277:50550-6.

32. Wiggin GR, Soloaga A, Foster JM, Murray-Tait V, Cohen P, Arthur JS. MSK1 and MSK2 are required for the mitogen- and stress-induced phosphorylation of CREB and ATF1 in fibroblasts. Molecular and cellular biology. 2002;22:2871-81.

33. Soloaga A, Thomson S, Wiggin GR, Rampersaud N, Dyson MH, Hazzalin CA, et al. MSK2 and MSK1 mediate the mitogen- and stress-induced phosphorylation of histone H3 and HMG-14. The EMBO journal. 2003;22:2788-97.

34. Marais R, Wynne J, Treisman R. The SRF accessory protein Elk-1 contains a growth factor-regulated transcriptional activation domain. Cell. 1993;73:381-93.

35. Sears R, Nuckolls F, Haura E, Taya Y, Tamai K, Nevins JR. Multiple Ras-dependent phosphorylation pathways regulate Myc protein stability. Genes & development. 2000;14:2501-14.

36. Felton-Edkins ZA, Fairley JA, Graham EL, Johnston IM, White RJ, Scott PH. The mitogen-activated protein (MAP) kinase ERK induces tRNA synthesis by phosphorylating TFIIIB. The EMBO journal. 2003;22:2422-32.

37. Stefanovsky VY, Pelletier G, Hannan R, Gagnon-Kugler T, Rothblum LI, Moss T. An immediate response of ribosomal transcription to growth factor stimulation in mammals is mediated by ERK phosphorylation of UBF. Molecular cell. 2001;8:1063-73.

38. Stephen AG, Esposito D, Bagni RK, McCormick F. Dragging ras back in the ring. Cancer cell. 2014;25:272-81.

39. Tian X, Rusanescu G, Hou W, Schaffhausen B, Feig LA. PDK1 mediates growth factor-induced Ral-GEF activation by a kinase-independent mechanism. The EMBO journal. 2002;21:1327-38.

40. Chong H, Vikis HG, Guan KL. Mechanisms of regulating the Raf kinase family. Cellular signalling. 2003;15:463-9.

41. Kato K, Cox AD, Hisaka MM, Graham SM, Buss JE, Der CJ. Isoprenoid addition to Ras protein is the critical modification for its membrane association and transforming

activity. Proceedings of the National Academy of Sciences of the United States of America. 1992;89:6403-7.

42. Gysin S, Salt M, Young A, McCormick F. Therapeutic strategies for targeting ras proteins. Genes & cancer. 2011;2:359-72.

43. Cho KN, Lee KI. Chemistry and biology of Ras farnesyltransferase. Archives of pharmacal research. 2002;25:759-69.

44. Berndt N, Hamilton AD, Sebti SM. Targeting protein prenylation for cancer therapy. Nature reviews Cancer. 2011;11:775-91.

45. Downward J. Targeting RAS signalling pathways in cancer therapy. Nature reviews Cancer. 2003;3:11-22.

46. Stanley LA. Molecular aspects of chemical carcinogenesis: the roles of oncogenes and tumour suppressor genes. Toxicology. 1995;96:173-94.

47. Johnson L, Mercer K, Greenbaum D, Bronson RT, Crowley D, Tuveson DA, et al. Somatic activation of the K-ras oncogene causes early onset lung cancer in mice. Nature. 2001;410:1111-6.

48. Barbacid M. ras genes. Annual review of biochemistry. 1987;56:779-827.

49. Prior IA, Lewis PD, Mattos C. A comprehensive survey of Ras mutations in cancer. Cancer research. 2012;72:2457-67.

50. Ihle NT, Byers LA, Kim ES, Saintigny P, Lee JJ, Blumenschein GR, et al. Effect of KRAS oncogene substitutions on protein behavior: implications for signaling and clinical outcome. Journal of the National Cancer Institute. 2012;104:228-39.

51. John J, Sohmen R, Feuerstein J, Linke R, Wittinghofer A, Goody RS. Kinetics of interaction of nucleotides with nucleotide-free H-ras p21. Biochemistry. 1990;29:6058-65.

52. Shirasawa S, Furuse M, Yokoyama N, Sasazuki T. Altered growth of human colon cancer cell lines disrupted at activated Ki-ras. Science. 1993;260:85-8.

53. Brummelkamp TR, Bernards R, Agami R. Stable suppression of tumorigenicity by virus-mediated RNA interference. Cancer cell. 2002;2:243-7.

54. Ghobrial IM, Adjei AA. Inhibitors of the ras oncogene as therapeutic targets. Hematology/oncology clinics of North America. 2002;16:1065-88.

55. End DW, Smets G, Todd AV, Applegate TL, Fuery CJ, Angibaud P, et al. Characterization of the antitumor effects of the selective farnesyl protein transferase inhibitor R115777 in vivo and in vitro. Cancer research. 2001;61:131-7.

56. Sun J, Qian Y, Hamilton AD, Sebti SM. Ras CAAX peptidomimetic FTI 276 selectively blocks tumor growth in nude mice of a human lung carcinoma with K-Ras mutation and p53 deletion. Cancer research. 1995;55:4243-7.

57. Sun J, Qian Y, Hamilton AD, Sebti SM. Both farnesyltransferase and geranylgeranyltransferase I inhibitors are required for inhibition of oncogenic K-Ras prenylation but each alone is sufficient to suppress human tumor growth in nude mouse xenografts. Oncogene. 1998;16:1467-73.

58. Gjertsen MK, Gaudernack G. Mutated Ras peptides as vaccines in immunotherapy of cancer. Vox sanguinis. 1998;74 Suppl 2:489-95.

59. Fossum B, Olsen AC, Thorsby E, Gaudernack G. CD8+ T cells from a patient with colon carcinoma, specific for a mutant p21-Ras-derived peptide (Gly13-->Asp), are cytotoxic towards a carcinoma cell line harbouring the same mutation. Cancer immunology, immunotherapy : CII. 1995;40:165-72.

60. Friday BB, Adjei AA. K-ras as a target for cancer therapy. Biochimica et biophysica acta. 2005;1756:127-44.

61. Sebolt-Leopold JS, Dudley DT, Herrera R, Van Becelaere K, Wiland A, Gowan RC, et al. Blockade of the MAP kinase pathway suppresses growth of colon tumors in vivo. Nature medicine. 1999;5:810-6.

62. Hynes NE, Lane HA. ERBB receptors and cancer: the complexity of targeted inhibitors. Nature reviews Cancer. 2005;5:341-54.

63. Pao W, Chmielecki J. Rational, biologically based treatment of EGFR-mutant non-small-cell lung cancer. Nature reviews Cancer. 2010;10:760-74.

64. Mendelsohn J, Baselga J. Status of epidermal growth factor receptor antagonists in the biology and treatment of cancer. Journal of clinical oncology : official journal of the American Society of Clinical Oncology. 2003;21:2787-99.

65. Fukuoka M, Yano S, Giaccone G, Tamura T, Nakagawa K, Douillard JY, et al. Multi-institutional randomized phase II trial of gefitinib for previously treated patients with advanced non-small-cell lung cancer (The IDEAL 1 Trial) [corrected]. Journal of clinical oncology : official journal of the American Society of Clinical Oncology. 2003;21:2237-46.

66. Lynch TJ, Bell DW, Sordella R, Gurubhagavatula S, Okimoto RA, Brannigan BW, et al. Activating mutations in the epidermal growth factor receptor underlying responsiveness of non-small-cell lung cancer to gefitinib. The New England journal of medicine. 2004;350:2129-39.

67. Pao W, Miller V, Zakowski M, Doherty J, Politi K, Sarkaria I, et al. EGF receptor gene mutations are common in lung cancers from "never smokers" and are associated with sensitivity of tumors to gefitinib and erlotinib. Proceedings of the National Academy of Sciences of the United States of America. 2004;101:13306-11.

68. Paez JG, Janne PA, Lee JC, Tracy S, Greulich H, Gabriel S, et al. EGFR mutations in lung cancer: correlation with clinical response to gefitinib therapy. Science. 2004;304:1497-500.

69. Riely GJ, Politi KA, Miller VA, Pao W. Update on epidermal growth factor receptor mutations in non-small cell lung cancer. Clinical cancer research : an official journal of the American Association for Cancer Research. 2006;12:7232-41.

70. Mok TS, Wu YL, Thongprasert S, Yang CH, Chu DT, Saijo N, et al. Gefitinib or carboplatin-paclitaxel in pulmonary adenocarcinoma. The New England journal of medicine. 2009;361:947-57.

71. Mitsudomi T, Morita S, Yatabe Y, Negoro S, Okamoto I, Tsurutani J, et al. Gefitinib versus cisplatin plus docetaxel in patients with non-small-cell lung cancer harbouring mutations of the epidermal growth factor receptor (WJTOG3405): an open label, randomised phase 3 trial. The Lancet Oncology. 2010;11:121-8.

72. Gong Y, Somwar R, Politi K, Balak M, Chmielecki J, Jiang X, et al. Induction of BIM is essential for apoptosis triggered by EGFR kinase inhibitors in mutant EGFR-dependent lung adenocarcinomas. PLoS medicine. 2007;4:e294.

73. Costa DB, Nguyen KS, Cho BC, Sequist LV, Jackman DM, Riely GJ, et al. Effects of erlotinib in EGFR mutated non-small cell lung cancers with resistance to gefitinib. Clinical cancer research : an official journal of the American Association for Cancer Research. 2008;14:7060-7.

74. Cragg MS, Kuroda J, Puthalakath H, Huang DC, Strasser A. Gefitinib-induced killing of NSCLC cell lines expressing mutant EGFR requires BIM and can be enhanced by BH3 mimetics. PLoS medicine. 2007;4:1681-89; discussion 90.

75. Deng J, Shimamura T, Perera S, Carlson NE, Cai D, Shapiro GI, et al. Proapoptotic BH3-only BCL-2 family protein BIM connects death signaling from epidermal growth factor receptor inhibition to the mitochondrion. Cancer research. 2007;67:11867-75.

76. Faber AC, Wong KK, Engelman JA. Differences underlying EGFR and HER2 oncogene addiction. Cell cycle. 2010;9:851-2.

77. Jackman DM, Yeap BY, Sequist LV, Lindeman N, Holmes AJ, Joshi VA, et al. Exon 19 deletion mutations of epidermal growth factor receptor are associated with prolonged survival in non-small cell lung cancer patients treated with gefitinib or erlotinib. Clinical cancer research : an official journal of the American Association for Cancer Research. 2006;12:3908-14.

78. Riely GJ, Pao W, Pham D, Li AR, Rizvi N, Venkatraman ES, et al. Clinical course of patients with non-small cell lung cancer and epidermal growth factor receptor exon 19 and exon 21 mutations treated with gefitinib or erlotinib. Clinical cancer research : an official journal of the American Association for Cancer Research. 2006;12:839-44.

79. Kobayashi S, Boggon TJ, Dayaram T, Janne PA, Kocher O, Meyerson M, et al. EGFR mutation and resistance of non-small-cell lung cancer to gefitinib. The New England journal of medicine. 2005;352:786-92.

80. Pao W, Miller VA, Politi KA, Riely GJ, Somwar R, Zakowski MF, et al. Acquired resistance of lung adenocarcinomas to gefitinib or erlotinib is associated with a second mutation in the EGFR kinase domain. PLoS medicine. 2005;2:e73.

81. Yun CH, Mengwasser KE, Toms AV, Woo MS, Greulich H, Wong KK, et al. The T790M mutation in EGFR kinase causes drug resistance by increasing the affinity for ATP. Proceedings of the National Academy of Sciences of the United States of America. 2008;105:2070-5.

82. Sos ML, Rode HB, Heynck S, Peifer M, Fischer F, Kluter S, et al. Chemogenomic profiling provides insights into the limited activity of irreversible EGFR Inhibitors in tumor cells expressing the T790M EGFR resistance mutation. Cancer research. 2010;70:868-74.

83. Kwak EL, Sordella R, Bell DW, Godin-Heymann N, Okimoto RA, Brannigan BW, et al. Irreversible inhibitors of the EGF receptor may circumvent acquired resistance to gefitinib. Proceedings of the National Academy of Sciences of the United States of America. 2005;102:7665-70.

84. Li D, Ambrogio L, Shimamura T, Kubo S, Takahashi M, Chirieac LR, et al. BIBW2992, an irreversible EGFR/HER2 inhibitor highly effective in preclinical lung cancer models. Oncogene. 2008;27:4702-11.

85. Cross DA, Ashton SE, Ghiorghiu S, Eberlein C, Nebhan CA, Spitzler PJ, et al. AZD9291, an Irreversible EGFR TKI, Overcomes T790M-Mediated Resistance to EGFR Inhibitors in Lung Cancer. Cancer discovery. 2014;4:1046-61.

86. Finlay MR, Anderton M, Ashton S, Ballard P, Bethel PA, Box MR, et al. Discovery of a Potent and Selective EGFR Inhibitor (AZD9291) of Both Sensitizing and T790M Resistance Mutations That Spares the Wild Type Form of the Receptor. Journal of medicinal chemistry. 2014;57:8249-67.

87. Regales L, Gong Y, Shen R, de Stanchina E, Vivanco I, Goel A, et al. Dual targeting of EGFR can overcome a major drug resistance mutation in mouse models of EGFR mutant lung cancer. The Journal of clinical investigation. 2009;119:3000-10.

88. Pirazzoli V, Nebhan C, Song X, Wurtz A, Walther Z, Cai G, et al. Acquired resistance of EGFR-mutant lung adenocarcinomas to afatinib plus cetuximab is associated with activation of mTORC1. Cell reports. 2014;7:999-1008.

89. Fei SJ, Zhang XC, Dong S, Cheng H, Zhang YF, Huang L, et al. Targeting mTOR to overcome epidermal growth factor receptor tyrosine kinase inhibitor resistance in non-small cell lung cancer cells. PloS one. 2013;8:e69104.

90. Laplante M, Sabatini DM. mTOR Signaling. Cold Spring Harbor perspectives in biology. 2012;4.

91. Zoncu R, Efeyan A, Sabatini DM. mTOR: from growth signal integration to cancer, diabetes and ageing. Nature reviews Molecular cell biology. 2011;12:21-35.

92. Franke TF, Yang SI, Chan TO, Datta K, Kazlauskas A, Morrison DK, et al. The protein kinase encoded by the Akt proto-oncogene is a target of the PDGF-activated phosphatidylinositol 3-kinase. Cell. 1995;81:727-36.

93. Pullen N, Thomas G. The modular phosphorylation and activation of p70s6k. FEBS letters. 1997;410:78-82.

94. del Peso L, Gonzalez-Garcia M, Page C, Herrera R, Nunez G. Interleukin-3-induced phosphorylation of BAD through the protein kinase Akt. Science. 1997;278:687-9.

95. Datta SR, Dudek H, Tao X, Masters S, Fu H, Gotoh Y, et al. Akt phosphorylation of BAD couples survival signals to the cell-intrinsic death machinery. Cell. 1997;91:231-41.

96. Sarbassov DD, Guertin DA, Ali SM, Sabatini DM. Phosphorylation and regulation of Akt/PKB by the rictor-mTOR complex. Science. 2005;307:1098-101.

97. Jacinto E, Loewith R, Schmidt A, Lin S, Ruegg MA, Hall A, et al. Mammalian TOR complex 2 controls the actin cytoskeleton and is rapamycin insensitive. Nature cell biology. 2004;6:1122-8.

98. Sparks CA, Guertin DA. Targeting mTOR: prospects for mTOR complex 2 inhibitors in cancer therapy. Oncogene. 2010;29:3733-44.

99. Sequist LV, Waltman BA, Dias-Santagata D, Digumarthy S, Turke AB, Fidias P, et al. Genotypic and histological evolution of lung cancers acquiring resistance to EGFR inhibitors. Science translational medicine. 2011;3:75ra26.

100. Yu HA, Arcila ME, Rekhtman N, Sima CS, Zakowski MF, Pao W, et al. Analysis of tumor specimens at the time of acquired resistance to EGFR-TKI therapy in 155 patients with EGFR-mutant lung cancers. Clinical cancer research : an official journal of the American Association for Cancer Research. 2013;19:2240-7.

101. Engelman JA, Zejnullahu K, Mitsudomi T, Song Y, Hyland C, Park JO, et al. MET amplification leads to gefitinib resistance in lung cancer by activating ERBB3 signaling. Science. 2007;316:1039-43.

102. Takezawa K, Pirazzoli V, Arcila ME, Nebhan CA, Song X, de Stanchina E, et al. HER2 amplification: a potential mechanism of acquired resistance to EGFR inhibition in EGFR-mutant lung cancers that lack the second-site EGFRT790M mutation. Cancer discovery. 2012;2:922-33.

103. Cortot AB, Repellin CE, Shimamura T, Capelletti M, Zejnullahu K, Ercan D, et al. Resistance to irreversible EGF receptor tyrosine kinase inhibitors through a multistep mechanism involving the IGF1R pathway. Cancer research. 2013;73:834-43.

104. Terai H, Soejima K, Yasuda H, Nakayama S, Hamamoto J, Arai D, et al. Activation of the FGF2-FGFR1 autocrine pathway: a novel mechanism of acquired resistance to gefitinib in NSCLC. Molecular cancer research : MCR. 2013;11:759-67.

105. Zhang Z, Lee JC, Lin L, Olivas V, Au V, LaFramboise T, et al. Activation of the AXL kinase causes resistance to EGFR-targeted therapy in lung cancer. Nature genetics. 2012;44:852-60.

106. Fritsche M, Haessler C, Brandner G. Induction of nuclear accumulation of the tumor-suppressor protein p53 by DNA-damaging agents. Oncogene. 1993;8:307-18.

107. Wang C, Youle RJ. The role of mitochondria in apoptosis*. Annual review of genetics. 2009;43:95-118.

108. Rich T, Allen RL, Wyllie AH. Defying death after DNA damage. Nature. 2000;407:777-83.

109. Brachmann SM, Hofmann I, Schnell C, Fritsch C, Wee S, Lane H, et al. Specific apoptosis induction by the dual PI3K/mTor inhibitor NVP-BEZ235 in HER2 amplified and PIK3CA mutant breast cancer cells. Proceedings of the National Academy of Sciences of the United States of America. 2009;106:22299-304.

110. Faber AC, Corcoran RB, Ebi H, Sequist LV, Waltman BA, Chung E, et al. BIM expression in treatment-naive cancers predicts responsiveness to kinase inhibitors. Cancer discovery. 2011;1:352-65.

111. Faber AC, Li D, Song Y, Liang MC, Yeap BY, Bronson RT, et al. Differential induction of apoptosis in HER2 and EGFR addicted cancers following PI3K inhibition. Proceedings of the National Academy of Sciences of the United States of America. 2009;106:19503-8.

112. Elmore S. Apoptosis: a review of programmed cell death. Toxicologic pathology. 2007;35:495-516.

113. Yang E, Zha J, Jockel J, Boise LH, Thompson CB, Korsmeyer SJ. Bad, a heterodimeric partner for Bcl-XL and Bcl-2, displaces Bax and promotes cell death. Cell. 1995;80:285-91.

114. Costa DB, Halmos B, Kumar A, Schumer ST, Huberman MS, Boggon TJ, et al. BIM mediates EGFR tyrosine kinase inhibitor-induced apoptosis in lung cancers with oncogenic EGFR mutations. PLoS medicine. 2007;4:1669-79; discussion 80.

115. Westphal D, Dewson G, Czabotar PE, Kluck RM. Molecular biology of Bax and Bak activation and action. Biochimica et biophysica acta. 2011;1813:521-31.

116. Warr MR, Shore GC. Unique biology of Mcl-1: therapeutic opportunities in cancer. Current molecular medicine. 2008;8:138-47.

117. Li P, Nijhawan D, Budihardjo I, Srinivasula SM, Ahmad M, Alnemri ES, et al. Cytochrome c and dATP-dependent formation of Apaf-1/caspase-9 complex initiates an apoptotic protease cascade. Cell. 1997;91:479-89.

118. Chinnaiyan AM. The apoptosome: heart and soul of the cell death machine. Neoplasia. 1999;1:5-15.

119. Nicholson DW, Ali A, Thornberry NA, Vaillancourt JP, Ding CK, Gallant M, et al. Identification and inhibition of the ICE/CED-3 protease necessary for mammalian apoptosis. Nature. 1995;376:37-43.

120. Sakahira H, Enari M, Nagata S. Cleavage of CAD inhibitor in CAD activation and DNA degradation during apoptosis. Nature. 1998;391:96-9.

121. Lazebnik YA, Kaufmann SH, Desnoyers S, Poirier GG, Earnshaw WC. Cleavage of poly(ADP-ribose) polymerase by a proteinase with properties like ICE. Nature. 1994;371:346-7.

122. Tewari M, Quan LT, O'Rourke K, Desnoyers S, Zeng Z, Beidler DR, et al. Yama/CPP32 beta, a mammalian homolog of CED-3, is a CrmA-inhibitable protease that cleaves the death substrate poly(ADP-ribose) polymerase. Cell. 1995;81:801-9.

123. Pasquale EB. Eph receptor signalling casts a wide net on cell behaviour. Nature reviews Molecular cell biology. 2005;6:462-75.

124. Pasquale EB. Eph-ephrin bidirectional signaling in physiology and disease. Cell. 2008;133:38-52.

125. Unified nomenclature for Eph family receptors and their ligands, the ephrins. Eph Nomenclature Committee. Cell. 1997;90:403-4.

126. Kullander K, Klein R. Mechanisms and functions of Eph and ephrin signalling. Nature reviews Molecular cell biology. 2002;3:475-86.

127. Gale NW, Holland SJ, Valenzuela DM, Flenniken A, Pan L, Ryan TE, et al. Eph receptors and ligands comprise two major specificity subclasses and are reciprocally compartmentalized during embryogenesis. Neuron. 1996;17:9-19.

128. Pasquale EB. The Eph family of receptors. Current opinion in cell biology. 1997;9:608-15.

129. Himanen JP, Rajashankar KR, Lackmann M, Cowan CA, Henkemeyer M, Nikolov DB. Crystal structure of an Eph receptor-ephrin complex. Nature. 2001;414:933-8.

130. Himanen JP, Nikolov DB. Eph signaling: a structural view. Trends in neurosciences. 2003;26:46-51.

131. Himanen JP, Nikolov DB. Eph receptors and ephrins. The international journal of biochemistry & cell biology. 2003;35:130-4.

132. Himanen JP, Goldgur Y, Miao H, Myshkin E, Guo H, Buck M, et al. Ligand recognition by A-class Eph receptors: crystal structures of the EphA2 ligand-binding domain and the EphA2/ephrin-A1 complex. EMBO reports. 2009;10:722-8.

133. Dodelet VC, Pasquale EB. Eph receptors and ephrin ligands: embryogenesis to tumorigenesis. Oncogene. 2000;19:5614-9.

134. Murai KK, Pasquale EB. 'Eph'ective signaling: forward, reverse and crosstalk. Journal of cell science. 2003;116:2823-32.

135. Wybenga-Groot LE, Baskin B, Ong SH, Tong J, Pawson T, Sicheri F. Structural basis for autoinhibition of the Ephb2 receptor tyrosine kinase by the unphosphorylated juxtamembrane region. Cell. 2001;106:745-57.

136. Davis TL, Walker JR, Loppnau P, Butler-Cole C, Allali-Hassani A, Dhe-Paganon S. Autoregulation by the juxtamembrane region of the human ephrin receptor tyrosine kinase A3 (EphA3). Structure. 2008;16:873-84.

137. Fang WB, Brantley-Sieders DM, Hwang Y, Ham AJ, Chen J. Identification and functional analysis of phosphorylated tyrosine residues within EphA2 receptor tyrosine kinase. The Journal of biological chemistry. 2008;283:16017-26.

138. Binns KL, Taylor PP, Sicheri F, Pawson T, Holland SJ. Phosphorylation of tyrosine residues in the kinase domain and juxtamembrane region regulates the biological and catalytic activities of Eph receptors. Molecular and cellular biology. 2000;20:4791-805.

139. Janes PW, Nievergall E, Lackmann M. Concepts and consequences of Eph receptor clustering. Seminars in cell & developmental biology. 2012;23:43-50.

140. Song J, Vranken W, Xu P, Gingras R, Noyce RS, Yu Z, et al. Solution structure and backbone dynamics of the functional cytoplasmic subdomain of human ephrin B2, a cell-surface ligand with bidirectional signaling properties. Biochemistry. 2002;41:10942-9.

141. Shamah SM, Lin MZ, Goldberg JL, Estrach S, Sahin M, Hu L, et al. EphA receptors regulate growth cone dynamics through the novel guanine nucleotide exchange factor ephexin. Cell. 2001;105:233-44.

142. Miao H, Burnett E, Kinch M, Simon E, Wang B. Activation of EphA2 kinase suppresses integrin function and causes focal-adhesion-kinase dephosphorylation. Nature cell biology. 2000;2:62-9.

143. Pratt RL, Kinch MS. Activation of the EphA2 tyrosine kinase stimulates the MAP/ERK kinase signaling cascade. Oncogene. 2002;21:7690-9.

144. Kikawa KD, Vidale DR, Van Etten RL, Kinch MS. Regulation of the EphA2 kinase by the low molecular weight tyrosine phosphatase induces transformation. The Journal of biological chemistry. 2002;277:39274-9.

145. Pandey A, Lazar DF, Saltiel AR, Dixit VM. Activation of the Eck receptor protein tyrosine kinase stimulates phosphatidylinositol 3-kinase activity. The Journal of biological chemistry. 1994;269:30154-7.

146. Pandey A, Duan H, Dixit VM. Characterization of a novel Src-like adapter protein that associates with the Eck receptor tyrosine kinase. The Journal of biological chemistry. 1995;270:19201-4.

147. Larsen AB, Pedersen MW, Stockhausen MT, Grandal MV, van Deurs B, Poulsen HS. Activation of the EGFR gene target EphA2 inhibits epidermal growth factor-induced cancer cell motility. Molecular cancer research : MCR. 2007;5:283-93.

148. Thelemann A, Petti F, Griffin G, Iwata K, Hunt T, Settinari T, et al. Phosphotyrosine signaling networks in epidermal growth factor receptor overexpressing squamous carcinoma cells. Molecular & cellular proteomics : MCP. 2005;4:356-76.

149. Brantley-Sieders DM, Zhuang G, Hicks D, Fang WB, Hwang Y, Cates JM, et al. The receptor tyrosine kinase EphA2 promotes mammary adenocarcinoma tumorigenesis and metastatic progression in mice by amplifying ErbB2 signaling. The Journal of clinical investigation. 2008;118:64-78.

150. Pratt RL, Kinch MS. Ligand binding up-regulates EphA2 messenger RNA through the mitogen-activated protein/extracellular signal-regulated kinase pathway. Molecular cancer research : MCR. 2003;1:1070-6.

151. Macrae M, Neve RM, Rodriguez-Viciana P, Haqq C, Yeh J, Chen C, et al. A conditional feedback loop regulates Ras activity through EphA2. Cancer cell. 2005;8:111-8.

152. Menges CW, McCance DJ. Constitutive activation of the Raf-MAPK pathway causes negative feedback inhibition of Ras-PI3K-AKT and cellular arrest through the EphA2 receptor. Oncogene. 2008;27:2934-40.

153. Amato KR, Wang S, Hastings AK, Youngblood VM, Santapuram PR, Chen H, et al. Genetic and pharmacologic inhibition of EPHA2 promotes apoptosis in NSCLC. The Journal of clinical investigation. 2014;124:2037-49.

154. Genander M, Halford MM, Xu NJ, Eriksson M, Yu Z, Qiu Z, et al. Dissociation of EphB2 signaling pathways mediating progenitor cell proliferation and tumor suppression. Cell. 2009;139:679-92.

155. Noren NK, Foos G, Hauser CA, Pasquale EB. The EphB4 receptor suppresses breast cancer cell tumorigenicity through an Abl-Crk pathway. Nature cell biology. 2006;8:815-25.

156. Noren NK, Pasquale EB. Eph receptor-ephrin bidirectional signals that target Ras and Rho proteins. Cellular signalling. 2004;16:655-66.

157. Fang WB, Brantley-Sieders DM, Parker MA, Reith AD, Chen J. A kinase-dependent role for EphA2 receptor in promoting tumor growth and metastasis. Oncogene. 2005;24:7859-68.

158. Fang WB, Ireton RC, Zhuang G, Takahashi T, Reynolds A, Chen J. Overexpression of EPHA2 receptor destabilizes adherens junctions via a RhoA-dependent mechanism. Journal of cell science. 2008;121:358-68.

159. Egea J, Klein R. Bidirectional Eph-ephrin signaling during axon guidance. Trends in cell biology. 2007;17:230-8.

160. Davy A, Gale NW, Murray EW, Klinghoffer RA, Soriano P, Feuerstein C, et al. Compartmentalized signaling by GPI-anchored ephrin-A5 requires the Fyn tyrosine kinase to regulate cellular adhesion. Genes & development. 1999;13:3125-35.

161. Davy A, Robbins SM. Ephrin-A5 modulates cell adhesion and morphology in an integrin-dependent manner. The EMBO journal. 2000;19:5396-405.

162. Lim YS, McLaughlin T, Sung TC, Santiago A, Lee KF, O'Leary DD. p75(NTR) mediates ephrin-A reverse signaling required for axon repulsion and mapping. Neuron. 2008;59:746-58.

163. Zhou R. The Eph family receptors and ligands. Pharmacology & therapeutics. 1998;77:151-81.

164. Henkemeyer M, Orioli D, Henderson JT, Saxton TM, Roder J, Pawson T, et al. Nuk controls pathfinding of commissural axons in the mammalian central nervous system. Cell. 1996;86:35-46.

165. Poliakov A, Cotrina M, Wilkinson DG. Diverse roles of eph receptors and ephrins in the regulation of cell migration and tissue assembly. Developmental cell. 2004;7:465-80.

166. Walker-Daniels J, Riese DJ, 2nd, Kinch MS. c-Cbl-dependent EphA2 protein degradation is induced by ligand binding. Molecular cancer research : MCR. 2002;1:79-87.

167. Miao H, Wei BR, Peehl DM, Li Q, Alexandrou T, Schelling JR, et al. Activation of EphA receptor tyrosine kinase inhibits the Ras/MAPK pathway. Nature cell biology. 2001;3:527-30.

168. Miao H, Li DQ, Mukherjee A, Guo H, Petty A, Cutter J, et al. EphA2 mediates ligand-dependent inhibition and ligand-independent promotion of cell migration and invasion via a reciprocal regulatory loop with Akt. Cancer cell. 2009;16:9-20.

169. Warner N, Wybenga-Groot LE, Pawson T. Analysis of EphA4 receptor tyrosine kinase substrate specificity using peptide-based arrays. The FEBS journal. 2008;275:2561-73.

170. Yokote H, Fujita K, Jing X, Sawada T, Liang S, Yao L, et al. Trans-activation of EphA4 and FGF receptors mediated by direct interactions between their cytoplasmic domains. Proceedings of the National Academy of Sciences of the United States of America. 2005;102:18866-71.

171. Fukai J, Yokote H, Yamanaka R, Arao T, Nishio K, Itakura T. EphA4 promotes cell proliferation and migration through a novel EphA4-FGFR1 signaling pathway in the human glioma U251 cell line. Molecular cancer therapeutics. 2008;7:2768-78.

172. Luo H, Yu G, Wu Y, Wu J. EphB6 crosslinking results in costimulation of T cells. The Journal of clinical investigation. 2002;110:1141-50.

173. Salvucci O, de la Luz Sierra M, Martina JA, McCormick PJ, Tosato G. EphB2 and EphB4 receptors forward signaling promotes SDF-1-induced endothelial cell chemotaxis and branching remodeling. Blood. 2006;108:2914-22.

174. Stein E, Lane AA, Cerretti DP, Schoecklmann HO, Schroff AD, Van Etten RL, et al. Eph receptors discriminate specific ligand oligomers to determine alternative signaling complexes, attachment, and assembly responses. Genes & development. 1998;12:667-78.

175. Huynh-Do U, Stein E, Lane AA, Liu H, Cerretti DP, Daniel TO. Surface densities of ephrin-B1 determine EphB1-coupled activation of cell attachment through alphavbeta3 and alpha5beta1 integrins. The EMBO journal. 1999;18:2165-73.

176. Sharfe N, Freywald A, Toro A, Dadi H, Roifman C. Ephrin stimulation modulates T cell chemotaxis. European journal of immunology. 2002;32:3745-55.

177. Deroanne C, Vouret-Craviari V, Wang B, Pouyssegur J. EphrinA1 inactivates integrin-mediated vascular smooth muscle cell spreading via the Rac/PAK pathway. Journal of cell science. 2003;116:1367-76.

178. Tanaka M, Kamata R, Sakai R. EphA2 phosphorylates the cytoplasmic tail of Claudin-4 and mediates paracellular permeability. The Journal of biological chemistry. 2005;280:42375-82.

179. Zantek ND, Azimi M, Fedor-Chaiken M, Wang B, Brackenbury R, Kinch MS. E-cadherin regulates the function of the EphA2 receptor tyrosine kinase. Cell growth & differentiation : the molecular biology journal of the American Association for Cancer Research. 1999;10:629-38.

180. Prevost N, Woulfe DS, Jiang H, Stalker TJ, Marchese P, Ruggeri ZM, et al. Eph kinases and ephrins support thrombus growth and stability by regulating integrin outside-in signaling in platelets. Proceedings of the National Academy of Sciences of the United States of America. 2005;102:9820-5.

181. Gu C, Park S. The EphA8 receptor regulates integrin activity through p110gamma phosphatidylinositol-3 kinase in a tyrosine kinase activity-independent manner. Molecular and cellular biology. 2001;21:4579-97.

182. Dalva MB, Takasu MA, Lin MZ, Shamah SM, Hu L, Gale NW, et al. EphB receptors interact with NMDA receptors and regulate excitatory synapse formation. Cell. 2000;103:945-56.

183. Cortina C, Palomo-Ponce S, Iglesias M, Fernandez-Masip JL, Vivancos A, Whissell G, et al. EphB-ephrin-B interactions suppress colorectal cancer progression by compartmentalizing tumor cells. Nature genetics. 2007;39:1376-83.

184. Ethell IM, Irie F, Kalo MS, Couchman JR, Pasquale EB, Yamaguchi Y. EphB/syndecan-2 signaling in dendritic spine morphogenesis. Neuron. 2001;31:1001-13.

185. Zisch AH, Stallcup WB, Chong LD, Dahlin-Huppe K, Voshol J, Schachner M, et al. Tyrosine phosphorylation of L1 family adhesion molecules: implication of the Eph kinase Cek5. Journal of neuroscience research. 1997;47:655-65.

186. Trivier E, Ganesan TS. RYK, a catalytically inactive receptor tyrosine kinase, associates with EphB2 and EphB3 but does not interact with AF-6. The Journal of biological chemistry. 2002;277:23037-43.

187. Drescher U, Kremoser C, Handwerker C, Loschinger J, Noda M, Bonhoeffer F. In vitro guidance of retinal ganglion cell axons by RAGS, a 25 kDa tectal protein related to ligands for Eph receptor tyrosine kinases. Cell. 1995;82:359-70.

188. Wang HU, Anderson DJ. Eph family transmembrane ligands can mediate repulsive guidance of trunk neural crest migration and motor axon outgrowth. Neuron. 1997;18:383-96.

189. Nieto MA, Gilardi-Hebenstreit P, Charnay P, Wilkinson DG. A receptor protein tyrosine kinase implicated in the segmental patterning of the hindbrain and mesoderm. Development. 1992;116:1137-50.

190. Gilardi-Hebenstreit P, Nieto MA, Frain M, Mattei MG, Chestier A, Wilkinson DG, et al. An Eph-related receptor protein tyrosine kinase gene segmentally expressed in the developing mouse hindbrain. Oncogene. 1992;7:2499-506.

191. Ganju P, Shigemoto K, Brennan J, Entwistle A, Reith AD. The Eck receptor tyrosine kinase is implicated in pattern formation during gastrulation, hindbrain segmentation and limb development. Oncogene. 1994;9:1613-24.

192. Becker N, Seitanidou T, Murphy P, Mattei MG, Topilko P, Nieto MA, et al. Several receptor tyrosine kinase genes of the Eph family are segmentally expressed in the developing hindbrain. Mechanisms of development. 1994;47:3-17.

193. Xu Q, Alldus G, Macdonald R, Wilkinson DG, Holder N. Function of the Eph-related kinase rtk1 in patterning of the zebrafish forebrain. Nature. 1996;381:319-22.

194. Adams RH, Wilkinson GA, Weiss C, Diella F, Gale NW, Deutsch U, et al. Roles of ephrinB ligands and EphB receptors in cardiovascular development: demarcation of arterial/venous domains, vascular morphogenesis, and sprouting angiogenesis. Genes & development. 1999;13:295-306.

195. Wang HU, Chen ZF, Anderson DJ. Molecular distinction and angiogenic interaction between embryonic arteries and veins revealed by ephrin-B2 and its receptor Eph-B4. Cell. 1998;93:741-53.

196. McBride JL, Ruiz JC. Ephrin-A1 is expressed at sites of vascular development in the mouse. Mechanisms of development. 1998;77:201-4.

197. Frieden LA, Townsend TA, Vaught DB, Delaughter DM, Hwang Y, Barnett JV, et al. Regulation of heart valve morphogenesis by Eph receptor ligand, ephrin-A1. Developmental dynamics : an official publication of the American Association of Anatomists. 2010;239:3226-34.

198. Gerety SS, Wang HU, Chen ZF, Anderson DJ. Symmetrical mutant phenotypes of the receptor EphB4 and its specific transmembrane ligand ephrin-B2 in cardiovascular development. Molecular cell. 1999;4:403-14.

199. Batlle E, Henderson JT, Beghtel H, van den Born MM, Sancho E, Huls G, et al. Beta-catenin and TCF mediate cell positioning in the intestinal epithelium by controlling the expression of EphB/ephrinB. Cell. 2002;111:251-63.

200. Miao H, Nickel CH, Cantley LG, Bruggeman LA, Bennardo LN, Wang B. EphA kinase activation regulates HGF-induced epithelial branching morphogenesis. The Journal of cell biology. 2003;162:1281-92.

201. Miao H, Wang B. Eph/ephrin signaling in epithelial development and homeostasis. The international journal of biochemistry & cell biology. 2009;41:762-70.

202. Vaught D, Chen J, Brantley-Sieders DM. Regulation of mammary gland branching morphogenesis by EphA2 receptor tyrosine kinase. Molecular biology of the cell. 2009;20:2572-81.

203. Munoz JJ, Alfaro D, Garcia-Ceca J, Alonso CL, Jimenez E, Zapata A. Thymic alterations in EphA4-deficient mice. Journal of immunology. 2006;177:804-13.

204. Chen J, Nachabah A, Scherer C, Ganju P, Reith A, Bronson R, et al. Germ-line inactivation of the murine Eck receptor tyrosine kinase by gene trap retroviral insertion. Oncogene. 1996;12:979-88.

205. Orsulic S, Kemler R. Expression of Eph receptors and ephrins is differentially regulated by E-cadherin. Journal of cell science. 2000;113 (Pt 10):1793-802.

206. Holmberg J, Armulik A, Senti KA, Edoff K, Spalding K, Momma S, et al. Ephrin-A2 reverse signaling negatively regulates neural progenitor proliferation and neurogenesis. Genes & development. 2005;19:462-71.

207. Conover JC, Doetsch F, Garcia-Verdugo JM, Gale NW, Yancopoulos GD, Alvarez-Buylla A. Disruption of Eph/ephrin signaling affects migration and proliferation in the adult subventricular zone. Nature neuroscience. 2000;3:1091-7.

208. Genander M, Frisen J. Ephrins and Eph receptors in stem cells and cancer. Current opinion in cell biology. 2010;22:611-6.

209. Yarden Y, Ullrich A. Growth factor receptor tyrosine kinases. Annual review of biochemistry. 1988;57:443-78.

210. Cross M, Dexter TM. Growth factors in development, transformation, and tumorigenesis. Cell. 1991;64:271-80.

211. Brantley-Sieders D, Schmidt S, Parker M, Chen J. Eph receptor tyrosine kinases in tumor and tumor microenvironment. Current pharmaceutical design. 2004;10:3431-42.

212. Merlos-Suarez A, Batlle E. Eph-ephrin signalling in adult tissues and cancer. Current opinion in cell biology. 2008;20:194-200.

213. Noren NK, Pasquale EB. Paradoxes of the EphB4 receptor in cancer. Cancer research. 2007;67:3994-7.

214. Wykosky J, Debinski W. The EphA2 receptor and ephrinA1 ligand in solid tumors: function and therapeutic targeting. Molecular cancer research : MCR. 2008;6:1795-806.

215. Surawska H, Ma PC, Salgia R. The role of ephrins and Eph receptors in cancer. Cytokine & growth factor reviews. 2004;15:419-33.

216. Pasquale EB. Eph receptors and ephrins in cancer: bidirectional signalling and beyond. Nature reviews Cancer. 2010;10:165-80.

217. Ding L, Getz G, Wheeler DA, Mardis ER, McLellan MD, Cibulskis K, et al. Somatic mutations affect key pathways in lung adenocarcinoma. Nature. 2008;455:1069-75.

218. Bardelli A, Parsons DW, Silliman N, Ptak J, Szabo S, Saha S, et al. Mutational analysis of the tyrosine kinome in colorectal cancers. Science. 2003;300:949.

219. Sjoblom T, Jones S, Wood LD, Parsons DW, Lin J, Barber TD, et al. The consensus coding sequences of human breast and colorectal cancers. Science. 2006;314:268-74.

220. Davies H, Hunter C, Smith R, Stephens P, Greenman C, Bignell G, et al. Somatic mutations of the protein kinase gene family in human lung cancer. Cancer research. 2005;65:7591-5.

221. Huusko P, Ponciano-Jackson D, Wolf M, Kiefer JA, Azorsa DO, Tuzmen S, et al. Nonsense-mediated decay microarray analysis identifies mutations of EPHB2 in human prostate cancer. Nature genetics. 2004;36:979-83.

222. Prickett TD, Agrawal NS, Wei X, Yates KE, Lin JC, Wunderlich JR, et al. Analysis of the tyrosine kinome in melanoma reveals recurrent mutations in ERBB4. Nature genetics. 2009;41:1127-32.

223. Davalos V, Dopeso H, Velho S, Ferreira AM, Cirnes L, Diaz-Chico N, et al. High EPHB2 mutation rate in gastric but not endometrial tumors with microsatellite instability. Oncogene. 2007;26:308-11.

224. Faoro L, Singleton PA, Cervantes GM, Lennon FE, Choong NW, Kanteti R, et al. EphA2 mutation in lung squamous cell carcinoma promotes increased cell survival, cell invasion, focal adhesions, and mammalian target of rapamycin activation. The Journal of biological chemistry. 2010;285:18575-85.

225. Kinch MS, Moore MB, Harpole DH, Jr. Predictive value of the EphA2 receptor tyrosine kinase in lung cancer recurrence and survival. Clinical cancer research : an official journal of the American Association for Cancer Research. 2003;9:613-8.

226. Brannan JM, Dong W, Prudkin L, Behrens C, Lotan R, Bekele BN, et al. Expression of the receptor tyrosine kinase EphA2 is increased in smokers and predicts

poor survival in non-small cell lung cancer. Clinical cancer research : an official journal of the American Association for Cancer Research. 2009;15:4423-30.

227. Brantley-Sieders DM, Jiang A, Sarma K, Badu-Nkansah A, Walter DL, Shyr Y, et al. Eph/ephrin profiling in human breast cancer reveals significant associations between expression level and clinical outcome. PloS one. 2011;6:e24426.

228. Duxbury MS, Ito H, Zinner MJ, Ashley SW, Whang EE. EphA2: a determinant of malignant cellular behavior and a potential therapeutic target in pancreatic adenocarcinoma. Oncogene. 2004;23:1448-56.

229. Miyazaki T, Kato H, Fukuchi M, Nakajima M, Kuwano H. EphA2 overexpression correlates with poor prognosis in esophageal squamous cell carcinoma. International journal of cancer Journal international du cancer. 2003;103:657-63.

230. Nakada M, Niska JA, Miyamori H, McDonough WS, Wu J, Sato H, et al. The phosphorylation of EphB2 receptor regulates migration and invasion of human glioma cells. Cancer research. 2004;64:3179-85.

231. Zhuang G, Brantley-Sieders DM, Vaught D, Yu J, Xie L, Wells S, et al. Elevation of receptor tyrosine kinase EphA2 mediates resistance to trastuzumab therapy. Cancer research. 2010;70:299-308.

232. Lu M, Miller KD, Gokmen-Polar Y, Jeng MH, Kinch MS. EphA2 overexpression decreases estrogen dependence and tamoxifen sensitivity. Cancer research. 2003;63:3425-9.

233. Miao B, Ji Z, Tan L, Taylor M, Zhang J, Choi HG, et al. EphA2 is a Mediator of Vemurafenib Resistance and a Novel Therapeutic Target in Melanoma. Cancer discovery. 2014.

234. Suzuki M, Abe A, Imagama S, Nomura Y, Tanizaki R, Minami Y, et al. BCR-ABL-independent and RAS / MAPK pathway-dependent form of imatinib resistance in Ph-positive acute lymphoblastic leukemia cell line with activation of EphB4. European journal of haematology. 2010;84:229-38.

235. Zelinski DP, Zantek ND, Stewart JC, Irizarry AR, Kinch MS. EphA2 overexpression causes tumorigenesis of mammary epithelial cells. Cancer research. 2001;61:2301-6.

236. Song W, Ma Y, Wang J, Brantley-Sieders D, Chen J. JNK signaling mediates EPHA2-dependent tumor cell proliferation, motility, and cancer stem cell-like properties in non-small cell lung cancer. Cancer research. 2014;74:2444-54.

237. Udayakumar D, Zhang G, Ji Z, Njauw CN, Mroz P, Tsao H. EphA2 is a critical oncogene in melanoma. Oncogene. 2011;30:4921-9.

238. Landen CN, Jr., Chavez-Reyes A, Bucana C, Schmandt R, Deavers MT, Lopez-Berestein G, et al. Therapeutic EphA2 gene targeting in vivo using neutral liposomal small interfering RNA delivery. Cancer research. 2005;65:6910-8.

239. Munarini N, Jager R, Abderhalden S, Zuercher G, Rohrbach V, Loercher S, et al. Altered mammary epithelial development, pattern formation and involution in transgenic mice expressing the EphB4 receptor tyrosine kinase. Journal of cell science. 2002;115:25-37.

240. Folkman J. Role of angiogenesis in tumor growth and metastasis. Seminars in oncology. 2002;29:15-8.

241. Brantley-Sieders DM, Chen J. Eph receptor tyrosine kinases in angiogenesis: from development to disease. Angiogenesis. 2004;7:17-28.

242. Chen J, Zhuang G, Frieden L, Debinski W. Eph receptors and Ephrins in cancer: common themes and controversies. Cancer research. 2008;68:10031-3.

243. Ogawa K, Pasqualini R, Lindberg RA, Kain R, Freeman AL, Pasquale EB. The ephrin-A1 ligand and its receptor, EphA2, are expressed during tumor neovascularization. Oncogene. 2000;19:6043-52.

244. Wu Q, Suo Z, Risberg B, Karlsson MG, Villman K, Nesland JM. Expression of Ephb2 and Ephb4 in breast carcinoma. Pathology oncology research : POR. 2004;10:26-33.

245. Brantley-Sieders DM, Caughron J, Hicks D, Pozzi A, Ruiz JC, Chen J. EphA2 receptor tyrosine kinase regulates endothelial cell migration and vascular assembly through phosphoinositide 3-kinase-mediated Rac1 GTPase activation. Journal of cell science. 2004;117:2037-49.

246. Hunter SG, Zhuang G, Brantley-Sieders D, Swat W, Cowan CW, Chen J. Essential role of Vav family guanine nucleotide exchange factors in EphA receptor-mediated angiogenesis. Molecular and cellular biology. 2006;26:4830-42.

247. Brantley-Sieders DM, Fang WB, Hwang Y, Hicks D, Chen J. Ephrin-A1 facilitates mammary tumor metastasis through an angiogenesis-dependent mechanism mediated by EphA receptor and vascular endothelial growth factor in mice. Cancer research. 2006;66:10315-24.

248. Brantley DM, Cheng N, Thompson EJ, Lin Q, Brekken RA, Thorpe PE, et al. Soluble Eph A receptors inhibit tumor angiogenesis and progression in vivo. Oncogene. 2002;21:7011-26.

249. Brantley-Sieders DM, Fang WB, Hicks DJ, Zhuang G, Shyr Y, Chen J. Impaired tumor microenvironment in EphA2-deficient mice inhibits tumor angiogenesis and metastatic progression. FASEB journal : official publication of the Federation of American Societies for Experimental Biology. 2005;19:1884-6.

250. Chen J, Hicks D, Brantley-Sieders D, Cheng N, McCollum GW, Qi-Werdich X, et al. Inhibition of retinal neovascularization by soluble EphA2 receptor. Experimental eye research. 2006;82:664-73.

251. Casanovas O, Hicklin DJ, Bergers G, Hanahan D. Drug resistance by evasion of antiangiogenic targeting of VEGF signaling in late-stage pancreatic islet tumors. Cancer cell. 2005;8:299-309.

252. Herbert SP, Huisken J, Kim TN, Feldman ME, Houseman BT, Wang RA, et al. Arterial-venous segregation by selective cell sprouting: an alternative mode of blood vessel formation. Science. 2009;326:294-8.

253. Erber R, Eichelsbacher U, Powajbo V, Korn T, Djonov V, Lin J, et al. EphB4 controls blood vascular morphogenesis during postnatal angiogenesis. The EMBO journal. 2006;25:628-41.

254. Noren NK, Lu M, Freeman AL, Koolpe M, Pasquale EB. Interplay between EphB4 on tumor cells and vascular ephrin-B2 regulates tumor growth. Proceedings of the National Academy of Sciences of the United States of America. 2004;101:5583-8.

255. Salvucci O, Maric D, Economopoulou M, Sakakibara S, Merlin S, Follenzi A, et al. EphrinB reverse signaling contributes to endothelial and mural cell assembly into vascular structures. Blood. 2009;114:1707-16.

256. Kumar SR, Scehnet JS, Ley EJ, Singh J, Krasnoperov V, Liu R, et al. Preferential induction of EphB4 over EphB2 and its implication in colorectal cancer progression. Cancer research. 2009;69:3736-45.

257. Zhuang G, Song W, Amato K, Hwang Y, Lee K, Boothby M, et al. Effects of cancer-associated EPHA3 mutations on lung cancer. Journal of the National Cancer Institute. 2012;104:1182-97.

258. Smith FM, Vearing C, Lackmann M, Treutlein H, Himanen J, Chen K, et al. Dissecting the EphA3/Ephrin-A5 interactions using a novel functional mutagenesis screen. The Journal of biological chemistry. 2004;279:9522-31.

259. Zogopoulos G, Jorgensen C, Bacani J, Montpetit A, Lepage P, Ferretti V, et al. Germline EPHB2 receptor variants in familial colorectal cancer. PloS one. 2008;3:e2885.

260. Shintani T, Ihara M, Sakuta H, Takahashi H, Watakabe I, Noda M. Eph receptors are negatively controlled by protein tyrosine phosphatase receptor type O. Nature neuroscience. 2006;9:761-9.

261. Carles-Kinch K, Kilpatrick KE, Stewart JC, Kinch MS. Antibody targeting of the EphA2 tyrosine kinase inhibits malignant cell behavior. Cancer research. 2002;62:2840-7.

262. Jackson D, Gooya J, Mao S, Kinneer K, Xu L, Camara M, et al. A human antibody-drug conjugate targeting EphA2 inhibits tumor growth in vivo. Cancer research. 2008;68:9367-74.

263. Annunziata CM, Kohn EC, LoRusso P, Houston ND, Coleman RL, Buzoianu M, et al. Phase 1, open-label study of MEDI-547 in patients with relapsed or refractory solid tumors. Investigational new drugs. 2013;31:77-84.

264. Mao W, Luis E, Ross S, Silva J, Tan C, Crowley C, et al. EphB2 as a therapeutic antibody drug target for the treatment of colorectal cancer. Cancer research. 2004;64:781-8.

265. Binda E, Visioli A, Giani F, Lamorte G, Copetti M, Pitter KL, et al. The EphA2 receptor drives self-renewal and tumorigenicity in stem-like tumor-propagating cells from human glioblastomas. Cancer cell. 2012;22:765-80.

266. Bruckheimer EM, Fazenbaker CA, Gallagher S, Mulgrew K, Fuhrmann S, Coffman KT, et al. Antibody-dependent cell-mediated cytotoxicity effector-enhanced EphA2 agonist monoclonal antibody demonstrates potent activity against human tumors. Neoplasia. 2009;11:509-17, 2 p following 17.

267. Koolpe M, Dail M, Pasquale EB. An ephrin mimetic peptide that selectively targets the EphA2 receptor. The Journal of biological chemistry. 2002;277:46974-9.

268. Murai KK, Nguyen LN, Koolpe M, McLennan R, Krull CE, Pasquale EB. Targeting the EphA4 receptor in the nervous system with biologically active peptides. Molecular and cellular neurosciences. 2003;24:1000-11.

269. Koolpe M, Burgess R, Dail M, Pasquale EB. EphB receptor-binding peptides identified by phage display enable design of an antagonist with ephrin-like affinity. The Journal of biological chemistry. 2005;280:17301-11.

270. Landen CN, Merritt WM, Mangala LS, Sanguino AM, Bucana C, Lu C, et al. Intraperitoneal delivery of liposomal siRNA for therapy of advanced ovarian cancer. Cancer biology & therapy. 2006;5:1708-13.

271. Bardelle C, Coleman T, Cross D, Davenport S, Kettle JG, Ko EJ, et al. Inhibitors of the tyrosine kinase EphB4. Part 2: structure-based discovery and optimisation of 3,5-bis substituted anilinopyrimidines. Bioorganic & medicinal chemistry letters. 2008;18:5717-21.

272. Bardelle C, Cross D, Davenport S, Kettle JG, Ko EJ, Leach AG, et al. Inhibitors of the tyrosine kinase EphB4. Part 1: Structure-based design and optimization of a series of 2,4-bis-anilinopyrimidines. Bioorganic & medicinal chemistry letters. 2008;18:2776-80.

273. Miyazaki Y, Nakano M, Sato H, Truesdale AT, Stuart JD, Nartey EN, et al. Design and effective synthesis of novel templates, 3,7-diphenyl-4-amino-thieno and furo-[3,2-c]pyridines as protein kinase inhibitors and in vitro evaluation targeting angiogenetic kinases. Bioorganic & medicinal chemistry letters. 2007;17:250-4.

274. Gendreau SB, Ventura R, Keast P, Laird AD, Yakes FM, Zhang W, et al. Inhibition of the T790M gatekeeper mutant of the epidermal growth factor receptor by EXEL-7647. Clinical cancer research : an official journal of the American Association for Cancer Research. 2007;13:3713-23.

275. Lafleur K, Huang D, Zhou T, Caflisch A, Nevado C. Structure-based optimization of potent and selective inhibitors of the tyrosine kinase erythropoietin producing human

hepatocellular carcinoma receptor B4 (EphB4). Journal of medicinal chemistry. 2009;52:6433-46.

276. Kolb P, Kipouros CB, Huang D, Caflisch A. Structure-based tailoring of compound libraries for high-throughput screening: discovery of novel EphB4 kinase inhibitors. Proteins. 2008;73:11-8.

277. Qiao L, Choi S, Case A, Gainer TG, Seyb K, Glicksman MA, et al. Structure-activity relationship study of EphB3 receptor tyrosine kinase inhibitors. Bioorganic & medicinal chemistry letters. 2009;19:6122-6.

278. Caligiuri M, Molz L, Liu Q, Kaplan F, Xu JP, Majeti JZ, et al. MASPIT: three-hybrid trap for quantitative proteome fingerprinting of small molecule-protein interactions in mammalian cells. Chemistry & biology. 2006;13:711-22.

279. Choi Y, Syeda F, Walker JR, Finerty PJ, Jr., Cuerrier D, Wojciechowski A, et al. Discovery and structural analysis of Eph receptor tyrosine kinase inhibitors. Bioorganic & medicinal chemistry letters. 2009;19:4467-70.

280. Melnick JS, Janes J, Kim S, Chang JY, Sipes DG, Gunderson D, et al. An efficient rapid system for profiling the cellular activities of molecular libraries. Proceedings of the National Academy of Sciences of the United States of America. 2006;103:3153-8.

281. Karaman MW, Herrgard S, Treiber DK, Gallant P, Atteridge CE, Campbell BT, et al. A quantitative analysis of kinase inhibitor selectivity. Nature biotechnology. 2008;26:127-32.

282. Bantscheff M, Eberhard D, Abraham Y, Bastuck S, Boesche M, Hobson S, et al. Quantitative chemical proteomics reveals mechanisms of action of clinical ABL kinase inhibitors. Nature biotechnology. 2007;25:1035-44.

283. Gurav SD, Gilibili RR, Jeniffer S, Mohd Z, Giri S, Govindarajan R, et al. Pharmacokinetics, tissue distribution and identification of putative metabolites of JI-101 - a novel triple kinase inhibitor in rats. Arzneimittel-Forschung. 2012;62:27-34.

284. Rix U, Remsing Rix LL, Terker AS, Fernbach NV, Hantschel O, Planyavsky M, et al. A comprehensive target selectivity survey of the BCR-ABL kinase inhibitor INNO-406 by kinase profiling and chemical proteomics in chronic myeloid leukemia cells. Leukemia. 2010;24:44-50.

285. Martiny-Baron G, Holzer P, Billy E, Schnell C, Brueggen J, Ferretti M, et al. The small molecule specific EphB4 kinase inhibitor NVP-BHG712 inhibits VEGF driven angiogenesis. Angiogenesis. 2010;13:259-67.

286. Shahzad MM, Lu C, Lee JW, Stone RL, Mitra R, Mangala LS, et al. Dual targeting of EphA2 and FAK in ovarian carcinoma. Cancer biology & therapy. 2009;8:1027-34.

287. Kumar SR, Masood R, Spannuth WA, Singh J, Scehnet J, Kleiber G, et al. The receptor tyrosine kinase EphB4 is overexpressed in ovarian cancer, provides survival signals and predicts poor outcome. British journal of cancer. 2007;96:1083-91.

288. Kumar SR, Singh J, Xia G, Krasnoperov V, Hassanieh L, Ley EJ, et al. Receptor tyrosine kinase EphB4 is a survival factor in breast cancer. The American journal of pathology. 2006;169:279-93.

289. Xia G, Kumar SR, Masood R, Zhu S, Reddy R, Krasnoperov V, et al. EphB4 expression and biological significance in prostate cancer. Cancer research. 2005;65:4623-32.

290. Xia G, Kumar SR, Stein JP, Singh J, Krasnoperov V, Zhu S, et al. EphB4 receptor tyrosine kinase is expressed in bladder cancer and provides signals for cell survival. Oncogene. 2006;25:769-80.

291. Campbell TN, Attwell S, Arcellana-Panlilio M, Robbins SM. Ephrin A5 expression promotes invasion and transformation of murine fibroblasts. Biochemical and biophysical research communications. 2006;350:623-8.

292. Cheng N, Brantley DM, Liu H, Lin Q, Enriquez M, Gale N, et al. Blockade of EphA receptor tyrosine kinase activation inhibits vascular endothelial cell growth factor-induced angiogenesis. Molecular cancer research : MCR. 2002;1:2-11.

293. Dobrzanski P, Hunter K, Jones-Bolin S, Chang H, Robinson C, Pritchard S, et al. Antiangiogenic and antitumor efficacy of EphA2 receptor antagonist. Cancer research. 2004;64:910-9.

294. Cheng N, Brantley D, Fang WB, Liu H, Fanslow W, Cerretti DP, et al. Inhibition of VEGF-dependent multistage carcinogenesis by soluble EphA receptors. Neoplasia. 2003;5:445-56.

295. Scehnet JS, Ley EJ, Krasnoperov V, Liu R, Manchanda PK, Sjoberg E, et al. The role of Ephs, Ephrins, and growth factors in Kaposi sarcoma and implications of EphrinB2 blockade. Blood. 2009;113:254-63.

296. Martiny-Baron G, Korff T, Schaffner F, Esser N, Eggstein S, Marme D, et al. Inhibition of tumor growth and angiogenesis by soluble EphB4. Neoplasia. 2004;6:248-57.

297. Kertesz N, Krasnoperov V, Reddy R, Leshanski L, Kumar SR, Zozulya S, et al. The soluble extracellular domain of EphB4 (sEphB4) antagonizes EphB4-EphrinB2 interaction, modulates angiogenesis, and inhibits tumor growth. Blood. 2006;107:2330-8.

298. Noberini R, Koolpe M, Peddibhotla S, Dahl R, Su Y, Cosford ND, et al. Small molecules can selectively inhibit ephrin binding to the EphA4 and EphA2 receptors. The Journal of biological chemistry. 2008;283:29461-72.

299. Fabes J, Anderson P, Brennan C, Bolsover S. Regeneration-enhancing effects of EphA4 blocking peptide following corticospinal tract injury in adult rat spinal cord. The European journal of neuroscience. 2007;26:2496-505.

300. Chrencik JE, Brooun A, Recht MI, Nicola G, Davis LK, Abagyan R, et al. Three-dimensional structure of the EphB2 receptor in complex with an antagonistic peptide reveals a novel mode of inhibition. The Journal of biological chemistry. 2007;282:36505-13.

301. Chrencik JE, Brooun A, Recht MI, Kraus ML, Koolpe M, Kolatkar AR, et al. Structure and thermodynamic characterization of the EphB4/Ephrin-B2 antagonist peptide complex reveals the determinants for receptor specificity. Structure. 2006;14:321-30.

302. Qin H, Shi J, Noberini R, Pasquale EB, Song J. Crystal structure and NMR binding reveal that two small molecule antagonists target the high affinity ephrin-binding channel of the EphA4 receptor. The Journal of biological chemistry. 2008;283:29473-84.

303. Coffman KT, Hu M, Carles-Kinch K, Tice D, Donacki N, Munyon K, et al. Differential EphA2 epitope display on normal versus malignant cells. Cancer research. 2003;63:7907-12.

304. Landen CN, Jr., Lu C, Han LY, Coffman KT, Bruckheimer E, Halder J, et al. Efficacy and antivascular effects of EphA2 reduction with an agonistic antibody in ovarian cancer. Journal of the National Cancer Institute. 2006;98:1558-70.

305. Kiewlich D, Zhang J, Gross C, Xia W, Larsen B, Cobb RR, et al. Anti-EphA2 antibodies decrease EphA2 protein levels in murine CT26 colorectal and human MDA-231 breast tumors but do not inhibit tumor growth. Neoplasia. 2006;8:18-30.

306. Wesa AK, Herrem CJ, Mandic M, Taylor JL, Vasquez C, Kawabe M, et al. Enhancement in specific CD8+ T cell recognition of EphA2+ tumors in vitro and in vivo after treatment with ligand agonists. Journal of immunology. 2008;181:7721-7.

307. Vearing C, Lee FT, Wimmer-Kleikamp S, Spirkoska V, To C, Stylianou C, et al. Concurrent binding of anti-EphA3 antibody and ephrin-A5 amplifies EphA3 signaling and downstream responses: potential as EphA3-specific tumor-targeting reagents. Cancer research. 2005;65:6745-54.

308. Noblitt LW, Bangari DS, Shukla S, Knapp DW, Mohammed S, Kinch MS, et al. Decreased tumorigenic potential of EphA2-overexpressing breast cancer cells following treatment with adenoviral vectors that express EphrinA1. Cancer gene therapy. 2004;11:757-66.

309. Lee JW, Han HD, Shahzad MM, Kim SW, Mangala LS, Nick AM, et al. EphA2 immunoconjugate as molecularly targeted chemotherapy for ovarian carcinoma. Journal of the National Cancer Institute. 2009;101:1193-205.

310. Hammond SA, Lutterbuese R, Roff S, Lutterbuese P, Schlereth B, Bruckheimer E, et al. Selective targeting and potent control of tumor growth using an EphA2/CD3-Bispecific single-chain antibody construct. Cancer research. 2007;67:3927-35.

311. van Geer MA, Bakker CT, Koizumi N, Mizuguchi H, Wesseling JG, Oude Elferink RP, et al. Ephrin A2 receptor targeting does not increase adenoviral pancreatic cancer transduction in vivo. World journal of gastroenterology : WJG. 2009;15:2754-62.

312. Wykosky J, Gibo DM, Debinski W. A novel, potent, and specific ephrinA1-based cytotoxin against EphA2 receptor expressing tumor cells. Molecular cancer therapeutics. 2007;6:3208-18.

313. Gobin AM, Moon JJ, West JL. EphrinA I-targeted nanoshells for photothermal ablation of prostate cancer cells. International journal of nanomedicine. 2008;3:351-8.

314. Noberini R, De SK, Zhang Z, Wu B, Raveendra-Panickar D, Chen V, et al. A disalicylic acid-furanyl derivative inhibits ephrin binding to a subset of Eph receptors. Chemical biology & drug design. 2011;78:667-78.

315. Giorgio C, Hassan Mohamed I, Flammini L, Barocelli E, Incerti M, Lodola A, et al. Lithocholic acid is an Eph-ephrin ligand interfering with Eph-kinase activation. PloS one. 2011;6:e18128.

316. Chaudhari A, Mahfouz M, Fialho AM, Yamada T, Granja AT, Zhu Y, et al. Cupredoxin-cancer interrelationship: azurin binding with EphB2, interference in EphB2 tyrosine phosphorylation, and inhibition of cancer growth. Biochemistry. 2007;46:1799-810.

317. Gnoni A, Marech I, Silvestris N, Vacca A, Lorusso V. Dasatinib: an anti-tumour agent via Src inhibition. Current drug targets. 2011;12:563-78.

318. Yamaguchi S, Tatsumi T, Takehara T, Sasakawa A, Hikita H, Kohga K, et al. Dendritic cell-based vaccines suppress metastatic liver tumor via activation of local innate and acquired immunity. Cancer immunology, immunotherapy : CII. 2008;57:1861-9.

319. Okada H, Kalinski P, Ueda R, Hoji A, Kohanbash G, Donegan TE, et al. Induction of CD8+ T-cell responses against novel glioma-associated antigen peptides and clinical activity by vaccinations with {alpha}-type 1 polarized dendritic cells and polyinosinic-polycytidylic acid stabilized by lysine and carboxymethylcellulose in patients with recurrent malignant glioma. Journal of clinical oncology : official journal of the American Society of Clinical Oncology. 2011;29:330-6.

320. Lindberg RA, Hunter T. cDNA cloning and characterization of eck, an epithelial cell receptor protein-tyrosine kinase in the eph/elk family of protein kinases. Molecular and cellular biology. 1990;10:6316-24.

321. Sulman EP, Tang XX, Allen C, Biegel JA, Pleasure DE, Brodeur GM, et al. ECK, a human EPH-related gene, maps to 1p36.1, a common region of alteration in human cancers. Genomics. 1997;40:371-4.

322. Ruiz JC, Robertson EJ. The expression of the receptor-protein tyrosine kinase gene, eck, is highly restricted during early mouse development. Mechanisms of development. 1994;46:87-100.

323. Mori T, Wanaka A, Taguchi A, Matsumoto K, Tohyama M. Differential expressions of the eph family of receptor tyrosine kinase genes (sek, elk, eck) in the developing nervous system of the mouse. Brain research Molecular brain research. 1995;29:325-35.

324. Fox BP, Kandpal RP. Invasiveness of breast carcinoma cells and transcript profile: Eph receptors and ephrin ligands as molecular markers of potential diagnostic and prognostic application. Biochemical and biophysical research communications. 2004;318:882-92.

325. Thaker PH, Deavers M, Celestino J, Thornton A, Fletcher MS, Landen CN, et al. EphA2 expression is associated with aggressive features in ovarian carcinoma. Clinical cancer research : an official journal of the American Association for Cancer Research. 2004;10:5145-50.

326. Lin YG, Han LY, Kamat AA, Merritt WM, Landen CN, Deavers MT, et al. EphA2 overexpression is associated with angiogenesis in ovarian cancer. Cancer. 2007;109:332-40.

327. Walker-Daniels J, Coffman K, Azimi M, Rhim JS, Bostwick DG, Snyder P, et al. Overexpression of the EphA2 tyrosine kinase in prostate cancer. The Prostate. 1999;41:275-80.

328. Mudali SV, Fu B, Lakkur SS, Luo M, Embuscado EE, Iacobuzio-Donahue CA. Patterns of EphA2 protein expression in primary and metastatic pancreatic carcinoma and correlation with genetic status. Clinical & experimental metastasis. 2006;23:357-65.

329. Wykosky J, Gibo DM, Stanton C, Debinski W. EphA2 as a novel molecular marker and target in glioblastoma multiforme. Molecular cancer research : MCR. 2005;3:541-51.

330. Wykosky J, Gibo DM, Stanton C, Debinski W. Interleukin-13 receptor alpha 2, EphA2, and Fos-related antigen 1 as molecular denominators of high-grade astrocytomas and specific targets for combinatorial therapy. Clinical cancer research : an official journal of the American Association for Cancer Research. 2008;14:199-208.

331. Liu F, Park PJ, Lai W, Maher E, Chakravarti A, Durso L, et al. A genome-wide screen reveals functional gene clusters in the cancer genome and identifies EphA2 as a mitogen in glioblastoma. Cancer research. 2006;66:10815-23.

332. Wang LF, Fokas E, Bieker M, Rose F, Rexin P, Zhu Y, et al. Increased expression of EphA2 correlates with adverse outcome in primary and recurrent glioblastoma multiforme patients. Oncology reports. 2008;19:151-6.

333. Herrem CJ, Tatsumi T, Olson KS, Shirai K, Finke JH, Bukowski RM, et al. Expression of EphA2 is prognostic of disease-free interval and overall survival in surgically treated patients with renal cell carcinoma. Clinical cancer research : an official journal of the American Association for Cancer Research. 2005;11:226-31.

334. Hess AR, Seftor EA, Gardner LM, Carles-Kinch K, Schneider GB, Seftor RE, et al. Molecular regulation of tumor cell vasculogenic mimicry by tyrosine phosphorylation: role of epithelial cell kinase (Eck/EphA2). Cancer research. 2001;61:3250-5.

335. Abraham S, Knapp DW, Cheng L, Snyder PW, Mittal SK, Bangari DS, et al. Expression of EphA2 and Ephrin A-1 in carcinoma of the urinary bladder. Clinical cancer

research : an official journal of the American Association for Cancer Research. 2006;12:353-60.

336. Nakamura R, Kataoka H, Sato N, Kanamori M, Ihara M, Igarashi H, et al. EPHA2/EFNA1 expression in human gastric cancer. Cancer science. 2005;96:42-7.

337. Kataoka H, Igarashi H, Kanamori M, Ihara M, Wang JD, Wang YJ, et al. Correlation of EPHA2 overexpression with high microvessel count in human primary colorectal cancer. Cancer science. 2004;95:136-41.

338. Wu D, Suo Z, Kristensen GB, Li S, Troen G, Holm R, et al. Prognostic value of EphA2 and EphrinA-1 in squamous cell cervical carcinoma. Gynecologic oncology. 2004;94:312-9.

339. Lu C, Shahzad MM, Wang H, Landen CN, Kim SW, Allen J, et al. EphA2 overexpression promotes ovarian cancer growth. Cancer biology & therapy. 2008;7:1098-103.

340. Shao Z, Zhang WF, Chen XM, Shang ZJ. Expression of EphA2 and VEGF in squamous cell carcinoma of the tongue: correlation with the angiogenesis and clinical outcome. Oral oncology. 2008;44:1110-7.

341. Miao H, Gale NW, Guo H, Qian J, Petty A, Kaspar J, et al. EphA2 promotes infiltrative invasion of glioma stem cells in vivo through cross-talk with Akt and regulates stem cell properties. Oncogene. 2015;34:558-67.

342. Dohn M, Jiang J, Chen X. Receptor tyrosine kinase EphA2 is regulated by p53-family proteins and induces apoptosis. Oncogene. 2001;20:6503-15.

343. Zelinski DP, Zantek ND, Walker-Daniels J, Peters MA, Taparowsky EJ, Kinch MS. Estrogen and Myc negatively regulate expression of the EphA2 tyrosine kinase. Journal of cellular biochemistry. 2002;85:714-20.

344. Walker-Daniels J, Hess AR, Hendrix MJ, Kinch MS. Differential regulation of EphA2 in normal and malignant cells. The American journal of pathology. 2003;162:1037-42.

345. Choi K, Creighton CJ, Stivers D, Fujimoto N, Kurie JM. Transcriptional profiling of non-small cell lung cancer cells with activating EGFR somatic mutations. PloS one. 2007;2:e1226.

346. Andres AC, Reid HH, Zurcher G, Blaschke RJ, Albrecht D, Ziemiecki A. Expression of two novel eph-related receptor protein tyrosine kinases in mammary gland development and carcinogenesis. Oncogene. 1994;9:1461-7.

347. Nasreen N, Mohammed KA, Lai Y, Antony VB. Receptor EphA2 activation with ephrinA1 suppresses growth of malignant mesothelioma (MM). Cancer letters. 2007;258:215-22.

348. Roux PP, Ballif BA, Anjum R, Gygi SP, Blenis J. Tumor-promoting phorbol esters and activated Ras inactivate the tuberous sclerosis tumor suppressor complex via p90

ribosomal S6 kinase. Proceedings of the National Academy of Sciences of the United States of America. 2004;101:13489-94.

349. Roux PP, Shahbazian D, Vu H, Holz MK, Cohen MS, Taunton J, et al. RAS/ERK signaling promotes site-specific ribosomal protein S6 phosphorylation via RSK and stimulates cap-dependent translation. The Journal of biological chemistry. 2007;282:14056-64.

350. Bonni A, Brunet A, West AE, Datta SR, Takasu MA, Greenberg ME. Cell survival promoted by the Ras-MAPK signaling pathway by transcription-dependent and -independent mechanisms. Science. 1999;286:1358-62.

351. Eisenmann KM, VanBrocklin MW, Staffend NA, Kitchen SM, Koo HM. Mitogen-activated protein kinase pathway-dependent tumor-specific survival signaling in melanoma cells through inactivation of the proapoptotic protein bad. Cancer research. 2003;63:8330-7.

352. Zhuang G, Hunter S, Hwang Y, Chen J. Regulation of EphA2 receptor endocytosis by SHIP2 lipid phosphatase via phosphatidylinositol 3-Kinase-dependent Rac1 activation. The Journal of biological chemistry. 2007;282:2683-94.

353. Beer DG, Kardia SL, Huang CC, Giordano TJ, Levin AM, Misek DE, et al. Gene-expression profiles predict survival of patients with lung adenocarcinoma. Nature medicine. 2002;8:816-24.

354. Rohrbeck A, Neukirchen J, Rosskopf M, Pardillos GG, Geddert H, Schwalen A, et al. Gene expression profiling for molecular distinction and characterization of laser captured primary lung cancers. Journal of translational medicine. 2008;6:69.

355. Zhu CQ, Ding K, Strumpf D, Weir BA, Meyerson M, Pennell N, et al. Prognostic and predictive gene signature for adjuvant chemotherapy in resected non-small-cell lung cancer. Journal of clinical oncology : official journal of the American Society of Clinical Oncology. 2010;28:4417-24.

356. Patricelli MP, Nomanbhoy TK, Wu J, Brown H, Zhou D, Zhang J, et al. In situ kinase profiling reveals functionally relevant properties of native kinases. Chemistry & biology. 2011;18:699-710.

357. Patricelli MP, Szardenings AK, Liyanage M, Nomanbhoy TK, Wu M, Weissig H, et al. Functional interrogation of the kinome using nucleotide acyl phosphates. Biochemistry. 2007;46:350-8.

358. Zha J, Harada H, Yang E, Jockel J, Korsmeyer SJ. Serine phosphorylation of death agonist BAD in response to survival factor results in binding to 14-3-3 not BCL-X(L). Cell. 1996;87:619-28.

359. Harada H, Andersen JS, Mann M, Terada N, Korsmeyer SJ. p70S6 kinase signals cell survival as well as growth, inactivating the pro-apoptotic molecule BAD. Proceedings of the National Academy of Sciences of the United States of America. 2001;98:9666-70.

360. Liu Y, Gray NS. Rational design of inhibitors that bind to inactive kinase conformations. Nature chemical biology. 2006;2:358-64.

361. Dzamko N, Inesta-Vaquera F, Zhang J, Xie C, Cai H, Arthur S, et al. The IkappaB kinase family phosphorylates the Parkinson's disease kinase LRRK2 at Ser935 and Ser910 during Toll-like receptor signaling. PloS one. 2012;7:e39132.

362. Brannan JM, Sen B, Saigal B, Prudkin L, Behrens C, Solis L, et al. EphA2 in the early pathogenesis and progression of non-small cell lung cancer. Cancer prevention research. 2009;2:1039-49.

363. Chen J. Regulation of tumor initiation and metastatic progression by Eph receptor tyrosine kinases. Advances in cancer research. 2012;114:1-20.

364. Siegel R, Ma J, Zou Z, Jemal A. Cancer statistics, 2014. CA: a cancer journal for clinicians. 2014;64:9-29.

365. Ladanyi M, Pao W. Lung adenocarcinoma: guiding EGFR-targeted therapy and beyond. Modern pathology : an official journal of the United States and Canadian Academy of Pathology, Inc. 2008;21 Suppl 2:S16-22.

366. Sordella R, Bell DW, Haber DA, Settleman J. Gefitinib-sensitizing EGFR mutations in lung cancer activate anti-apoptotic pathways. Science. 2004;305:1163-7.

367. Barquilla A, Pasquale EB. Eph Receptors and Ephrins: Therapeutic Opportunities. Annual review of pharmacology and toxicology. 2014.

368. Selamat SA, Chung BS, Girard L, Zhang W, Zhang Y, Campan M, et al. Genome-scale analysis of DNA methylation in lung adenocarcinoma and integration with mRNA expression. Genome research. 2012;22:1197-211.

369. Chmielecki J, Pietanza MC, Aftab D, Shen R, Zhao Z, Chen X, et al. EGFR-mutant lung adenocarcinomas treated first-line with the novel EGFR inhibitor, XL647, can subsequently retain moderate sensitivity to erlotinib. Journal of thoracic oncology : official publication of the International Association for the Study of Lung Cancer. 2012;7:434-42.

370. Chmielecki J, Foo J, Oxnard GR, Hutchinson K, Ohashi K, Somwar R, et al. Optimization of dosing for EGFR-mutant non-small cell lung cancer with evolutionary cancer modeling. Science translational medicine. 2011;3:90ra59.

371. Regales L, Balak MN, Gong Y, Politi K, Sawai A, Le C, et al. Development of new mouse lung tumor models expressing EGFR T790M mutants associated with clinical resistance to kinase inhibitors. PloS one. 2007;2:e810.

372. Tichelaar JW, Lu W, Whitsett JA. Conditional expression of fibroblast growth factor-7 in the developing and mature lung. The Journal of biological chemistry. 2000;275:11858-64.

373. Politi K, Zakowski MF, Fan PD, Schonfeld EA, Pao W, Varmus HE. Lung adenocarcinomas induced in mice by mutant EGF receptors found in human lung

cancers respond to a tyrosine kinase inhibitor or to down-regulation of the receptors. Genes & development. 2006;20:1496-510.

374. Fisher GH, Wellen SL, Klimstra D, Lenczowski JM, Tichelaar JW, Lizak MJ, et al. Induction and apoptotic regression of lung adenocarcinomas by regulation of a K-Ras transgene in the presence and absence of tumor suppressor genes. Genes & development. 2001;15:3249-62.

375. Ohashi K, Sequist LV, Arcila ME, Moran T, Chmielecki J, Lin YL, et al. Lung cancers with acquired resistance to EGFR inhibitors occasionally harbor BRAF gene mutations but lack mutations in KRAS, NRAS, or MEK1. Proceedings of the National Academy of Sciences of the United States of America. 2012;109:E2127-33.

376. Bean J, Brennan C, Shih JY, Riely G, Viale A, Wang L, et al. MET amplification occurs with or without T790M mutations in EGFR mutant lung tumors with acquired resistance to gefitinib or erlotinib. Proceedings of the National Academy of Sciences of the United States of America. 2007;104:20932-7.

377. Li X, Wang L, Gu JW, Li B, Liu WP, Wang YG, et al. Up-regulation of EphA2 and down-regulation of EphrinA1 are associated with the aggressive phenotype and poor prognosis of malignant glioma. Tumour biology : the journal of the International Society for Oncodevelopmental Biology and Medicine. 2010;31:477-88.

378. Meador CB, Jin H, de Stanchina E, Nebhan CA, Pirazzoli V, Wang L, et al. Optimizing the Sequence of Anti-EGFR-Targeted Therapy in EGFR-Mutant Lung Cancer. Molecular cancer therapeutics. 2014.

379. Riely GJ, Kris MG, Zhao B, Akhurst T, Milton DT, Moore E, et al. Prospective assessment of discontinuation and reinitiation of erlotinib or gefitinib in patients with acquired resistance to erlotinib or gefitinib followed by the addition of everolimus. Clinical cancer research : an official journal of the American Association for Cancer Research. 2007;13:5150-5.

380. Chaft JE, Oxnard GR, Sima CS, Kris MG, Miller VA, Riely GJ. Disease flare after tyrosine kinase inhibitor discontinuation in patients with EGFR-mutant lung cancer and acquired resistance to erlotinib or gefitinib: implications for clinical trial design. Clinical cancer research : an official journal of the American Association for Cancer Research. 2011;17:6298-303.

381. Becker A, Crombag L, Heideman DA, Thunnissen FB, van Wijk AW, Postmus PE, et al. Retreatment with erlotinib: Regain of TKI sensitivity following a drug holiday for patients with NSCLC who initially responded to EGFR-TKI treatment. European journal of cancer. 2011;47:2603-6.

382. Oxnard GR, Janjigian YY, Arcila ME, Sima CS, Kass SL, Riely GJ, et al. Maintained sensitivity to EGFR tyrosine kinase inhibitors in EGFR-mutant lung cancer recurring after adjuvant erlotinib or gefitinib. Clinical cancer research : an official journal of the American Association for Cancer Research. 2011;17:6322-8.

383. Eisinger-Mathason TS, Andrade J, Lannigan DA. RSK in tumorigenesis: connections to steroid signaling. Steroids. 2010;75:191-202.

384. Young A, Lou D, McCormick F. Oncogenic and wild-type Ras play divergent roles in the regulation of mitogen-activated protein kinase signaling. Cancer discovery. 2013;3:112-23.

385. Finke J, Ferrone S, Frey A, Mufson A, Ochoa A. Where have all the T cells gone? Mechanisms of immune evasion by tumors. Immunology today. 1999;20:158-60.

386. Pardoll D. Does the immune system see tumors as foreign or self? Annual review of immunology. 2003;21:807-39.

387. Marincola FM, Wang E, Herlyn M, Seliger B, Ferrone S. Tumors as elusive targets of T-cell-based active immunotherapy. Trends in immunology. 2003;24:335-42.

388. Mahnke YD, Devevre E, Baumgaertner P, Matter M, Rufer N, Romero P, et al. Human melanoma-specific CD8(+) T-cells from metastases are capable of antigen-specific degranulation and cytolysis directly ex vivo. Oncoimmunology. 2012;1:467-530.

389. Baitsch L, Baumgaertner P, Devevre E, Raghav SK, Legat A, Barba L, et al. Exhaustion of tumor-specific CD8(+) T cells in metastases from melanoma patients. The Journal of clinical investigation. 2011;121:2350-60.

390. Ahmadzadeh M, Johnson LA, Heemskerk B, Wunderlich JR, Dudley ME, White DE, et al. Tumor antigen-specific CD8 T cells infiltrating the tumor express high levels of PD-1 and are functionally impaired. Blood. 2009;114:1537-44.

391. Zou W, Chen L. Inhibitory B7-family molecules in the tumour microenvironment. Nature reviews Immunology. 2008;8:467-77.

392. Pardoll DM. The blockade of immune checkpoints in cancer immunotherapy. Nature reviews Cancer. 2012;12:252-64.

393. Lennerz V, Fatho M, Gentilini C, Frye RA, Lifke A, Ferel D, et al. The response of autologous T cells to a human melanoma is dominated by mutated neoantigens. Proceedings of the National Academy of Sciences of the United States of America. 2005;102:16013-8.

394. Castle JC, Kreiter S, Diekmann J, Lower M, van de Roemer N, de Graaf J, et al. Exploiting the mutanome for tumor vaccination. Cancer research. 2012;72:1081-91.

395. Badovinac VP, Harty JT. Intracellular staining for TNF and IFN-gamma detects different frequencies of antigen-specific CD8(+) T cells. Journal of immunological methods. 2000;238:107-17.

396. Betts MR, Brenchley JM, Price DA, De Rosa SC, Douek DC, Roederer M, et al. Sensitive and viable identification of antigen-specific CD8+ T cells by a flow cytometric assay for degranulation. Journal of immunological methods. 2003;281:65-78.